AN ABSTRACT OF THE DISSERTATION OF

Geoffrey R. Hosack for the degree of Doctor of Philosophy in Fisheries Science presented on June 27 2008.

Title: Predicting the Stability, Equilibrium response, and Nonequilibrium Dynamics of Ecological Systems.

Abstract approved:

_____

      Philippe A. Rossignol   Hiram W. Li

In this dissertation, new theory and its applications are developed to predict three properties of complex ecological communities: stability, equilibrium response, and non-equilibrium dynamics. First, a graph-theoretic analysis identifies the interconnections in a complex ecosystem that promote or diminish stability (Chapter 2). The hierarchy of interactions that influences stability and feedback processes can guide resource allocation for environmental monitoring, investigate alternative management strategies, and help formulate novel research hypotheses. Second, a combined graph-theoretic and probabilistic approach evaluates the potential for long-term changes in equilibrium (Chapter 3). Conditional probabilities of long-term increase and decrease in variables are transferred from the graph-theoretic models into a Bayesian network. The Bayesian network allows researchers both to predict how an ecosystem might change given a perturbation and to diagnose which model structure best matches empirical observations. Third, a threshold index predicts whether or not large-magnitude short-term transitory changes in disease prevalence can occur (Chapter 4). The concept of reactivity is used to derive a threshold index for epidemicity, E_0, which gives the maximum number of new infections produced by an infective individual at a disease free equilibrium. This index provides a threshold that determines whether or not major epidemics are possible. The relative importance of parameters differs between control strategies that seek to reduce endemicity and those

that seek to reduce epidemicity. The index $\mathbf{E}_0$ therefore is an important measure of epidemic potential that may assist efforts to control epidemics. Together these approaches provide new theory that help bridge the gap between our need to understand complex ecological systems and the empirical data available for their characterization.

Predicting the Stability, Equilibrium Response, and Nonequilibrium Dynamics of Ecological Systems.

by

Geoffrey R. Hosack

A DISSERTATION

submitted to

Oregon State University

in partial fulfillment of
the requirements for the
degree of

Doctor of Philosophy

Presented June 27, 2008
Commencement June 2009

Doctor of Philosophy dissertation of Geoffrey R. Hosack presented on June 27, 2008

APPROVED:

_____

Co-Major Professor, representing Fisheries Science

_____

Co-Major Professor, representing Fisheries Science

_____

Head of the Department of Fisheries and Wildlife

_____

Dean of the Graduate School

I understand that my dissertation will become part of the permanent collection of Oregon State University libraries. My signature below authorizes release of my dissertation to any reader upon request.

_____

Geoffrey R. Hosack, Author

ACKNOWLEDGMENTS

CONTRIBUTIONS OF AUTHORS

The following authors contributed to the writing and research design of this dissertation: Hiram Li (Chapter 2), Philippe Rossignol (Chapters 2 and 4), Keith Hayes (Chapter 3), Jeffrey Dambacher (Chapter 3), and Pauline van den Driessche (Chapter 4).

TABLE OF CONTENTS

LIST OF FIGURES

LIST OF TABLES

LIST OF APPENDICES

LIST OF APPENDIX TABLES

1 GENERAL INTRODUCTION

Ecological researchers and managers often have to make decisions and recommendations while working in complex and often poorly understood systems. Species exist in interconnected communities that demand a multispecies perspective for evaluating mechanisms that govern the viability of a population of interest (Sih et al. 1985, Wootton 1994), but learning how species within complex communities respond to human and environmental pressures remains one of the great challenges for community ecology (Ives and Carpenter 2007). Ecologists are forced to conduct their research and decision-making responsibilities amidst uncertainty with respect to the processes, the structure, and the dynamics of complex communities (Francis and Shotton 1997, Ruckelshaus et al. 2002, Fairbrother and Turnley 2005). New theoretic tools are needed that allow ecologists and managers to deal with the uncertainty that usually characterizes ecological systems. In this dissertation, three such tools are contributed to narrow the gap between the uncertainties inherent within complex ecological systems and the empirical data available for their characterization.

A graph-theoretic approach is proposed that identifies critical linkages between members within a complex system (Chapter 2). Graphical models are used to create complex models that relate the influence of each variable on another (Levins 1974, Dambacher et al. 2002). These graphical models are food-web models with the addition of non-trophic interactions such as interference competition, mutualism, and modified interactions (Dambacher and Ramos-Jilliberto 2007). These graphical models are used to derive positive and negative feedback cycles that determine the stability of the system. A sensitivity analysis is developed that identifies the critical linkages that contribute to stabilizing or destabilizing processes within the system. The approach is demonstrated using two theoretical models and two empirical models, each taken from the published literature. Non-trophic interactions are investigated as critical interactions that determine the success of species invasions and the development of alternative stable states.

If a system is stable, the next question is often: how will the system respond to an anthropogenic or environmental pressure over the long-term? In these situations, ecological predictions and management strategies can be more sensitive to the structural uncertainty of a model than parametric uncertainty. In addition, when faced with insufficient quantitative knowledge, ecologists may forgo quantitative analysis and fill in this gap of empirical data with expert opinion incorporated into a Bayesian Belief Network (BBN). Including expert elicitation in BBNs can have the following disadvantages: (1) specifying conditional probabilities can be time-consuming, (2) expert opinion can be subject to cognitive bias, (3) expert opinion can be confounded with linguistic uncertainty, and (4) feedback cycles can be difficult to parameterize within a dynamic Bayesian network. In Chapter 3, we present a method that addresses the problems highlighted above by merging BBNs with the form of graphical modeling used in Chapter 2. This method is designed to assist ecologists, risk practitioners and natural resources managers in understanding how ecosystems might respond to a changing pressures in the environment.

Whereas Chapter 2 asks if a system exhibits a long-term return to equilibrium following a perturbation, and Chapter 3 asks how presses to ecological systems change the long-term levels of variables, Chapter 4 investigates whether or not important ecological changes may develop over the short-term. For example, clinically important changes in disease infection may develop over the short-term in vector-borne diseases (Lotka 1923). A threshold index, $\mathbf{E}_0$, is developed that predicts whether or not a short-term epidemic can occur within a system of vector-borne disease. The index $\mathbf{E}_0$ is used to investigate if vector behavior has a larger influence on the severity of epidemics than on the level of epidemicity within a given area of disease transmission.

Each of the chapters 2-4 contributes a new theoretic approach designed to improve our understanding and our prediction of complex ecological systems. The general conclusions are outlined in Chapter 5.

2 SENSITIVITY OF SYSTEM STABILITY TO MODEL STRUCTURE

Geoffrey R. Hosack
Department of Fisheries and Wildlife, Oregon State University, Corvallis, OR 97331
Geoff.Hosack@oregonstate.edu

Hiram W. Li
Oregon Cooperative Fish and Wildlife Research Unit, U. S. Geological Survey
Department of Fisheries and Wildlife, Oregon State University, Corvallis, OR 97331
Hiram.Li@oregonstate.edu

Philippe A. Rossignol
Department of Fisheries and Wildlife, Oregon State University, Corvallis, OR 97331
Phil.Rossignol@oregonstate.edu

2.1 Abstract

A community's structure is formed by the direct effects among the species and variables within the community. The direct effects within a community form feedback cycles that confer the dynamical aspects of stability and resilience to the community. A community is stable, and resilient, if the levels of all community variables return to the original steady state following a perturbation. Although feedback cycles (loops) have an intuitive interpretation, identifying how they form the feedback properties of a particular community can be intractably complicated. Furthermore, the role that any specific direct effect plays in the stability of a system is not fully understood. Such information would allow experimental and management manipulation of complex communities. We therefore provide a sensitivity analysis that identifies the structural role of the direct effects among species using graph theory techniques. We formalize the model structure using a signed digraph that in turn has a mathematical representation. A sensitivity analysis then summarizes the degree to which each of these direct effects contributes to stabilizing feedback within the community. Sensitivity analysis is useful for identifying ecologically important feedback cycles within the structure of a particular community and for detecting direct effects that have strong influences on community stability. It may guide the development of management interventions and research designs. We demonstrate the power of this approach using two theoretical models and two empirical examples of different levels of complexity. Sensitivity analysis provides insight on how stability and coexistence is maintained within ecological communities.

2.2 Keywords

feedback cycle, signed directed graph, species interaction, qualitative modeling

2.3 Introduction

Understanding how species stably coexist within complex communities remains one of the great challenges for community ecology (Ives and Carpenter 2007). Species coexist not in a vacuum but in large interconnected communities where they interact, sometimes very strongly, with other species whose vital rates are influenced by yet other species (Sih et al. 1985, Wootton 1994). Many species and populations appear to exhibit stability (Sibly et al. 2007). Stability is linked to other important ecological concepts such as resilience (Neubert and Caswell 1997) and alternative stable states (Scheffer et al. 2001), and as such is an important concept with a long history of applied use in ecology. Although stability has a clear mathematical definition (May 1974), it is not simply a theoretical measure, but also an applied one that asks how communities of species persist and respond to anthropogenic, climatic, and ecological pressures.

The structure of the entire community is defined by the direct effects—also referred to as species interactions (e.g., Berlow et al. 2004)—between community members, and a community's structure has important implications for its stability (Puccia and Levins 1985, Dambacher et al. 2003b). Feedback cycles are formed by combinations of the direct effects among community members. Understanding these cycles leads to improved insight into the mechanisms that govern the dynamics of a community (Dambacher et al. 2002) or population (Guneralp 2007). Although feedback cycles may be conceptually identified in a community, the way that these cycles interact to form feedback for the entire community is often complicated and counter-intuitive (Levins 1974) and is particularly so in large communities (Dambacher et al. 2002). As we will show, sensitivity analysis of a community's structural stability can elucidate why particular feedback cycles are important and resolve issues that appear to be counter-intuitive.

Within population models, sensitivity analyses that determine the effect of life stage interactions on the long-term growth rate within population models have provided a very effective modeling tool for ecologists (Caswell 2001); these models usually rely on quantified life-table data. Sensitivity analyses applied to community models, however, have been restricted because community

models are more difficult to parameterize (Wootton and Emmerson 2005). Quantifying the direct effects in communities is expensive, time-consuming, and rarely possible (Bender et al. 1984, Yodzis 1988, Schmitz 1997). A need exists for an approach that, based on the structure of communities, interprets how the direct effects influence feedback cycles and hence stability.

Sensitivity analysis of a community's structural stability is introduced as one such way to identify how each direct effect influences the stability of the community as a whole. Feedback cycles may exert stabilizing effects, destabilizing effects, or even both effects simultaneously on the community as a whole. Sensitivity analysis for community stability provides a method that establishes how each direct effect participates in stabilizing or destabilizing feedback cycles and thereby determines community stability. We illustrate from four examples the variety of mechanisms that influence coexistence among species and community stability, as revealed by this approach. The examples are (1) keystone predator model, (2) competitive exclusion modified by mutualism, (3) effect of introduced species in modifying interspecific interactions and subsidies between ecosystems, and (4) relative role of trophic versus non-trophic interactions influencing the structural stability of shallow lake communities. A computer program is provided that conducts the sensitivity analysis.

2.4 Methods

In the Methods, we first introduce definitions necessary for understanding a graph-theoretic approach to modeling communities. Second, we use a toy example to explore graphically these new definitions and introduce the concept of structural stability. Third, sensitivity analysis is heuristically defined, and then applied to this same example. The mathematical details that underlie sensitivity analysis are found in Appendix A. A computer program that implements the sensitivity analysis is provided in Appendix B.

2.4.1 Preliminary definitions

Community structure is represented by a *signed digraph* (signed directed graph) that denotes the positive and negative direct effects between variables (Figure 2.1). A *path* is a sequence of these direct effects that starts at one variable and ends at another without crossing any variable more than once. A path that ends at the starting variable is a *cycle* (loop). Cycles that have no shared variables are *disjunct*. A *cycle product* is a product of one or more disjunct cycles. Cycle products define *feedback*. *Feedback level* is the number of variables included within a cycle product. *Positive feedback* occurs when an increase (decrease) is made to a variable and feedback further increases (decreases) that variable. *Negative feedback* occurs when an increase (decrease) is made to a variable and feedback decreases (increases) that variable.

2.4.2 Structural stability of a simple model

To better visualize feedback cycles, it is convenient to diagram the interrelationships between the species within a community using a signed digraph. A signed digraph depicts the direct effects that occur between species. For example, Figure 2.1 shows a three trophic level model: species 1 is the basal resource, species 2 is an intermediate consumer, and species 3 is the top level consumer. In addition, the model specifies that species 3 has a positive direct effect on the basal resource as might occur through nutrient recycling.

The signed digraph has an associated symbolic matrix, **A**. The matrix **A** represents the system linearized at a steady state, (i.e., it is the Jacobian matrix; May 1974). The matrix entry in the ith row and the jth column shows the magnitude (a_{ij}), and the sign ($+$, $-$) of the direct effect of species j on species i. The a_{ij}, which we assume are unknown, and their associated signs describe the direct effect of species j on species i. These direct effects incorporate parameters such as species interaction magnitudes and rates of growth and decay at a steady state. In practice, these direct effects are difficult to quantify (Bender et al. 1984, Wootton and Emmerson 2005). In this paper, we focus

instead on identifying ecologically important feedback cycles that arise from these mechanistic interconnections within the community.

Every system requires negative feedback cycles as a necessary condition for stability. A necessary condition for stability is that all the feedback levels must be negative. In the above example model, feedback cycles can affect the system at 3 different feedback levels because there are 3 species in this community (Figure 2.2).

For example, the growth equation of species 1 draws resources from variables not explicitly modeled in Figure 2.1, such as from light or nutrients; that is, species 1 has a carrying capacity set by external factors and exhibits logistic-type growth. Such a variable may be considered self-regulated (Levins 1998) and, in the signed digraph, a single negative feedback cycle starts and ends at the basal resource, species 1. This negative feedback cycle product, which only includes one variable, contributes stabilizing negative feedback to the first feedback level.

Trophic interactions involve two variables: the consumer has a negative direct effect on the prey, and the prey has a positive direct effect on the consumer. A positive direct effect multiplied by a negative direct effect creates a negative feedback cycle. In this model, two such trophic relationships exist because species 2 feeds on species 1 and species 3 feeds on species 2. Thus, two negative feedback cycles contribute stabilizing negative feedback to the second feedback level.

A single feedback cycle may affect the stability of the community at multiple feedback levels. Feedback cycles from lower feedback levels may combine with other disjunct cycles to form cycle products at higher feedback levels. An example of this can be seen in the third feedback level. The self-regulation of species 1 is multiplied by the disjunct trophic relationship between species 2 and 3. This cycle product is stabilizing because it is the product of two negative feedback cycles. In contrast, a long feedback cycle that includes all three species introduces destabilizing positive feedback at the third feedback level. This long feedback cycle is positive because the product of the 3 direct effects from which it is composed has a positive sign ($+a_{13}a_{32}a_{21}$). If this positive cycle product is stronger than the negative cycle product, then the community cannot be stable.

A set of necessary and sufficient conditions for stability, given by the far less intuitive Hurwitz determinants, takes into consideration the relative strength of the different feedback levels. There are n Hurwtiz determinants, denoted Δ_k, constructed from the F_k, and these must all be positive for an equilibrium to be stable (Hurwitz [1895] 1964, Dambacher et al. 2003b; see Appendix A). For this example model, if all feedback levels are negative, then the remaining condition for stability as derived from the Hurwitz determinants is

$$F_1 F_2 + F_3 = \left(-a_{11}\right)\left(-a_{12}a_{21} - a_{23}a_{32}\right) + \left(a_{13}a_{32}a_{21} - a_{11}a_{23}a_{32}\right) > 0 . \tag{2.1}$$

The inequality in Equation (2.1) always holds for this model system. Thus, if all feedback levels are negative, then the model system is stable.

2.4.3 Sensitivity of the tri-trophic example

The next question centers on how a particular direct effect influences the stability of the system, that is, its sensitivity. We introduce the concept of sensitivity weight, $\mathbf{W}_{ij}^{F_k}$, to determine how each direct effect contributes to negative and positive feedback cycle products. Below, we provide a heuristic definition of sensitivity weight; the mathematical derivation is given in Appendix A. We measure the sensitivity of the kth feedback level F_k, $k = 1 \ldots n$, using the metric:

$$\mathbf{W}_{ij}^{F_k} = \frac{net\ \#\ of\ cycle\ products\ in\ F_k\ that\ contains\ a_{ij}}{total\ \#\ of\ cycle\ products\ in\ F_k\ that\ contains\ a_{ij}} . \tag{2.2}$$

The sensitivity weight $\mathbf{W}_{ij}^{F_k}$ is the ratio of the net number of cycle products to the total number of cycle products appearing within the kth feedback level that contain the direct effect's a_{ij}. A sensitivity weight of -1.0 ($+1.0$) indicates that a direct effect's a_{ij} is represented only within negative (positive) cycle products in the coefficient F_k. The sensitivity weight is 0 if an equal number of negative and positive cycle products that contain a_{ij} are present. Sensitivity weights between 0 and -1.0 ($+1.0$) indicate that more negative (positive) cycle products contain a_{ij} than positive (negative) cycle products.

For each Hurwitz determinant Δ_k, $k = 1 \ldots n$, we use an analogous metric $\mathbf{W}_{ij}^{\Delta_k}$ to count the number of positive versus negative occurrences of a direct effect's a_{ij} (see Appendix A). Since the Hurwitz determinants must be positive in stable systems, however, positive net sensitivity weights for Hurwitz determinants correspond to stabilizing feedback. This contrasts with the sensitivity weights of the feedback levels in Equation (2.2), where negative values correspond to stabilizing feedback.

We apply these sensitivity weights to the feedback levels within the example model (Figure 2.2). The positive direct effect of the top-level consumer, species 3, on the basal resource, species 1, denoted a_{13}, occurs only once within the system's feedback, at the third feedback level. The net sensitivity weight for a_{13} at the third feedback level is $\mathbf{W}_{13}^{F_3} = +1/1$, and this direct effect contributes only to destabilizing positive feedback.

In contrast, the positive direct effect of the intermediate consumer, species 2, on the top-level consumer (a_{32}) occurs not only in both negative and positive feedback cycle products at the third feedback level, $\mathbf{W}_{32}^{F_3} = 0/2$, but also in a single negative cycle product at the second feedback level, $\mathbf{W}_{32}^{F_2} = -1/1$. Although the direct effect a_{32} contributes to stabilizing feedback in F_2, its effect in F_3 is ambiguous. In the same trophic relationship, but unlike its partner a_{32}, the direct effect $-a_{23}$ contributes only stabilizing feedback ($\mathbf{W}_{23}^{F_2} = -1/1$ and $\mathbf{W}_{23}^{F_3} = -1/1$). The net sensitivity weights thus inform how each direct affect affects the stability of the community.

The mathematical derivation of the sensitivity weight matrices for the feedback levels and the Hurwitz determinants are provided in Appendix A. A computer program that implements the sensitivity analysis is provided in the Appendix B.

2.5 Results

Sensitivity analysis identifies the role and relative importance that each direct effect plays within community stability. This is a general mathematical method applicable to the structure of any complex system that can be represented using a signed digraph. We first illustrate sensitivity analysis

by applying it to two small theoretical communities. We interpret how the direct effects affect community stability at multiple levels of feedback and in the Hurwitz determinants. Second, after investigating these theoretical models, we apply sensitivity analysis to two empirical examples of community structures taken from the published literature.

2.5.1 The keystone predator model

The keystone predator model consists of an unstable subsystem of two interference competitors stabilized by the presence of a predator (Levins 1975, Vance 1978; Figure 3). The predator exerts a negative direct effect on prey through consumption; assimilation of prey produces a positive direct effect of prey on the predator. Multiplying these direct effects together forms a negative (stabilizing) cycle for each predator-prey relationship. Each prey species also engages in competition such that one exerts a negative direct effect on the other. Multiplying these direct effects together forms a positive (destabilizing) cycle for the competitive relationship. In the absence of the predator, the interspecific competition between the two prey species produces destabilizing positive feedback that, if stronger than the stabilizing intraspecific competition within the prey species, precludes stable coexistence. The presence of the predator produces stabilizing negative feedback such that coexistence among prey species becomes possible, even if interspecific competition between prey is stronger than their intraspecific competition. Adding a predator may change feedback quality from positive to negative, and so the predator is a keystone for community stability (Levins 1975). We use sensitivity analysis to derive this conclusion.

Sensitivity analysis determines the contribution of each direct effect within these feedback cycle products. The weighted sensitivity matrices for each feedback level $\mathbf{W}^{F_k}$ are given in Table 2.1. The sensitivity analysis shows that self-regulation of prey is stabilizing because the weighted sensitivity of -1.0 is observed in all three feedback levels F_k for the direct effects $-a_{11}$ and $-a_{22}$. This means that self-regulation only occurs in negative cycle products that contribute negative (stabilizing) feedback to the community. In contrast, the interspecific competition occurring among prey, given by

$-a_{12}$ and $-a_{21}$, has a weight of +1.0 at feedback levels F_2 and F_3. Interspecific competition contributes only positive (destabilizing) feedback to the community. In the absence of the keystone predator, stability is impossible if the interspecific competition between prey species is stronger than their self-regulation.

The weighted sensitivity matrices also show that the predator creates negative feedback cycles, associated with predation, at level F_2. Sensitivity analysis shows that if the strength of predation is greater than the interspecific competition, then the predator stabilizes an otherwise unstable system at this intermediate level of feedback, as in (Levins 1975). Each direct effect involving the predator, however, also occurs in both one positive and one negative feedback cycle product at the highest feedback level F_3. This ambiguity at the highest feedback level indicates that the keystone predator does not guarantee stability for a community with strong interspecific competition between prey species, but only permits it. The sensitivity analysis demonstrates how the keystone predator makes the stable coexistence of an otherwise unstable community possible.

2.5.2 Competitive exclusion modified by commensalism

In the above keystone predator model, a predator stabilized its community by forming negative feedback at an intermediate feedback level. In this example, we will investigate how negative feedback may sometimes destabilize communities. We take an example where positive feedback is absent from all feedback levels and yet the community structure may be unstable.

An axiom of ecology is that "complete competitors cannot coexist" (Hardin 1960). Two consumers completely dependent on a single resource, if described by a signed digraph equivalent to Figure 2.4 without the dotted path, cannot coexist at a stable equilibrium because the community lacks feedback cycle products at the highest feedback level, F_3. That is, no products of disjunct cycles exist that involve all three variables. In contrast, the two lower feedback levels each have negative feedback cycles resulting from predation and self-regulation.

Stability is possible, however, if one consumer has a commensal relationship with its competitor. For instance, one consumer may excrete a substance or modify a habitat to benefit the other. This modification creates a single negative feedback cycle at the highest level: the product of the three direct effects contributing to this feedback cycle has a negative sign ($-a_{13}a_{21}a_{32}$). All feedback levels in this modified community are unambiguously negative.

This commensal relationship permits stability by forming a negative feedback cycle at level F_3, but the community may yet be unstable because of the length of this cycle. Long negative feedback cycles that involve more than two variables can overwhelm lower level negative feedback and subsequently lead to overcorrection and instability (Puccia and Levins 1985, Dambacher et al. 2003b). This form of instability is detected by the Hurwitz determinants, and can usually be traced to the n–1st Hurwitz determinant (Dambacher et al. 2003b).

Sensitivity analysis of the modified competitive exclusion community shows that the commensalism in this system, denoted by a_{32}, contributes only to destabilizing feedback within the n–1st Hurwitz determinant (Table 2.2). Two of the direct effects that correspond to resource consumption, $-a_{13}$ and a_{21}, which as noted above are stabilizing at feedback level 2, also participate in the long negative feedback cycle. Note that the weighted sensitivities show that these direct effects in turn contribute to both stabilizing and destabilizing feedback ($\mathbf{W}_{13}^{\Delta_2} = \mathbf{W}_{21}^{\Delta_2} = 0.0$) in the second Hurwitz determinant. The sensitivity analysis straightforwardly identifies an interesting property of this community. The community may be unstable even though only negative feedback is present at all feedback levels, and the sensitivity analysis identifies the source of this phenomenon.

2.5.3 Modified interactions and subsidy

In riparian forests of northern Japan, both benthic and terrestrial insects provide food for native Dolly Varden charr (*Salvelinus malma*). Emerging benthic insects subsidize riparian spiders. Nonnative rainbow trout (*Oncorhynchus mykiss*) feed on terrestrial, but not benthic, insects. Rainbow trout also modify the foraging of Dolly Varden by inhibiting their feeding on terrestrial insects and

enhancing their feeding on benthic insects. Experimental manipulations show that these variables

form an interconnected community (Baxter et al. 2004). Baxter et al. (2004) postulated that the

addition of nonnative rainbow trout may displace native Dolly Varden and preclude the coexistence of

the fish species in some natural settings. We use sensitivity analysis to identify which of the above

direct effects produce destabilizing positive feedback, and thereby distinguish how each direct effect

influences the stable coexistence of this community.

In addition to the direct effects described above, the rainbow trout also modify the foraging

behavior of Dolly Varden and form direct effects that arise from these modified interactions (*sensu*

Dambacher and Ramos-Jiliberto 2007). Two such direct effects that can emerge are depicted in Figure

2.5: rainbow trout greatly reduce the uptake of terrestrial insects by Dolly Varden (negative direct

effect from rainbow trout to Dolly Varden) and simultaneously increase predation by Dolly Varden on

benthic invertebrates (negative direct effect from rainbow trout to benthic invertebrates). For the

purposes of this analysis, we focus on the signed digraph of Figure 2.5, but other alternatives are

possible (see Dambacher and Ramos-Jiliberto 2007).

The signed digraph that describes the above community structure assumes self-regulation

(e.g., logistic growth) for all variables. Terrestrial invertebrates are assumed to enter the stream

community at a constant rate, and some number is eaten by trout or charr with the remainder exiting

the community by drift or decomposition. Benthic invertebrates emerge from the stream community

and subsidize riparian spiders; this subsidy is represented as a positive direct effect from benthic

invertebrates to spiders.

For this example, we use the highest feedback level F_5 as a guide for identifying important

positive and negative cycles that affect the stability of this stream community. Although a full

sensitivity analysis could be conducted, the highest feedback level often provides a synopsis of the

salient feedback characteristics within a system (e.g., Thomas and Kaufman 2005, Dambacher and

Ramos-Jiliberto 2007, Letellier et al. 2007).

Sensitivity analysis of the stream community's trophic relationships at the highest feedback

level indicates that the negative direct effect of rainbow trout on terrestrial invertebrates, $-a_{TR}$,

contributes only stabilizing negative feedback (Table 2.3). Inspecting Figure 2.5, it is seen that this direct effect participates in a single negative feedback cycle that corresponds to the predator-prey relationship between rainbow trout and terrestrial invertebrates. Within this same predator-prey relationship is the positive direct effect of terrestrial invertebrates on rainbow trout, a_{RT}. Unlike the above associated negative direct effect $-a_{TR}$, this positive direct effect has an ambiguous weighted sensitivity ($\mathbf{W}_{RT}^{F_5} = 0$). Again inspecting Figure 2.5, it is seen that this direct effect a_{RT} occurs not only in the predator-prey negative feedback cycle ($-a_{RT}a_{TR}$), but also in the positive feedback cycle ($a_{RT}a_{DR}$ a_{TD}); it therefore occurs in both positive and negative cycle products at the highest feedback level. Sensitivity weights similarly yield information on the other trophic relationships within the community.

The negative paths created by the modified interactions, $-a_{DR}$ and $-a_{BR}$, in contrast to the above trophic relationships, occur only in positive feedback cycles (Table 2.3). The analysis shows that the modifying effect of rainbow trout on Dolly Varden foraging, if strong enough, will preclude the stable coexistence of the stream community. The sensitivity analysis therefore supports the hypothesis of Baxter et al. (2004) that the rainbow trout may displace the Dolly Varden because of the modified foraging behavior.

The subsidy offered by emerging benthic invertebrates to riparian spiders exhibits no return feedback because spiders do not directly affect the density of benthic invertebrates. This subsidy a_{SB} does not appear in the highest feedback level ($\mathbf{W}_{SB}^{F_5} = \{\}$, the empty set), nor does this direct effect occur at any other feedback level. The sensitivity analysis confirms the perhaps intuitive expectation that the rate of subsidy from the stream community to riparian spiders does not affect the stability of the community as a whole.

2.5.4 Stability of shallow lake communities

Dramatic shifts between steady states in natural communities may result from structural instability. Positive feedback cycles, although not necessary for ecological communities constrained to the nonnegative domain, are generally thought to engender alternative stable states (Soule 2003). The shallow lake community tends to exhibit two alternative stable states: a vegetated clear state and an algal dominated turbid state. Scheffer et al. (2001) described a conceptual model for shallow lake communities under nutrient loading. This conceptual model is translated into a corresponding signed digraph (Figure 2.6).

We use sensitivity analysis to identify positive feedback cycles within shallow lake communities under nutrient loading. As in the above stream community example, we begin by using the highest feedback level F_6 as a guide for identifying these feedback cycles. Sensitivity analysis of this feedback level indicates that most direct effects participate in both positive and negative cycle products (Table 2.4). A majority of these paths occur in more positive cycle products than negative cycle products, suggesting that the community structure promotes instability.

A few of the non-trophic paths that incorporate vegetation occur only in positive feedback cycle products at the highest feedback level ($-a_{VP}$, $-a_{SV}$, $-a_{FV}$). Inspecting Figure 2.6, the non-trophic paths leading between vegetation and the other community variables appear to form triangles, or loops involving three variables, within the signed digraph. This observation suggests that important feedback properties may arise at the feedback level involving three variables.

A sensitivity analysis of feedback level F_3 confirms this suspicion (Table 2.4). Every non-trophic direct effect is present only in positive cycle products in F_3. The non-trophic interactions introduce only destabilizing feedback into the shallow-lake community at this feedback level. In contrast, every trophic relationship contains at least one direct effect that is present only in negative cycle products in F_3. The trophic interactions thus appear to have a stabilizing influence on the shallow lake community. The sensitivity analysis of feedback level F_3 indicates that the non-trophic

direct effects created by vegetation are the primary source of structural instability within the shallow lake community.

2. 6 Discussion

Sensitivity analysis of structural stability identifies the important direct effects that determine the stability of a community. The capability to scale direct effects along their relative importance provides theoretical insight into complex communities as well as a new tool for generating experimental hypotheses. It is now possible to see how and why a small number of direct effects may strongly influence stability. Identifying such key direct effects may help guide the formulation of research hypotheses, the prioritization of data-collection efforts for quantifying important interactions, and the development of alternative management strategies. This contribution is made possible by the development of an index, sensitivity weight, which considers the relative number of times a particular direct effect appears in all the feedback cycles involved in stability. To facilitate this analysis, we developed an algorithm based on a graph-theoretic approach. The approach presented here is based on community structure and is thus broadly applicable across systems that have either quantifiable or non-quantifiable direct effects, or have elements of both.

Applying sensitivity analysis to theoretical and empirical communities revealed the presence of key direct effects that determined the stability of their communities. For instance, some species or variables may have very important effects on community stability by forming key direct effects with other constituent variables, and these species or variables may deserve greater focus from research and management efforts. Sensitivity analysis can inform decision-making that targets specific species by identifying not only strong and weak stabilizing direct effects, but also those direct effects that contribute to destabilizing feedback within the community. Stability thus becomes more than a numeric index, as the sensitivity analysis shows how some community parts are more important than others for stability. Sensitivity analysis pinpoints the degree to which component species and variables have unequal contributions to the stability of their community.

The term "sensitivity", in the context of community matrix models, has been applied to the magnitude of the response of a community following an external perturbation (Cottingham and Schindler 2000) and to a change in equilibrium levels due to a press perturbation (Nakajima 1992). Sensitivity analyses have been discussed in the context of measuring the effect of small changes in the magnitudes of species interactions, that is, elements of the community matrix, on both overall return time (Carpenter et al. 1992; Neubert and Caswell 1997), on the rate of initial displacement from equilibrium after a pulse perturbation (Neubert and Caswell 1997), and on transient dynamics in populations (Caswell 2007). Sensitivity analyses have also been applied on probabilistic models of community composition (Tanner et al. 1994, Wootton 2001, Hill et al. 2004). Population-based sensitivity analysis, as shown by its widespread use and popularity (Caswell 2001), is one of the great recent developments in ecology. All the above studies, however, rely on quantified interaction terms. Our use of the term more closely matches that used by ecologists in population studies.

If the interactions among every community member could be accurately measured, then it would be a simple matter to calculate whether or not a community is stable and the degree to which it is resilient. Direct effects among community members are, unfortunately, difficult to measure (Bender et al. 1984). Quantifying direct effects in the field is expensive and time-consuming (Yodzis 1988, Schmitz 1997) and is not always possible (Bender et al. 1984, Wootton and Emmerson 2005). Even if all direct effects are observable, their exact specification is complicated by the measurement error and the natural variability that occurs in most community settings (Wooton and Emmerson 2005). Although quantification is and should be desired (Berlow et al. 2004), an unquestioning adherence to quantifying every direct effect may discourage the consideration of important aspects of the system. For instance, useful natural history information or variables that are known to be important, but are difficult to measure, may not be included in the analysis. Perhaps more dangerously, reasonable hypotheses may be discarded or not fully considered in an attempt to reduce a complex system into measurable components.

Community sensitivity assessments have been hamstrung because of the paucity of experimentally verified interaction strengths (Wootton and Emmerson 2005). In this study, we present

novel theory and approach to the sensitivity analysis of a community and its structural stability. Although this sensitivity analysis cannot provide a single quantitative number as in the above numerical studies, the approach does yield a depth of understanding that is difficult to ascertain in numerical black-box methods. In the examples above, we demonstrate instances where a particular direct effect may contribute both negative and positive feedback that affects overall community stability. The sensitivity analysis parses the feedback contribution made by each direct effect at different levels within the community, and so identifies how each direct effect promotes or diminishes the stability of its community.

The results of community sensitivity analysis suggest that the approach may provide insight for strategic management intervention. Understanding feedback properties provides an avenue for insight into the mechanisms that influence community stability. In the well-studied shallow lake example, vegetation was identified as the nexus of several positive feedback cycles. These feedback cycles were formed by non-trophic interactions, such as the refugia from foraging fish that vegetation provides for zooplankton. This finding agrees with empirical evidence suggesting that vegetation enhances itself through positive feedback mechanisms (Scheffer et al. 1993). Sensitivity analysis may similarly identify variables central to the dynamics of systems that are as yet not so well-understood.

Sensitivity analysis should provide information on how the system might respond to a change in the magnitude of a direct effect following management action. First, the sensitivity analysis suggests that strategic intervention may have unexpected consequences for community stability. Altering the magnitude of a direct effect through management action may have very different consequences for stability depending on how the direct effect influences feedback cycles. For instance, direct effects may have simultaneously stabilizing and destabilizing influences on the same community. Sensitivity analysis identifies these scenarios. Second, the sensitivity analysis can identify direct effects that primarily form destabilizing positive feedback. Increasing the magnitude of these direct effects may lead to (1) a destabilized steady state or (2) a shift to an alternative signed digraph, as might occur at a boundary equilibrium where one or more species goes extinct. The predictive power of sensitivity analysis for empirical systems deserves further investigation.

The feedback sensitivity analysis is based on a signed digraph representing the interactions within the community at steady state. This graphical approach, which is meant to complement traditional quantitative techniques, is useful for building complex models that cross discipline boundaries (e.g., Dambacher et al. 2007). The ease of examining alternative signed digraphs makes the approach particularly useful for generating and evaluating alternative hypotheses during model formulation (Hosack et al. 2008). Variables that are difficult to measure, but are known to be important components, may be included within the community model. As such, the signed digraph may help to build an inclusive model that improves our understanding of the important mechanisms that underlie the community, and thereby inform future modeling efforts and hypotheses.

The signed digraph represents a dynamical system of ordinary differential equations (ODEs) linearized at a steady state (May 1974). Any system that can be represented using ODEs that has a feasible steady state can also be represented with a signed digraph. The underlying ODEs, however, do contain more information. For instance, self-regulation in a signed digraph often corresponds to logistic growth, but it might also represent another ecological process (Levins 1998). In the above stream community example, there is a constant input of terrestrial invertebrates into the stream community that are consumed by fish. A simple ODE for terrestrial insects (*T*) with fish (*F*) predation and drift is $dT/dt = I - \alpha_{TF}TF - dT$, where *I* is the constant input, α_{TF} is the predation coefficient, and *d* is the rate of loss due to drift and export from the stream community. The growth equation linearized at steady state for terrestrial invertebrates is then $\partial dT/\partial Tdt \big|_{T=T^*, F=F^*} = -\alpha_{TF}F^* - d < 0$, where *T** and *F** corresponds to the terrestrial invertebrate and fish populations at steady state. In this example, negative self-regulation is placed on terrestrial invertebrates, not because of logistic growth, but because of predation and drift. Dambacher and Ramos-Jilliberto (2007) have recently demonstrated how functional responses, modified interactions, and other ODE modeling techniques may also be represented using signed digraphs; we apply their analysis in an example of modified interactions occurring between a native and a non-native species of fish.

Sensitivity analysis deepens our understanding of the mechanisms that determine community stability. Stability is arguably the most important mathematical concept—and the most debated—in community ecology, and it is closely linked to other important concepts in community ecology such as resilience and alternative stable states. The sensitivity analysis approach presented here is holistic and is capable of incorporating models that are informed by data or expert opinion, or constructed from existing knowledge of natural history. The ultimate goal is to increase our understanding of how species coexist and recover from perturbations, which is desirable as we attempt to predict the impacts of natural and anthropogenic change on ecological communities.

2. 7 Acknowledgements

Table 2.1. Sensitivity weights $\mathbf{W}_{ij}^{F_k}$ for the direct effects within each feedback level of the keystone predator model (Figure 2.3). The empty set {} indicates a lack of feedback. The symbol • indicates that the direct effect is absent from the community structure. The direct effects that correspond to the interspecific competition relationship are in bold, the predator-prey relationships are in italics, and the intraspecific competition relationships are in plain text.

$$\mathbf{W}_{ij}^{F_1} \qquad\qquad \mathbf{W}_{ij}^{F_2} \qquad\qquad \mathbf{W}_{ij}^{F_3}$$

	Sp1	*Sp2*	*Sp3*		*Sp1*	*Sp2*	*Sp3*		*Sp1*	*Sp2*	*Sp3*
Sp1	−1/1	{}	{}	*Sp1*	−1/1	**1/1**	*−1/1*	*Sp1*	−1/1	**1/1**	*0/2*
Sp2	{}	−1/1	{}	*Sp2*	**1/1**	−1/1	*−1/1*	*Sp2*	**1/1**	−1/1	*0/2*
Sp3	{}	{}	•	*Sp3*	*−1/1*	*−1/1*	•	*Sp3*	*0/2*	*0/2*	•

Table 2.2. Sensitivity weight $\mathbf{W}_{ij}^{\Delta_2}$ for each direct effect within the n–1st Hurwitz determinant of the competitive exclusion community modified with commensalism (Figure 2.4). The sensitivity weight of the commensal direct effect a_{32} is in bold.

$$\mathbf{W}_{ij}^{\Delta_2}$$

	Sp1	*Sp2*	*Sp3*
Sp1	1	1	0
Sp2	0	•	•
Sp3	1	**−1**	•

Table 2.3. Sensitivity weight $\mathbf{W}_{ij}^{F_5}$ for each direct effect within the highest feedback level F_5 of the stream community (Figure 2.5). The modified foraging of Dolly Varden by rainbow trout generates additional direct effects in the community structure; these are in bold. *R*, rainbow trout; *D*, Dooly Varden charr; *T*, terrestrial invertebrates; *B*, benthic invertebrates; *S*, spiders.

$$\mathbf{W}_{ij}^{F_5}$$

	R	D	T	B	S
R	−1.00	•	0.00	•	•
D	**1.00**	−1.00	−1.00	−0.33	•
T	−1.00	0.33	−1.00	•	•
B	**1.00**	−1.00	•	−0.50	•
S	•	•	•	•	−0.43

Table 2.4. Sensitivity weights $\mathbf{W}_{ij}^{F_k}$ for the direct effects within feedback levels F_3 and F_6 of the shallow lake community. Non-trophic direct effects are in boldface.

$$\mathbf{W}_{ij}^{F_3} \qquad\qquad \mathbf{W}_{ij}^{F_6}$$

	V	N	P	G	F	S		V	N	P	G	F	S
V	−1.00	−1.00	**1.00**	•	•	**1.00**	V	1.00	0.20	**1.00**	•	•	**0.64**
N	−0.60	−0.85	−1.00	•	•	•	N	0.00	0.27	0.25	•	•	•
P	•	−0.60	−0.85	−0.60	•	•	P	•	0.33	−0.25	0.50	•	•
G	**1.00**	•	−1.00	−0.85	−1.00	•	G	**0.00**	•	0.20	0.25	0.25	•
F	**1.00**	•	•	−1.00	−0.86	•	F	1.00	•	•	−0.11	0.09	•
S	**1.00**	•	•	•	**1.00**	−1.00	S	1.00	•	•	•	**0.33**	−0.14

$$\mathbf{A} = \begin{bmatrix} -a_{11} & -a_{12} & a_{13} \\ a_{21} & 0 & -a_{23} \\ 0 & a_{32} & 0 \end{bmatrix}$$

Figure 2.1. The signed digraph and its associated matrix **A** for a 3 trophic level system with nutrient recycling. The signed digraph describes the direct effects between a basal resource (species 1) with self-regulating logistic growth, a herbivore (species 2), and a predator (species 3) that in turn subsidizes the basal resource through nutrient recycling. Negative direct effects are shown by lines ending in a filled circle and positive direct effects are shown by lines ending in arrowheads. In trophic relationships, a consumer exerts a negative direct effect on its resource through consumption; assimilation of the resource produces a positive direct effect of the resource on the consumer. The subscripts of the a_{ij} are read as the magnitude of the direct effect of species j on species i.
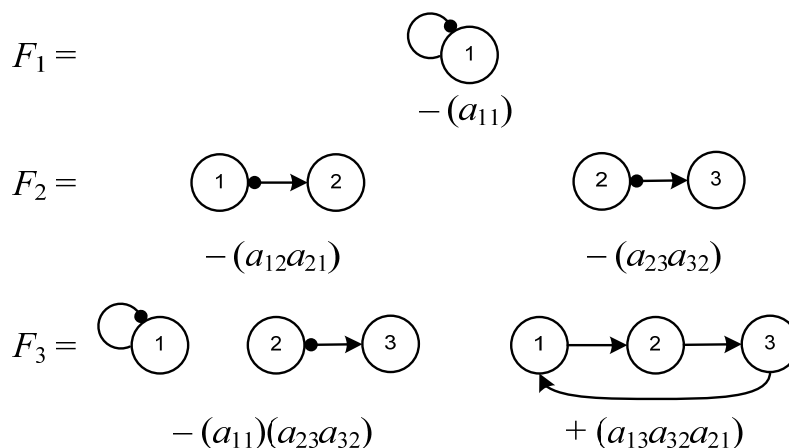
Figure 2.2. Feedback within the 3 trophic level model (Figure 1) for each feedback level F_k, $k = 1\ldots3$. The disjunct feedback cycles that form each cycle product are identified by parentheses.

$$F_1 = -(a_{11}) - (a_{22})$$

$$F_2 = -(a_{11})(a_{22}) - (a_{13}a_{31}) - (a_{23}a_{32})$$
$$+ (a_{12}a_{21})$$

$$F_3 = -(a_{11})(a_{23}a_{32}) - (a_{22})(a_{13}a_{31})$$
$$+ (a_{12}a_{23}a_{31}) + (a_{13}a_{32}a_{21})$$
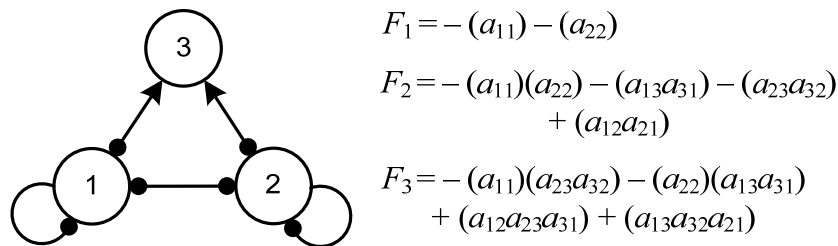
Figure 2.3. The signed digraph for the keystone predator model and its associated feedback levels. Variables 1 and 2 are self-regulated resources engaged in destabilizing interference competition. Variable 3 is a predator of both species 1 and 2. At feedback level F_1, self-regulation (intraspecific competition) forms two negative cycle products. Feedback level F_2 consists of three negative cycle products, formed by the two predation cycles plus the product of the two disjunct self-regulation cycles, and a single positive feedback cycle, formed by the interspecific competition. At feedback level F_3, the disjunct products of self-regulation cycles and predation cycles form two negative cycle products, whereas two positive cycle products are formed by the long feedback cycles that include all three variables.
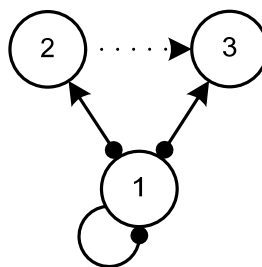
Figure 2.4. The modified competitive exclusion system with commensalism. Two consumers compete for a single resource. The resource contributes negative feedback at the lowest level through logistic growth ($-a_{11}$). The positive direct effect of the resource on each consumer taken together with the negative direct effect of each consumer on the resource creates two negative feedback cycles at the intermediate level ($-a_{12}a_{21}$, $-a_{13}a_{31}$). The addition of a commensal direct effect from species 2 to species 3 (a_{32}, dotted line) creates a single negative feedback cycle at the highest level ($-a_{13}a_{32}a_{21}$).
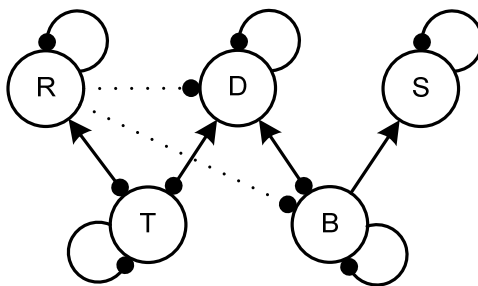
Figure 2.5. Stream community of fish and invertebrates in northern Japan. Rainbow trout (*R*) consume terrestrial invertebrates (*T*). Dolly Varden charr (*D*) consume terrestrial and benthic (*B*) invertebrates. Emergent benthic invertebrates subsidize riparian spiders (*S*). The dotted lines denote direct effects that arise from rainbow trout modifying the foraging behavior of Dolly Varden on terrestrial and benthic invertebrates (*sensu* Dambacher and Ramos-Jiliberto 2007).

Direct effect	Mechanism
$-a_{NP}, -a_{NV}$	Nutrient depletion by phytoplankton and vegetation
a_{PN}, a_{VN}	Nutrient uptake by phytoplankton and vegetation
$-a_{PG}, -a_{GF}$	Prey removal by consumers
a_{GP}, a_{FG}	Prey absorption by consumers
$-a_{VP}$	Phytoplankton shade vegetation
$-a_{VS}$	Suspended solids shade vegetation
$-a_{SV}$	Vegetation prevents sediment resuspension
$-a_{FV}$	Vegetation reduces foraging efficiency of fish on grazers
a_{GV}	Vegetation provides prey refugia for grazers from fish
a_{SF}	Fish resuspend sediments

Figure 2.6. The shallow lake community signed digraph representing the direct effects among nutrients (*N*), phytoplankton (*P*), vegetation (*V*), suspended sediments (*S*), grazers (*G*), and fish (*F*) as described by Scheffer et al. (2001). Self-regulation is assumed for all variables.

3 ASSESSING MODEL STRUCTURE UNCERTAINTY THROUGH AN ANALYSIS OF SYSTEM FEEDBACK AND BAYESIAN NETWORKS

Geoffrey R. Hosack[1], Keith R. Hayes[2] and Jeffrey M. Dambacher[2]

[1]Department of Fisheries and Wildlife, Oregon State University, 104 Nash Hall, Corvallis, OR 97331, USA
[2]CSIRO Marine and Atmospheric Research, GPO Box 1538, Hobart, Tasmania 7001, Australia

3.1 Abstract

Ecological predictions and management strategies are sensitive to variability in model parameters as well as uncertainty in model structure. Systematic analysis of the effect of alternative model structures, however, is often beyond the resources typically available to ecologists, ecological risk practitioners, and natural resource managers. Many of these practitioners are also using Bayesian Belief Networks based on expert opinion to fill gaps in empirical information. The practical application of this approach can be limited by the need to populate large conditional probability tables and the complexity associated with ecological feedback cycles. In this paper, we describe a modelling approach that helps solve these problems by embedding a qualitative analysis of sign directed graphs into the probabilistic framework of a Bayesian Belief Network. Our approach incorporates the effects of feedback on the model's response to a sustained change in one or more of its parameters, provides an efficient means to explore the effect of alternative model structures, mitigates the cognitive bias in expert opinion, and is amenable to stakeholder input. We demonstrate our approach by examining two published case studies: a host-parasitoid community centered on a non-native, agricultural pest of citrus cultivars and the response of an experimental lake mesocosm to nutrient input. Observations drawn from these case studies are used to diagnose alternative model structures and to predict the system's response following management intervention.

3.2 Keywords

Bayesian Belief Network, risk assessment, feedback, expert opinion, model uncertainty, signed directed graphs

3.3 Introduction

Ecologists, natural resource managers, and practitioners of ecological risk assessment operate in complex and often poorly understood settings. Each is forced to design experiments, make predictions or assess decisions without completely understanding the underlying processes, structure, and dynamics of complex ecosystems (Francis and Shotton 1997, Ruckelshaus et al. 2002, Fairbrother and Turnley 2005). The predictive, numeric, process-based models that each employs typically address parametric uncertainty using Monte Carlo simulations (Metropolis and Ulam 1949). However, process-based models of ecological systems inevitably have many possible alternative structures. A systematic analysis of the effects of different model structures is often not practicable with the limited resources available for any single study (Hoffman and Hammonds 1994, Reckhow 1994, Ferson 1996), despite the fact that ecological predictions and management strategies may be more sensitive to the structural uncertainty of a model than parametric uncertainty (Punt and Hilborn 1997, Varis and Kuikka 1999, Dambacher et al. 2002).

Besides the problem of choosing an appropriate model structure, practitioners of ecological risk assessment and natural resource managers, when faced with insufficient quantitative knowledge to adequately capture parametric uncertainty, typically eschew quantitative analysis methods in favor of methods based on expert opinion (see Burgman 2005, p. 381; OGTR 2005, p. 25). A popular way to fill gaps in empirical information is to incorporate expert opinion into a Bayesian Belief Network, or BBN, (Varis and Kuikka 1999, Marcot et al. 2001, Borusk et al. 2004, Pollino et al. 2007). Without empirical data, however, experts must, in what is typically a laborious and time-consuming process, specify the relevant conditional probabilities in the BBN (Ticehurst et al. 2007). Furthermore, expert opinion can be subject to cognitive bias unless carefully elicited (Morgan and Henrion 1990, Burgman 2005), and might be further confounded by linguistic uncertainty (Regan et al. 2002). Another difficulty is that including feedbacks via cyclic network structures requires dynamic time-explicit BBNs that depend on extensive parameterization (Burger and Gochfeld 1997, Ong et al. 2002, Borusk

et al. 2004, Dojer et al. 2006). Hence, BBNs based on expert opinion do not usually include ecological feedbacks in their network structure (e.g., Marcot et al. 2001, Stiber et al. 2004).

Here we present a method that addresses the problems highlighted above by merging BBNs with another form of graphical model used in ecology - signed directed graphs (Levins 1974, Dambacher 2002, 2003b). This new method incorporates ecological feedback and facilitates comparison of alternative model structures and thereby provides a practical way to explore the effects of model structure uncertainty in complex ecosystems. This method is designed to assist ecologists, risk practitioners and natural resources managers in predicting how ecosystems might respond to a disturbance, in exploring the dynamics of alternative model structures, in performing model diagnosis, and in optimizing the allocation of resources for monitoring programs. It also eliminates the need for experts to estimate complex conditional probabilities, thereby reducing opportunities for the introduction of cognitive bias into the BBN.

3.3 Materials and Methods

3.3.1 Analyzing the Effect of Press Perturbations

Bayesian Belief Networks allow the probabilistic representation of a system based on multiple sources of knowledge. The conditional relationships between a system's variables (nodes) are visually depicted using directed acyclic graphs (Pearl 2000). By definition, a directed acyclic graph lacks feedback; that is, a path traced along its links cannot pass through a variable more than once. Signed directed graphs (SDGs), however, can incorporate feedback cycles, provide predictions of increase (+), decrease (-), or no change (0) for specified variables, and can quickly evaluate the consequences of alternative model structures (Levins 1974, Dambacher 2002).

Just as the DAG graphically describes the probabilistic relationships within a Bayes network, the SDG describes an underlying deterministic, mathematical model. The model underlying a SDG describes the dynamics of n number of variables X_i in a system of differential equations

$$\frac{dX_i}{dt} = f_i\left(X_1,\ldots X_n; p_1 \ldots p_k\right); \ i=1\ldots n, k=1\ldots m,$$ (3.1)

where m number of parameters p_k control the rates of increase or decrease. The Jacobian matrix **A** is composed of the first partial derivatives of the growth functions f_i taken with respect to the variables and evaluated at equilibrium, such that

$$a_{ij} = \left.\frac{\partial f_i}{\partial X_j}\right|_*,$$ (3.2)

where * denotes evaluation at equilibrium (May 1974).

Both the SDG and the matrix **A** represent the qualitative relationship between variables in a model ecosystem (Levins 1974). A three-variable SDG model (Fig. 3.1) translated into matrix form is

$$\mathbf{A} = \begin{bmatrix} -a_{1,1} & -a_{1,2} & -a_{1,3} \\ a_{2,1} & -a_{2,2} & -a_{2,3} \\ a_{3,1} & a_{3,2} & -a_{3,3} \end{bmatrix},$$

where the matrix entry in the ith row and the jth column shows the magnitude (a_{ij}), and the sign (+, -) of the direct effect of species j on species i. The rows are the receiving variables and the columns are the source variables of the direct effects shown in Fig. 3.1. For example, the direct effect of X_3 on X_2 is negative and is represented by $-a_{2,3}$ since the predator imparts mortality to its prey.

A sustained change to a parameter, referred to here as a "press perturbation" (Bender et al. 1984) will shift the system to a new equilibrium. The average values of the system's variables at this new equilibrium point (which variously may have increased, decreased, or remained unchanged) can be estimated by inverting the negative of the matrix **A** in the equation

$$\frac{\partial \mathbf{X}^*}{\partial p_k} = -\mathbf{A}^{-1}\frac{\partial \mathbf{f}}{\partial p_k},$$ (3.3)

where ∂p_k is the parameter shift in the press perturbation, and **f** is the vector of growth functions for the system of Eq. (3.1). The inverse matrix $-\mathbf{A}^{-1}$ accounts for both direct and indirect effects resulting from the press perturbation, and is equivalent to the classical adjoint of $-\mathbf{A}$ divided by its determinant

$$-\mathbf{A}^{-1} = \frac{\text{adj}(-\mathbf{A})}{\det(-\mathbf{A})} .$$ (3.4)

Because det($-\mathbf{A}$) is a common denominator for all entries within the adjoint matrix, the long-term direction of change in the levels of the variables X_i following a press perturbation on parameter p_k can be determined by examining elements of the adjoint matrix (Dambacher et al. 2002, 2005). The entries of adj($-\mathbf{A}$), are feedback cycles (addends) that are the direct and indirect effects which govern the response of each variable to a press perturbation (Dambacher et al. 2002, 2003a).

3.3.2 Analyzing the Qualitative Effect of Feedback

The elements of a quantitatively specified Jacobian matrix (denoted $^{\#}\mathbf{A}$) contain numerical

entries, such as $^{\#}\mathbf{A} = \begin{bmatrix} -0.9 & -0.8 & -0.7 \\ 0.6 & -.5 & -0.4 \\ 0.3 & 0.2 & -.1 \end{bmatrix}$. Note, however, that n^2 experiments are needed to

empirically estimate the magnitude of all entries within $\mathbf{A}$ (Bender et al. 1984), an arduous task for even a moderately complex system. This clearly limits the applicability of quantitative approaches (Levins 1998). Further, the predictions of numeric matrices can be overly sensitive to the exact values of the matrix entries (Yodzis 1988). For instance, if the magnitude of $^{\#}a_{1,2}$ in the above system was increased by just ten percent to –0.88, then the prediction given by $-^{\#}\mathbf{A}_{1,3}^{-1}$ would shift from a negative to a positive value. Here, we instead focus on a qualitative specification of $\mathbf{A}$, and define the matrix $^{\circ}\mathbf{A}$ with entries that are either +1, –1, or 0, depending on whether a variable acts to increase, decrease, or exert no direct influence on the growth rate of another variable (the matrix $^{\circ}\mathbf{A}$ can be formally defined as a transposed signed adjacency matrix).

The sign of an entry within adj($-^{\circ}\mathbf{A}$) gives the net number of feedback cycles that contribute to a variable's response. It provides a prediction of whether the equilibrium values of a variable will increase, decrease, or remain unchanged following a press perturbation (Dambacher et al. 2002). If the feedback cycles in an adjoint matrix entry are all of the same sign, then the prediction is completely determined. But the prediction sign will be ambiguous if both positive and negative feedback cycles

are present. To measure the degree to which there are feedback cycles with countervailing sign, we

consider the ratio of the net to the total number of feedback cycles in an adjoint matrix entry. The total

number of cycles is calculated by use of an adjacency matrix $^\bullet\mathbf{A}$, with entries of +1 corresponding to

each nonzero entry in the matrix $^\circ\mathbf{A}$. A matrix of absolute feedback $\mathbf{T}$ is calculated by use of the

matrix permanent (Minc 1978) in each matrix minor of $^\bullet\mathbf{A}$, where $\mathbf{T} = \text{permanent}(\text{minor}(^\bullet\mathbf{A})_{ij})^{\text{Transpose}}$.

The prediction weights associated with elements of the adjoint matrix are given by $\mathbf{W} = \dfrac{\left|\overrightarrow{\text{adj}\left(-^\circ\mathbf{A}\right)}\right|}{\mathbf{T}}$,

where the arrow superscript is a vectorized matrix operator denoting element-by-element division and

"$|\ |$" denotes absolute value—see Dambacher et al. (2002) for a detailed discussion of these matrix

operations.

Elements of $\mathbf{W}$ range from 0 to 1. A value of zero indicates an equal number of both positive

and negative cycles. As prediction weights approach 1 then relatively more cycles are of the same

sign, and elements with a weight of exactly 1 have cycles that are all of the same sign. When there are

no feedback cycles in a response, such that $\mathbf{T}_{ij}$ equals zero, then the variable is predicted to remain

unchanged following a press perturbation. In this circumstance the sign of $\text{adj}(-^\circ\mathbf{A})_{ij}$ will be zero and

the associated prediction weight is set equal to 1.

3.3.3 Verifying sign determinacy

Dambacher et al. (2003a) tested the sign determinacy of elements within $\text{adj}(-^\circ\mathbf{A})$ by

randomly allocating values to a_{ij} from a uniform distribution, and comparing the qualitative

predictions from the adjoint matrix with responses calculated from the inverse of quantitatively

specified matrices. The sign determinacy of responses (i.e., the proportion of quantitative response

signs that have the same sign as the qualitative prediction) with prediction weights ≥ 0.5 was shown to

generally exceed >90%; below this threshold the sign determinacy of responses declined to 50% for

weighted predictions that approached zero. While these tests of sign determinacy were based on a

uniform distribution of random interaction strengths, recent studies emphasize the importance of

considering skewed distributions in simulations applied to model ecosystems (Berlow et al. 2004, Emmerson and Yearsley 2004, Wootton and Emmerson 2005).

We evaluated the effect of strong and weak interactions on the sign determinacy of adj($-$ $^{\circ}\textbf{A}$)$_{ij}$, for the models tested by Dambacher et al. (2003a), by randomly allocating values to a_{ij} from four different distributions with markedly different types of skew. We also introduced "trophic dependence" by forcing ecologically realistic trophic transfer efficiencies into each simulation. Trophic relationships occur when a variable X_2 consumes another and thus has a negative direct effect, $-a_{1,2}$, on the prey X_1. The prey X_1 provides a positive direct effect $a_{2,1}$ on the predator. However, $|a_{2,1}|$ $< |-a_{1,2}|$ because of energetic costs resulting from the metabolization of ingested matter and the typically pyramidal distribution of predator and prey population abundances. We use the notation $^{\#}\textbf{A}$ to denote a simulated matrix with numeric entries. Dependence between $^{\#}a_{1,2}$ and $^{\#}a_{2,1}$ is invoked by first drawing the magnitude of the direct effect of predator on prey, $|^{\#}a_{1,2}|$, from its respective distribution (Fig. 3.3a). This value of $|^{\#}a_{1,2}|$ is then multiplied by a random variable with a Uniform (0, 0.01) distribution that reflects the constraints on density and energy transfer to produce the magnitude of $^{\#}a_{2,1}$. The 0.01 upper limit reflects the assumption that the equilibrium biomass between the prey and its consumer differ tenfold, and the assumption that maximum ecological efficiency is 10%. Other forms of trophic dependence with different upper limits gave qualitatively similar results (see Appendix C for details).

We used Monte Carlo simulations to create 500 stable numeric matrices (May 1974, Dambacher et al. 2003a), where stability was determined by the real parts of all eigenvalues of $^{\#}\textbf{A}$ being negative. We assume that the simulated matrices represent generalized Lotka–Volterra systems with non-zero equilibriums for all species. Separate simulations were done for each model structure under each combination of parameter shape and dependence assumptions.

We examined the proportion of simulations with the "correct" sign, i.e., $\text{sgn}(\text{adj}(-^{\circ}\textbf{A})_{ij}) = \text{sgn}(\text{adj}(-^{\#}\textbf{A})_{ij})$, for all elements of adjoint matrices combined across all 18 model systems. We used a least squares fit to the nonlinear function

$$\Pr\left[\mathrm{sgn}\left(\mathrm{adj}\left(-^{\circ}\mathbf{A}\right)_{ij}\right) = \mathrm{sgn}\left(\mathrm{adj}\left(-^{\#}\mathbf{A}\right)_{ij}\right)\right] = \frac{\exp\left(\beta_W \mathbf{W}_{ij} + \beta_{WT} \mathbf{W}_{ij}\mathbf{T}_{ij}\right)}{1 + \exp\left(\beta_W \mathbf{W}_{ij} + \beta_{WT} \mathbf{W}_{ij}\mathbf{T}_{ij}\right)}. \tag{3.5}$$

Eq. 3.5 is a logistic-type function that incorporates the influence of prediction weights and absolute

feedback on the expected proportion of correct sign. The logistic form allows a flexible curve to be fit

to the simulation results with *a priori* bounds between 0.5 and an upper asymptote of 1.0. The

parameter β_W incorporates the direct effect of the prediction weights, and β_{WT} the interaction between

prediction weights and total feedback. The intercept at $\mathbf{W}_{ij} = 0$ is fixed at a value of 0.5 to impose an

equal chance of the response being either positive or negative when it is composed of an equal

number of positive and negative feedback cycles contributing to a response. Note that a variety of

different functions could be used to translate the simulation results into the probabilities of having the

correct sign (e.g., see Appendix C for a 95% lower bound on the proportions of correct sign).

3.3.4 Translating Model Predictions into Conditional Probabilities

The transition from SDGs to BBNs is completed by translating the prediction weights

associated with each element of adj($-^{\circ}\mathbf{A}$) into a probability that is then incorporated into the

conditional probability tables of a BBN. A choice needs to be made about how the BBN will be

implemented and we suggest two possible conventions. The first preserves the three categories of

response predicted by the SDG. That is, in addition to the binary response fit by Eq. (3.5) for

predictions with feedback, there may also be predictions of no change due to a lack of feedback (see

Materials and Methods - *Analyzing the Qualitative Effect of Feedback*). In this approach the binary

response of Eq. 3.5 is translated to the three-category BBN via the linear relationship

$$\Pr\left(\mathrm{sgn}(\mathrm{adj}(-^{\circ}\mathbf{A})_{ij}\right) = \frac{4g\left(\mathbf{W}_{ij}, \mathbf{T}_{ij}\right) - 1}{3}, \tag{3.6}$$

where $g(\mathbf{W}_{ij}, \mathbf{T}_{ij})$ is the function given by Eq. 3.5. The remaining probability $1 - \Pr\left(\mathrm{sgn}(\mathrm{adj}(-^{\circ}\mathbf{A})_{ij}\right)$

must then be divided in some proportion between the two other categories at the analyst's discretion.

In the examples presented here the remaining probability is simply apportioned equally. For instance,

if adj($-^{\circ}\mathbf{A})_{ij}$ is negative, then Pr(*Decrease*) is substituted into the left-hand side of Eq. 3.6, and the

remaining probability 1 – Pr(*Decrease*) is equally apportioned to the categories of increase and no observable (obs.) change. If, however, $\mathbf{W}_{ij} = 0$ and $\mathbf{T}_{ij} > 0$, the SDG is uninformative and Eq. 3.6 assigns probability equally among the three categories.

The second convention allows the assignment of nonzero observation likelihoods only to the categories of increase or decrease, and Eq. 3.5 is applied without the linear transformation in Eq. 3.6 to give probabilities of increase and decrease. If $\mathbf{W}_{ij} = 0$ and $\mathbf{T}_{ij} > 0$, Eq. 3.5 automatically allocates equal probability to increase and decrease. The implications of these two conventions are discussed further in the Discussion.

3.3.5 From Signed Directed Graphs to Bayesian Belief Networks

Here we embed the consequences of cyclical SDGs into the conditional probabilities of an acyclic BBN (Fig. 3.2). Each variable in the SDG has a corresponding observation-prediction node that denotes a set of conditional probabilities (a conditional probability table; CPT) in the BBN. For a given SDG, Eq. (3.5) and Eq. (3.6) are used to estimate the probability of predicted response for all possible inputs (press perturbations) to the SDG. The CPTs within the observation-prediction nodes record the probability of observing an increase, decrease, or no apparent response conditional on: 1) *l* input nodes that have probabilities of positive input, negative input, or no input where *l* is the number of variables in the SDG that are subject to a press perturbation; and, 2) a structure node that represents all alternative model structures (SDGs) that describe the system. We define the probability of a model being "true" as the degree to which it is consistent with observations relative to the other alternative models. It is always possible, however, that none of the SDGs accurately depict the sign response of the system in question. A "null model" is therefore introduced as a benchmark to judge the performance of the SDGs. The null model allocates equal probabilities of observing an increase, decrease, or no response across every possible prediction given a press perturbation, and is structurally equivalent to a fully connected matrix (i.e., a matrix of size *n* filled with +1's). For details on the process of constructing BBNs from conditional probabilities see, for example, Cain (2001).

3.4. Results

3.4.1 Verifying sign determinacy

Our results showed that prediction weights are informative when strong and weak interactions, and ecologically realistic trophic transfer efficiencies (i.e., trophic dependence) are introduced into the simulations. Sign determinacy was strongly related to prediction weights ($\mathbf{W}_{ij}$) for all parameter distribution shapes and forms of dependence tested (Fig. 3.3). Moreover, sign determinacy of adj($-^{o}\mathbf{A}$)$_{ij}$ for a given prediction weight was found to increase as a function of the absolute number of feedback cycles ($\mathbf{T}_{ij}$). The parameters β_W and β_{WT} were highly significant for all fits (Table C.1).

Introducing trophic dependence among the elements of $\mathbf{A}$ had a much greater effect on sign determinacy than did the skewness of the distribution of interaction strengths. The relative frequency of strong and weak links, described by the different distribution types, was relatively unimportant and had only a minor effect on the fitted values of β_W and β_{WT}. Conversely, trophic dependence between the elements of matrix $\mathbf{A}$ introduced a non-random pattern of weak interaction strengths that diminished the proportion of correct qualitative predictions (Fig. 3.3c), and increased the standard error of β_W and β_{WT} (Table C.1). Even with this increased scatter, however, the parameters of Eq. 3.5 remained significant, and therefore informative, under all the scenarios examined in our simulations. In the succeeding examples, we employ the fit of Eq. 3.5 with trophic dependency and uniformly distributed magnitudes of interactions (Fig. 3.3c, top) to generate the conditional probability tables for the example BBNs. In Appendix C, we provide a more conservative alternative to Eq. 3.5 for calculating proportion of correct sign, and apply a 95% bound to the points in Fig. 3.3c.

3.4.2 Example Applications

The red scale *Aonidiella aurantii* is a common non-native insect pest of orange, grapefruit, and lemon crops in California. The red scale is parasitized by two non-native wasps *Encarsia perniciosi* and *Aphytis melinus*. A SDG of this host-parasitoid community is identical to the model introduced in Fig. 3.1. Rather than explicitly including the three species of scale insect and wasps, we identify three variables describing different states of parasitization among the red scale host: unparasitized hosts (X_1), hosts parasitized by *E. perniciosi* (X_2), and hosts parasitized by *A. melinus* (X_3). Unparasitized hosts are transferred into a parasitized state following an attack by either *E. perniciosi* or *A. melinus*. These parasitoids are assumed to attack scale hosts at a rate proportional to the number of scale hosts already parasitized; this produces a predator-prey type relationship of parasitized hosts on their "prey", the unparasitized hosts. In another predator-prey type relationship, attacks by *A. melinus* on scale hosts already parasitized by *E. perniciosi* are assumed to transfer these hosts into a state of parasitization by *A. melinus* (Borer et al. 2003, 2004). All three variables exhibit intraspecific density-dependent growth; for unparasitized hosts it is via intra-specific competition for the basal citrus resource (Borer et al. 2003); for hosts parasitized by *A. melinus* and *E. perniciosi*, it is via intraspecific reattack on previously parasitized hosts (Murdoch et al. 2005). The underlying system of equations for this host-parasitoid community model and instructions for constructing the associated BBN are given in the

Supplement. We use a BBN to test whether the host-parasitoid community (H-PC) model is consistent with the observational results of Borer et al. (2003). The corresponding BBN has three observation-prediction nodes, an input node, and a model structure model node (Fig. 3.4). The performance of the H-PC model is judged against the null model.

We begin by allocating equal prior probabilities to the H-PC model and the null model within the model structure node. Setting the probability of a positive press perturbation, or input, to the scale pest X_1 equal to 1.0 represents an unequivocal increase in the reproductive rate of unparasitized scale pests (Fig. 3.4a). In practice this could correspond to regional increase in red scale

reproduction across grapefruit, orange, and lemon crops (Borer et al. 2003). If the number of red scale hosts that are parasitized by *A. melinus* (X_3) was observed to increase, then the H-PC model becomes more likely than the null model, i.e., Pr(H-PC model is True) = 0.74. Given this updated information, the BBN now predicts that unparasitized hosts have an 80% chance of increase whereas before it was 65% (Fig. 3.4b). Since the H-PC model has been supported, it has contributed more to this subsequent prediction than the null model, and the probability of increase for the density of unparasitized hosts has also risen. If, as in the field observations of Borer et al. (2003), the density of unparasitized hosts was also observed to increase, then the estimated probability that the H-PC model is true increases to 0.89 (Fig. 3.4c). Note how the density of red scale parasitized by *E. perniciosi* remains ambiguous (equal probability of observing increase, decrease or no change) and is therefore uninformative.

A researcher, with limited resources, who wishes to test the H-PC model by experimentally increasing red scale reproduction, might ask "What variable should be measured to falsify the H-PC model?" For instance, it may be least costly to measure the density of red scale hosts parasitized by *A. melinus* wasps that develop outside the host (Luck and Podoler 1985), rather than *E. perniciosi* wasps that develop inside the host (Yu et al. 1990). A sensitivity analysis shows how the probabilities of one node are affected by changes made to other nodes; that is, the analysis shows whether or not one node is sensitive to another. A sensitivity analysis on the top node "Alternative Models" within the BBN (Table 3.1) suggests that the researcher should measure the density of scale hosts parasitized by *A. melinus* and the density of unparasitized scale hosts. These nodes best discriminate between the hypothesized H-PC model and the null model because they are the most informative: the probabilities of the alternative models are most sensitive to observations made on these variables. Within the context of our qualitative analysis, the researcher would be ill-advised to measure the density of hosts parasitized by *E. perniciosi*, because this variable is uninformative, as both the H-PC and the null model provide equal probabilities of observing an increase, decrease, or no response.

3.4.3 Analyzing the effect of alternative model structures

The previous example compared a single model structure with a null model. Where there are alternative models to be considered with the same number of variables, then it is a straightforward matter to incorporate multiple alternative models in the structure node of the BBN. Here we explore a slightly more complicated BBN structure that allows comparison of SDG models having a different number of variables, and thus a different number of observation-prediction nodes in the BBN. Hulot et al. (2000) explored the ability of alternative SDGs to explain the response of experimental lake mesocosms to nutrient input. Their experimental mesocosms consisted of nutrients (phosphorus) and three trophic levels: autotrophs, herbivores, and carnivores. They used SDGs to analyze two alternative four-variable food chain models (with assumptions of either prey- or ratio-dependence) and an eight-variable model based on functional groups (Fig. 3.5).

We recast the mesocosm lake experiment into an example BBN, and show how it can synthesize empirical data into a common framework facilitating model diagnosis and prediction, as well as suggest management options. We consider a nutrient input into the experimental mesocosm BBN (Fig. 3.6). First, we use the BBN to predict how variables might respond to the experimental nutrient input if the prey dependent model or the functional group model are true (Fig. 3.6a). Second, we use the BBN to determine which model structure may be best supported by the observations (Fig. 3.6b). As a starting point, the alternative model structures and the null models are assigned equal prior probability within their respective model structure nodes, and an experimental input to phosphorus is assumed.

To incorporate empirical observations, we use the statistical results of Hulot et al. (2000) to assign the likelihood of having observed an increase, decrease and no response in the levels of the variables. These observation likelihoods may reflect our belief of the applicability of the statistical tests, the power of the tests, interpretation of classical hypothesis testing, and so forth. For purposes of this example, we allocate 100% likelihood that there was an observed increase (decrease) in a variable if the statistical result was classified by Hulot et al. (2000) as significant, and the variable was

observed to increase (decrease) in the nutrient-enriched treatment versus the control. If the statistical test was categorized as nonsignificant, then the variable is assumed to have a 100% likelihood of remaining unchanged. While there are a number of ways to assign these likelihoods, our purpose here is simply to demonstrate how observational data can be incorporated into a BBN to yield information on hypothesized model structures.

Sensitivity analysis (Table 3.2) of the food chain models reveals that, given an unequivocal increase in phosphorus due to an experimental manipulation, monitoring the levels of phosphorus and herbivores would best discriminate between the prey-dependence model, ratio-dependence model, and the null model. Entering into the BBN the observed significant increase in phosphorus and the nonsignificant effect of nutrient enrichment on herbivores updates the probability of the null model being true to about 85%; the alternative models of prey and ratio dependence have a 0% and 15% chance of being true. Including the additional observation of no significant change in algae elevates the estimated probability of the null model being true to 99% (Fig. 3.6b). Clearly, neither linear food chain model finds much support within the experimental lake mesocosm data observed by Hulot et al. (2000).

Conducting a sensitivity analysis on the functional group model node (Fig. 3.6), again with an unequivocal increase in phosphorus, suggests that observations on phosphorus (P), large herbivores (H_2), and periphyton (A_P) would best discriminate between the null model and the functional group model (Table 3.2). Hulot et al. (2000) observed a significant increase in these three variables. Entering these findings into the respective nodes of the BBN gives an estimated probability of about 0.96 that the functional group model is true. The sensitivity analysis also suggests that fish (C_2) and small herbivores (H_1) would not distinguish between alternative model structures. In fact, the response of fish and small herbivores is invariant to the alternative model structures, and observations of these nodes would not improve model diagnosis.

Given these observations the BBN now predicts a 50% chance for a decrease in edible algae (A_1), a 56% chance for a decrease in invertebrate carnivores (C_1), and a 47% chance for an increase in protected algae (A_2). In the lake mesocosms, the observed effect of nutrient enrichment on these three

variables was nonsignificant (Hulot et al. 2000). Entering these remaining observations drops the probability that the functional group model is true to 0.90 (Fig. 3.6b). Although this functional group model is not perfect and, as Hulot et al. (2000) state, there are other conceivable alternative model structures possible, nevertheless, the functional group model appears more consistent with the data compared to either of the food chain models or the null model.

3.5 Discussion

Ecologists and natural resource managers often represent impacts to ecological systems as a linear sequence of cause and effect relationships using methods such as fault and event trees (Hayes 2002), path analysis (Shipley 2000), and non-dynamic belief networks (Marcot et al. 2001, Borusk et al. 2004, Pollino et al. 2007). These approaches, however, do not explicitly account for complex dynamics driven by feedbacks in ecological systems. Feedback cycles can create counterintuitive results that confound predictions and effective management interventions. The modeling framework presented here addresses this problem by embedding the feedback properties of signed directed graphs into the conditional probability tables of a Bayesian Belief Network.

The basic structure of the BBNs used here is relatively simple, yet reflects the essential features of the qualitative dynamics of complex systems in a probabilistic framework. The SDG has a probabilistic interpretation within a BBN that addresses three basic questions: 1) *Prediction*—what are the probabilities that equilibrium levels will change given a sustained change to a parameter that affects the dynamics of the system? These probabilities are conditional upon a) the likelihoods of observing an increase, decrease, or no change in the level of the system's variables, b) likelihood of an input to one or more of the system's variables; and, c) prior belief in model structure. 2) *Diagnosis*—which alternative model structure provides predictions that best match the field observations? A model will increase in probability of being true when its predictions are consistent with observations, whereas inconsistent models will decrease in probability. Alternative models are diagnosed based on their probabilities relative to each other and to the null model. (3) *Sensitivity*—

which nodes are most sensitive to press perturbations on other nodes? Sensitivity analyses deduce the influence of one node on another (e.g., Marcot et al. 2001). This technique is especially useful in deciding which variables to measure or observe in order to distinguish between competing alternative models, and is readily available for use in BBN software packages (e.g., Norsys 2006).

Incorporating the cyclic behavior of feedback systems within the acyclic framework of a BBN provides a novel way to address uncertainty in the structure of ecological models, and to validate qualitative model predictions with field observations. More importantly, this approach provides an explicit means to record and compare the assumptions that underpin the model and uncertainty in its structure. One of the advantages of this framework is that it eliminates many of the problems associated with traditional BBNs. The conditional probability tables that underlie a BBN must usually be pre-specified by experts, who are set the task of allocating probabilities to an event occurring over an array of varying conditions (Borusk et al. 2004, Ticehurst et al. 2007). For complex BBNs, these tables can be difficult and time consuming to complete. Our approach constructs the conditional probability tables at a key-stroke and thereby encourages ecologists and managers to explore a fuller range of alternative model structures and impact scenarios.

The use of the SDG allows continuous time models to inform BBN parameterization. We have used simulations to test the robustness of SDG predictions for an array of network structures to establish a general rule, and provide an alternative to direct parameterization of conditional probabilities by expert opinion (Marcot et al. 2001) or empirical data (Pollino et al. 2007). However, if a particular community structure is of concern, then simulations generated from that model could be used to inform conditional probabilities directly. Implicit is the assumption that dynamics return to approximately steady-state between observations. Otherwise, a time-explicit dynamic Bayes network would be required to estimate transient behavior between successive observations. Once the conditional probability tables and the BBN are created, the modularity of BBNs (Mortera et al. 2003, Borusk et al. 2004) allows interconnection with other models developed outside the system described by the SDG. For instance, the lake mesocosm BBN described in the results may be combined into a

larger BBN that addresses management options, water quality monitoring programs, and risk pathway analyses.

Our simulation studies allowed us to translate the prediction weights of the SDG into conditional probabilities, and they are based upon the distributions of the interaction strengths and also the structure of the 18 models used in our simulations. Application of these probabilities within the BBN contains an important challenge and a choice among alternative conventions. The challenge is associated with the dependency both in ecological interactions and in feedback cycles. The convention is associated with the two-sign state versus three-sign state versions of a BBN, with the latter requiring one to choose how to allocate prior probability in the conditional probability tables.

We recognize two forms of dependence that will affect the conditional probabilities derived from the qualitative predictions of the SDG: dependence between pairwise interaction terms (i.e., including but not limited to trophic dependence) and the dependence created between different elements of the adjoint matrix that have feedback cycles with common combinations of terms (feedback dependence). We discovered that trophic dependence had a greater effect on sign determinacy than the distribution of interaction strengths, but did not seriously undermine the significance and utility of the prediction weights. Feedback dependence is important because it affects the likelihood of multiple observations following an input to the system. In our approach these are treated as independent entities in our BBN structure, but the effect of feedback dependence on the qualitative predictions and diagnosis of alternative model structures, given multiple observations, is in theory available in the SDG and is an avenue for future research.

The practical implications of the convention regarding a two- or three-sign state BBN depends on: a) how observation likelihoods are subsequently entered into the BBN; and, b) how the prior probabilities are allocated in the three state case. In both conventions, the focus during model diagnosis is on the relative probabilities of alternative models. We have not fully explored the implications of different prior probability assignations and different observational likelihoods for the two conventions. We note that the two conventions produce identical ranks in model diagnosis if prior probability is allocated equally between the two cases not predicted by the SDG (for the three-sign

case), and 100% observational likelihood is apportioned to any single sign prediction. This will not be true, however, if one of the models being compared produces an unambiguous prediction of a zero response, and the other does not. This is because the three state case can discriminate between uninformative prediction weights (i.e., $\mathbf{W}_{ij} = 0$ and $\mathbf{T}_{ij} > 0$) and unambiguous predictions of no response (i.e., $\mathbf{W}_{ij} = 1$ and $\mathbf{T}_{ij} = 0$), whereas the two state convention disallows both ambiguous and unambiguous predictions of no response. It is therefore misleading to compare the rank order diagnosis between the two conventions in this situation.

The decision to use the two- or three-state convention depends on the particular application. Under certain circumstances it may be desirable to disallow predictions of zero response, for example, when there is a zero probability of precisely measuring two identical sample means from a continuous probability distribution. It is also easier in the two state case to assign non-zero observation likelihood across the two categories of increase and decrease. In the three-sign state examples provided here, we have avoided assigning non-zero observation likelihood to more than one category because the effects of such an approach on the rank ordering of alternative models are confounded with the potentially arbitrary prior probability allocations that are necessitated by the three state case. Thus, in applying the three state case as developed in this work, we recommend that the observation likelihood entered for a particular category should be either 0 or 1.0.

Incorporating the graphical BBN and SDG allows the analyst to quickly compare the effects of different model structures. Traditional simulations studies typically emphasize parameter uncertainty rather than model uncertainty (Reckhow 1994, Ferson 1996, Punt and Hilborn 1997, Levins 1998). We do not present this approach as an alternative to traditional simulation studies, but rather as a complement, or precursor, to such studies. In the context of ecological risk assessment, the approach provides a valuable tool for the problem formulation stage in risk analysis (USEPA 1992, Hayes et al. 2007). The graphical nature of the underlying dynamical model, in particular, lends a common symbolic language capable of capturing the understanding and opinions of researchers and stakeholders across a broad array of disciplines (Dambacher et al. 2007). This approach thus

documents and enhances understanding in systems that are poorly understood, difficult to quantify, or both.

3.6 Acknowledgments

Table 3.1. Sensitivity analysis of the agricultural pest BBN given a positive input to X_1. High values indicate shared information between the structure node and a finding at a node; the structure node in such a case is sensitive to findings at that node (Norsys 2006)[†].

Finding Node	Mutual Information
Alternative models	*1.00*
X_1	0.36
X_3	0.36
X_2	0.00

[†]Sensitivity analysis uses the change in mutual information between two nodes due to the reduction of entropy in node X because of a finding at node Y. The expected reduction in entropy of X due to a finding at Y is zero if X is independent of Y. The mutual information for a finding at the query node Q is the maximum possible for a finding at any node and is included here for scale (italics).

Table 3.2. Sensitivity analysis of the structure nodes for the BBN in Fig. 3.6. High values indicate increasing shared information between the observation nodes and their respective structure node. The values of the structure nodes serve as a reference (italics).

Food Chain		Functional Group	
Node	Mutual	Node	Mutual
Food Chain Models	Information	*Func Group Models*	information
Phosphorus (food chain),	*1.585*	Large herbivores, H_2	*1.000*
P_{fc}	0.787	Phosphorus (func. groups),	0.358
Herbivores, H	0.783	P_{fg}	0.358
Autotrophs, A	0.345	Periphyton, A_p	0.358
Carnivores, C	0.343	Invertebrate carnivores, C_1	0.039
		Edible algae, A_1	0.022
		Protected algae, A_2	0.014
		Small herbivores, H_1	0.000
		Fish, C_2	0.000
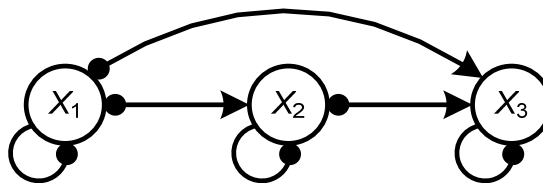
Figure 3.1. Signed directed graph depicting a top predator X_3 consuming prey X_1 and X_2 from two different trophic levels. Negative direct effects are shown by lines ending in a filled circle (——•) and positive direct effects are depicted with arrows (——→). Intraspecific density-dependent processes are represented by a line returning to the source variable.
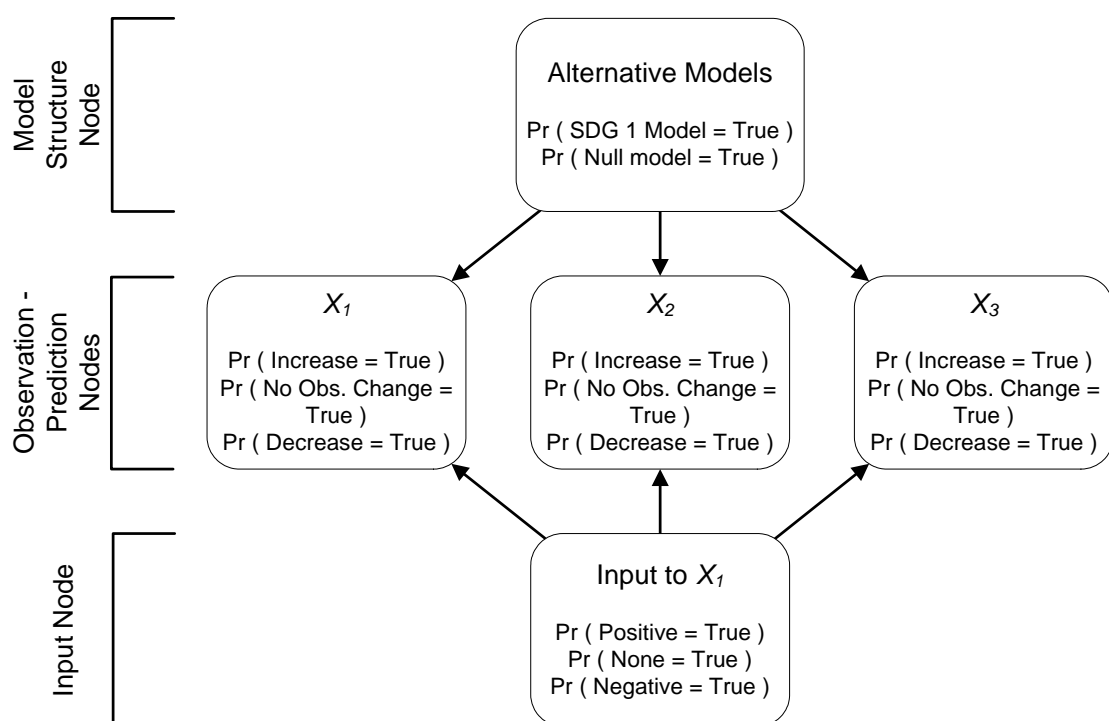
Figure 3.2. Bayesian Belief Network of the signed directed graph model from Fig. 3.1 (SDG 1) and competing null model. A press perturbation is made only on variable X_1.
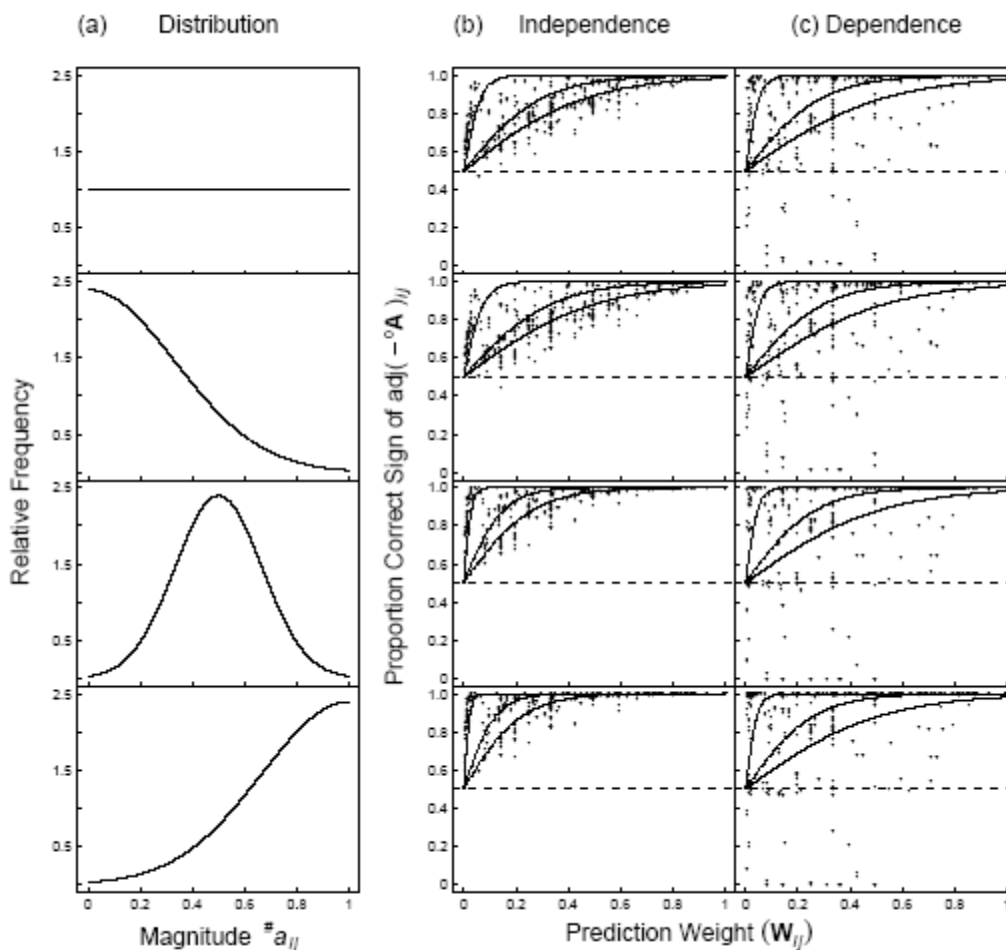
Figure 3.3. The influence of interaction magnitude and interdependency on prediction weight accuracy. (a) The four different distributions used to simulate the relative frequency of strong and weak interactions between the matrix elements $^{\#}a_{ij}$. The $^{\#}a_{ij}$'s of 500 stable matrices were drawn independently from each these distributions for eighteen different community models (Dambacher et al.2003a). (b) The proportion of qualitative response predictions with the same sign as the quantitative response predictions plotted against the prediction weight of the qualitative model. Each point represents the proportion of the $^{\#}a_{ij}$ elements whose sign is correctly predicted by the qualitative model, for all community models. The fitted curves denote the expected correct proportion given prediction weight and total feedback (Eq. 3.5, Table C.1), for three values of total feedback, **T** (from bottom to top): $\mathbf{T}_{ij} = 10$, $\mathbf{T}_{ij} = 100$, $\mathbf{T}_{ij} = 1000$. (c) As in (b), but with $^{\#}a_{ij}$ of a predator-prey relationship conditionally dependent such that if the predator is species i and the prey species j, then $0 < {}^{\#}a_{ij} < 0.01 \times {}^{\#}a_{ji}$, where the $^{\#}a_{ji}$ are drawn independently from the distribution in the corresponding row of Fig. 3.3(a) (see Appendix A). Non-trophic $^{\#}a_{ij}$ are drawn independently from the distribution in the corresponding row of Fig. 3.3(a). Note that points are overlapping.

Figure 3.4. Bayesian Belief Network of the Californian red scale pest community (Borer et al. 2003), where X_1 is unparasitized red scale (*Aonidiella aurantii*), X_2 is red scale parasitized by the wasp *Encarsia perniciosi*, and X_3 is red scale parasitized by the wasp *Aphytis melinus*. In this example, there has been a positive input (e.g., increased rate of birth) to unparasitized red scale as shown by 100% chance of a positive input to X_1. Nodes that have specified observation likelihoods are darker than those that do not. In (a), equal prior probabilities are allocated to the competing models in the structure node. In (b), an observed increase in X_3 supports the H-PC model, thereby increasing the probability of observing an increase in X_1. In (c), observing an increase in X_1 further supports the H-PC model. BBNs were created using Netica 3.14 (Norsys 2006).

a)
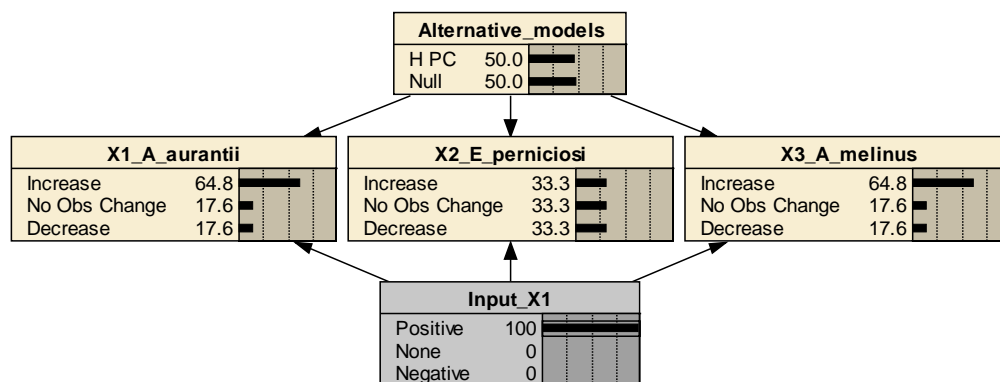
b)
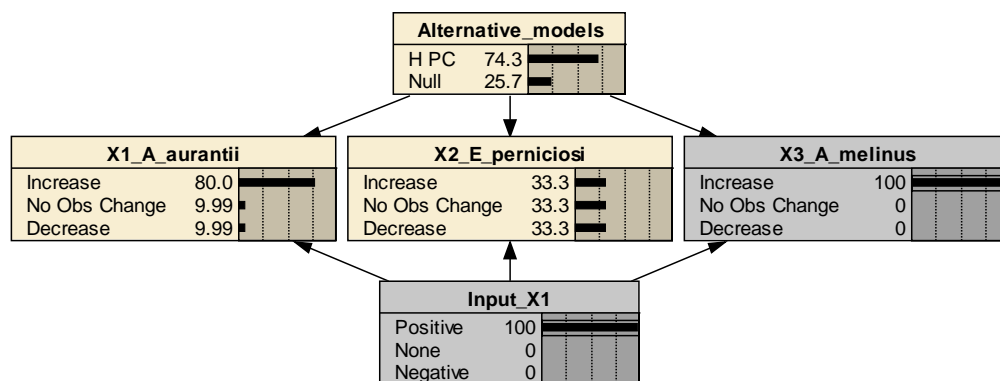
c)
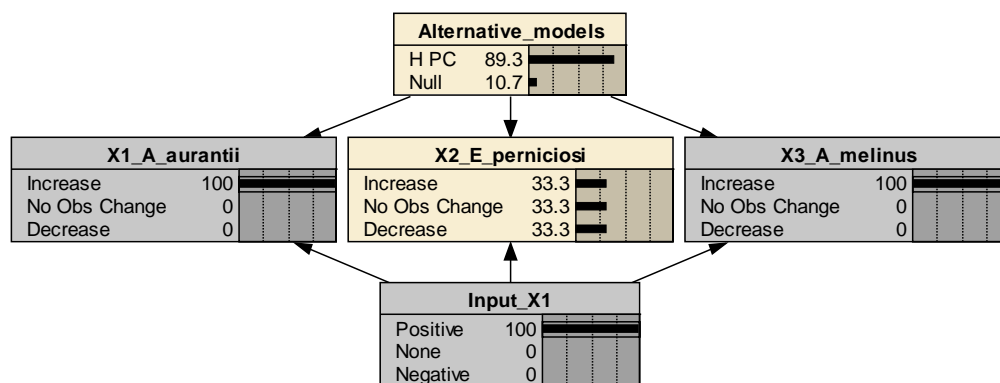
Figure 3.4.
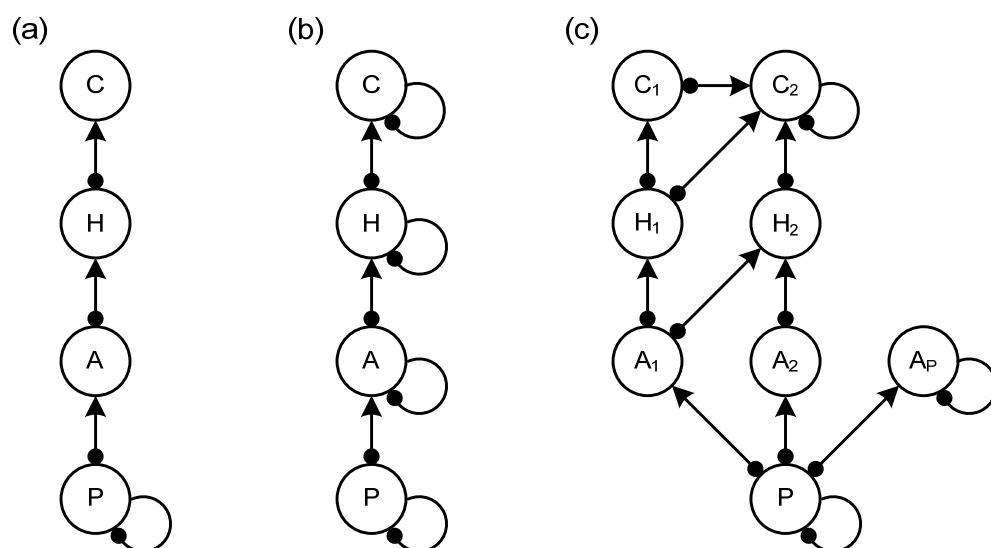
Figure 3.5. Alternative model structures of experimental lake mesocosms tested by Hulot et al. (2000). SDG representation of linear trophic food chains with (a) prey dependence, (b) ratio dependence, and (c) a model separating trophic levels into functional groups. A: algae, A_1: edible algae, A_2: protected algae, A_P: periphyton, C: carnivores, C_1: invertebrate carnivores, C_2: fish, H: herbivores, H_1: small herbivores, H_2: large herbivores, P: Phosphorus. Adapted by permission from Macmillan Publishers Ltd: Nature (Hulot et al. 2000), copyright (2000).
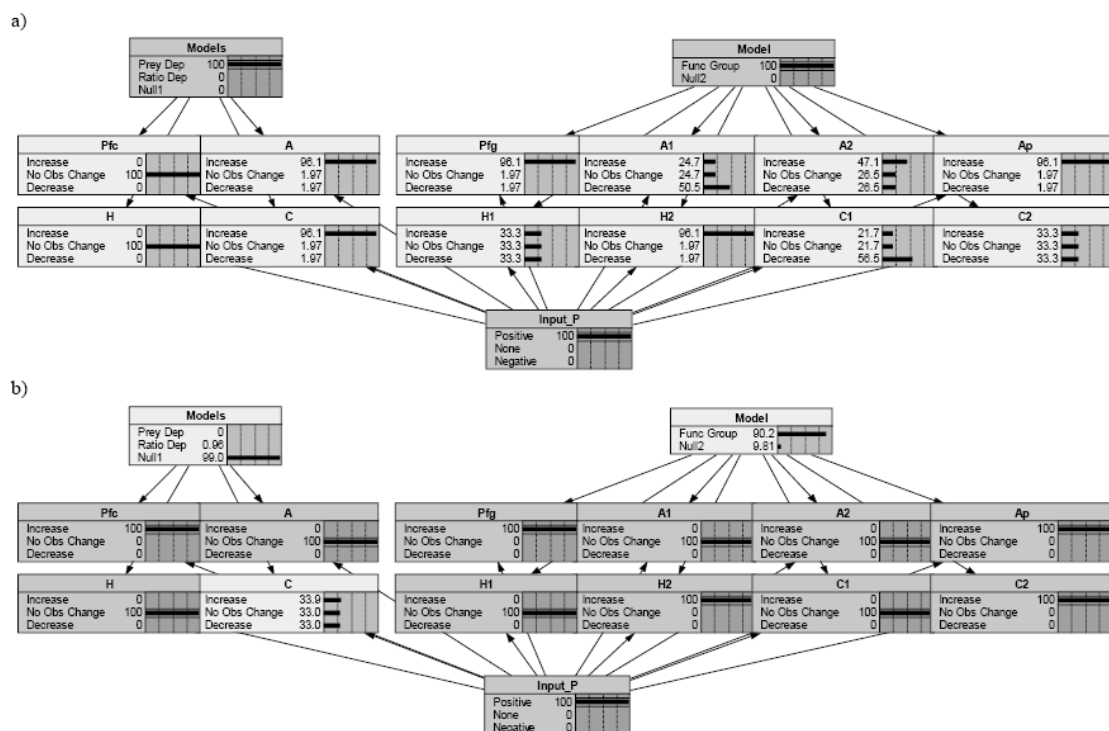
Figure 3.6. General structure of Bayesian Belief Network incorporating both four and eight variable SDG models corresponding to Hulot et al's (2000) lake mesocosm experiments. Separate structure nodes correspond to the comparison of four variable models and to the comparison of eight variable models. The two structure nodes each have a set of corresponding observation nodes. Since all of the models describe the system's response to the same experimental manipulation, the probability of input to phosphorus is a node common to all observation nodes. A: algae, A1: edible algae, A2: protected algae, AP: periphyton, C: carnivores, C1: invertebrate carnivores, C2: fish, H: herbivores, H1: small herbivores, H2: large herbivores, P(fc): Phosphorus in food chain model, P(fg): Phosphorus in functional group model. In this example, there is a positive input of phosphorus. In (a), prior probabilities are allocated to the competing models in each structure node such that the prey dependent and functional group models have 100% chance of being correct. The predictions of these models are given in the observation-prediction nodes. In (b), the prior probabilities of competing models within each model structure node are given equal probabilities and observation likelihoods are entered as described in 3.4.3 Analyzing the effect of alternative model structures. Nodes that have specified observation likelihoods are darker than those that do not.

4 THE CONTROL OF VECTOR-BORNE DISEASE EPIDEMICS

Geoffrey R. Hosack [a], Philippe A. Rossignol [a],

and P. van den Driessche [b]

[a] Department of Fisheries and Wildlife

Oregon State University

104 Nash Hall

Corvallis, OR 97331-3803 USA

[b] Department of Mathematics and Statistics

University of Victoria, BC, V8W 3R4, Canada

4.1 Abstract

The theoretical underpinning of our struggle with vector-borne disease, and still our strongest tool, remains the basic reproduction number, $\mathbf{R}_0$, the measure of long term endemicity. Despite its widespread application, $\mathbf{R}_0$ does not address the dynamics of epidemics in a model that has an endemic equilibrium. We use the concept of reactivity to derive a threshold index for epidemicity, $\mathbf{E}_0$, which gives the maximum number of new infections produced by an infective individual at a disease free equilibrium. This index describes the transitory behavior of disease following a temporary perturbation in prevalence. We demonstrate that if the threshold for epidemicity is surpassed, then an epidemic peak can occur, that is, prevalence can increase further, even when the disease is not endemic and so dies out. The hierarchy of parameters in $\mathbf{E}_0$ may differ from that in $\mathbf{R}_0$ and lead to different strategies for control. Both the transmission efficiency from hosts to vectors and the vector-host ratio may have a stronger effect on epidemicity than endemicity. The duration of the extrinsic incubation period required by the pathogen to transform an infected vector to an infectious vector, however, may have a stronger effect on endemicity than epidemicity. We use the index $\mathbf{E}_0$ to examine how vector behavior affects epidemicity. We find that parasite modified behavior, feeding bias by vectors for infected hosts, and heterogeneous host attractiveness contribute significantly to transitory epidemics. We anticipate that the epidemicity index will lead to a reevaluation of control strategies for vector-borne disease and be applicable to other disease transmission models.

4.2 Keywords

4.3 Introduction

Soon after proving the transmission of malaria by biting mosquitoes, Ronald Ross (1911) demonstrated that the prevalence of malaria tends to a fixed limit depending on the rates of transmission, recovery, and mortality within the host and vector populations. Ross's model showed that the prevalence of malaria tends toward zero, in the long-term, if a control strategy holds the number of vectors at a sufficiently low level. The realization that malaria transmission could be halted by reducing, but not eradicating, the vector population greatly influenced the modeling and control of infectious disease (Bailey 1982). Macdonald (1952) suggested that targeting the rate of vector mortality more effectively reduced malaria prevalence than targeting other rates. Macdonald (1952) placed these rates into an index that we denote by $\mathbf{R}_0$. If $\mathbf{R}_0 < 1$ then malaria prevalence declines to zero in the long-term. Otherwise, malaria can become endemic. The index $\mathbf{R}_0$ was used to develop and evaluate control strategies meant to reduce malaria prevalence (Garret-Jones 1964, World Health Organization 1975).

The index $\mathbf{R}_0$ is widely applied to the mathematical modeling of diseases in general (Diekmann and Heesterbeek 2000, van den Driessche and Watmough 2002, Thieme 2003). Early in the mathematical study of malaria, however, Lotka (1923) used Ross's model to show that significant, but transitory, changes in prevalence often occur before reaching the long-term equilibrium determined by $\mathbf{R}_0$. We use this model to investigate potential causes of transitory epidemics within vector-borne disease.

The model first proposed by Ross (1911) and subsequently modified by Macdonald (1952) has influenced both the modeling and the application of control strategies to vector-borne disease. Models of malaria that investigate complications arising from host superinfection, immunity, and other factors are based on this fundamental model (Aron and May 1982, Dietz 1988, Koella, 2003). The model has also influenced the mathematical analysis of many other vector-borne diseases (Dye 1992), including dengue fever (Feng and Velasco-Hernandez 1997), rickettsia in cattle (Yonow et al.

1998), trypanosomiasis (McDermott and Coleman 2001), and West Nile Virus (Foppa and Spielman 2007). A standard model consistent with the assumptions of Ross (1911) and Macdonald (1952) that relates the proportion of infected hosts x to the proportion of infected vectors y is given by,

$$\frac{dx}{dt} = ab_x my(1-x) - rx$$
$$\frac{dy}{dt} = ab_y x\left(e^{-\mu n} - y\right) - \mu y. \tag{4.1}$$

The standard model consists of two coupled ordinary differential equations that describe the change in prevalence for the vector and host populations. This model uses several assumptions to simplify the complexity of malaria transmission and identify the important aspects of malaria transmission between vector and host (Bailey 1982, Aron and May 1982, Smith and McKenzie 2004). Each equation corresponds to a Susceptible-Infected-Susceptible model for the vector and host populations. Infected vectors do not recover but die at rate μ, and newly born vectors are susceptible. The specific effects of immunity and superinfection on hosts are ignored such that hosts recover at rate r and again become immediately susceptible. Vectors bite hosts at rate a and transmit infection with efficiency b_x. The proportion of vectors that acquire infection by biting infected hosts is b_y. The number of vectors per host is m, and n is the length of the extrinsic incubation period.

In vector-borne disease, the period of time between a vector becoming infected to becoming infectious may be long compared to the lifespan of the vector. Vector mortality during this extrinsic incubation period of the pathogen within the vector has important consequences for endemicity (Macdonald 1952). The growth equation for prevalence within vectors includes vector mortality during the extrinsic incubation period. In the standard model, the probability of an infected vector surviving the extrinsic incubation period is given by the quantity $e^{-\mu n}$ (see Smith and McKenzie 2004, Smith *et al.* 2007). Other formulations have explicitly modeled the time lag between when a vector becomes infected and when it becomes infectious (Aron and May 1982, Ruan et al. 2008) but

we do not consider this here. We refer to the model given by Eq. (4.1) as the standard model because it reflects the assumptions of both Ross (1911) and Macdonald (1952) as contained in the original index $\mathbf{R}_0$ for malaria.

Unlike the long-term case for endemicity, no index has summarized the short-term behavior of transitory epidemics in vector-borne disease. We therefore derive a threshold index for transitory epidemics $\mathbf{E}_0$, such that if $\mathbf{E}_0 > 1$ then transitory epidemics are possible; otherwise, transitory epidemics are not possible (Section 4.2). The index $\mathbf{E}_0$ contains the same parameters as $\mathbf{R}_0$, but the way in which these rates affect each index differs (Section 4.3). For example, we demonstrate how the vector-host ratio m has a greater influence on epidemicity than endemicity. We investigate how the hierarchy of potential target rates differs for control strategies that reduce epidemicity versus endemicity. We determine the conditions for which epidemics preferentially elevate prevalence within the host population versus the vector population (Section 4.4). We also show that epidemics, although transitory, have lasting effects on disease prevalence. The index $\mathbf{E}_0$ permits comparison of epidemicity across models, and we use it to show how different assumptions of vector feeding behavior and host susceptibility affect epidemicity (4.5). The models in this paper assume constant population sizes and can be formulated in terms of either the change in prevalence or the change in prevalent number over time. We apply these indices to prevalence and in Section 4.6 discuss how the alternative formulation for prevalent number affects the results.

Section 4. 2 Derivation of threshold indices

The index $\mathbf{R}_0$, which we refer to as the basic reproduction number, can be calculated using established methods (Diekmann and Heesterbeek 2000, van den Driessche and Watmough 2002). For a matrix $\mathbf{A}$, let $s(\mathbf{A})$ denote the spectral abscissa (i.e., the largest real part of any eigenvalue of $\mathbf{A}$) and $\rho(\mathbf{A})$ denote the spectral radius (i.e., the maximum modulus of any eigenvalue of $\mathbf{A}$). For an ordinary differential equation system with a unique disease free equilibrium (DFE), the Jacobian

matrix evaluated at the DFE is written as $\mathbf{J}_0 = \mathbf{F}_{\mathbf{J}_0} - \mathbf{V}_{\mathbf{J}_0}$, where the matrix $\mathbf{F}_{\mathbf{J}_0}$ contains the rates of

new infection in vectors and hosts linearized at the DFE, and the matrix $\mathbf{V}_{\mathbf{J}_0}$ contains the rates of

recovery and mortality linearized at the DFE. The basic reproduction number is

$$\mathbf{R}_0 = \rho\left(\mathbf{F}_{\mathbf{J}_0}\mathbf{V}_{\mathbf{J}_0}^{-1}\right) \tag{4.2}$$

For a model defined in terms of prevalent numbers, the basic reproduction number $\mathbf{R}_0$ is defined as

the expected number of new infections produced by an infective individual in a population at a DFE.

The DFE is locally stable if $\mathbf{R}_0 < 1$ (equivalently $s(\mathbf{J}_0) < 0$), but unstable if $\mathbf{R}_0 > 1$ (equivalently

$s(\mathbf{J}_0) > 0$) (van den Driessche and Watmough 2002).

Reactivity is the maximum instantaneous amplification rate of the state variables from

equilibrium in Euclidean distance following a perturbation, and is equivalent to the maximum of the

Rayleigh quotient (Neubert and Caswell 1997). Thus reactivity is equal to the maximum eigenvalue,

$s(H(\mathbf{J}_0))$, of the Hermitian part $H(\mathbf{J}_0)$ of the system's Jacobian matrix evaluated at the DFE, where

$H(\mathbf{J}_0) = \left(\mathbf{J}_0 + \mathbf{J}_0^T\right)/2$. By Bendixson's theorem, the risk of endemicity given by $s(\mathbf{J}_0)$ is always less

than or equal to the risk of epidemicity given by $s(H(\mathbf{J}_0))$ (Householder 1964). In the models

examined in this paper, $H(\mathbf{J}_0)$ is quasipositive (i.e., has off-diagonal entries nonnegative). The

eigenvector associated with $s(H(\mathbf{J}_0))$ is in the nonnegative orthant (Berman et al. 1989), as is the

predicted cone of epidemicity in systems with positive reactivity. We determine a threshold index for

epidemicity $\mathbf{E}_0$ such that if $\mathbf{E}_0 > 1$, then $s(H(\mathbf{J}_0)) > 0$ and the system is reactive, and, if $\mathbf{E}_0 < 1$, then

$s(H(\mathbf{J}_0)) < 0$ and the system is non-reactive. Set $H(\mathbf{F}_{\mathbf{J}_0}) = \left(\mathbf{F}_{\mathbf{J}_0} + \mathbf{F}_{\mathbf{J}_0}^T\right)/2$, and, since $\mathbf{V}_{\mathbf{J}_0}$ is diagonal,

$H(\mathbf{V}_{\mathbf{J}_0}) = \left(\mathbf{V}_{\mathbf{J}_0} + \mathbf{V}_{\mathbf{J}_0}^T\right)/2 = \mathbf{V}_{\mathbf{J}_0}$. The threshold for epidemicity is

$$\mathbf{E}_0 = \rho\left(H(\mathbf{F}_{\mathbf{J}_0})H(\mathbf{V}_{\mathbf{J}_0})^{-1}\right) = \rho\left(\frac{\mathbf{F}_{\mathbf{J}_0} + \mathbf{F}_{\mathbf{J}_0}^T}{2}\mathbf{V}_{\mathbf{J}_0}^{-1}\right). \tag{4.3}$$

The first equality comes from the definition of $\mathbf{E}_0$ and an equivalent condition (as stated above for $\mathbf{R}_0$), and the second comes from $\mathbf{V}_{\mathbf{J}_0}$ being diagonal.

Consider the linear system,

$$\frac{d\mathbf{x}}{dt} = H(\mathbf{J}_0)\mathbf{x}, \tag{4.4}$$

where the vector $\mathbf{x}$ refers to the number of infected hosts and infected vectors. As the time t after a perturbation goes to infinity, the vector $\mathbf{x}$ will approach the eigenvector $\mathbf{u}_1$ that corresponds to the maximum eigenvalue of $H(\mathbf{J}_0)$. The eigenvector $\mathbf{u}_1$ maximizes the Rayleigh quotient formed with the Hermitian matrix $H(\mathbf{J}_0)$ (Horn and Johnson, 1985). For any non-zero perturbation, the linear system, in the long-term, provides the maximum amplification rate of infection near the DFE for the original linearized system, $\frac{d\mathbf{x}}{dt} = \mathbf{J}_0\mathbf{x}$. The matrix $H(\mathbf{J}_0)$, as with the partition of the matrix $\mathbf{J}_0$ above, may be partitioned such that $H(\mathbf{J}_0) = H(\mathbf{F}_{\mathbf{J}_0}) - H(\mathbf{V}_{\mathbf{J}_0})$, where the matrix $H(\mathbf{F}_{\mathbf{J}_0})$ is nonnegative and the matrix $H(\mathbf{V}_{\mathbf{J}_0})$ is nonsingular and has a nonnegative inverse. Without reinfection, the change in the number of infected individuals is $\frac{d\mathbf{z}(t)}{dt} = -H(\mathbf{V}_{\mathbf{J}_0})\mathbf{z}(t)$, where $\mathbf{z}(t)$ gives the number of individuals infected at time t. This has the solution $\mathbf{z}(t) = e^{-H(\mathbf{V}_{\mathbf{J}_0})t}\mathbf{z}(0)$. The maximum number of infected individuals at time t is given by $H(\mathbf{F}_{\mathbf{J}_0})\mathbf{z}(t)$. We integrate this expression, from zero to infinity with reinfection turned off,

$$\begin{aligned}\int_0^\infty H(\mathbf{F}_{\mathbf{J}_0})\mathbf{z}(t)dt &= \int_0^\infty H(\mathbf{F}_{\mathbf{J}_0})e^{-H(\mathbf{V}_{\mathbf{J}_0})t}\mathbf{z}(0)dt \\ &= H(\mathbf{F}_{\mathbf{J}_0})H(\mathbf{V}_{\mathbf{J}_0})^{-1}\mathbf{z}(0).\end{aligned} \tag{4.5}$$

We call $H(\mathbf{F}_{\mathbf{J}_0})H(\mathbf{V}_{\mathbf{J}_0})^{-1}$ the maximum next generation matrix. We are interested in the multiplicative growth per generation of the maximum next generation matrix over all generations, and so examine the quantity $\left\| \left[H(\mathbf{F}_{\mathbf{J}_0})H(\mathbf{V}_{\mathbf{J}_0})^{-1} \right]^k \right\|^{1/k}$ as $k \to \infty$. This is given by the spectral radius of the

maximum next generation matrix. Thus, for a model defined in terms of prevalent numbers, the threshold index for epidemicity $\mathbf{E}_0$ gives the maximum number of new infections produced by an infective individual at a DFE. For a model defined in terms of prevalence, as in Eq. 4.1, the analyses for the threshold indices $\mathbf{R}_0$ and $\mathbf{E}_0$ are similar, and give threshold conditions for the proportion of infected individuals.

4.3 Standard model and epidemicity

The standard model either has a globally asymptotically stable DFE, or a globally asymptotically stable endemic equilibrium with $x > 0$, $y > 0$ (Lotka 1923, Bailey 1982). The DFE is stable if $\mathbf{R}_0 = \sqrt{\frac{a^2 b_x b_y m e^{-\mu n}}{r\mu}} < 1$; endemicity occurs if $\mathbf{R}_0 > 1$ (Table 4.1, Section 4.2). The basic reproduction number (also called the reproductive rate), $\mathbf{R}_0$, is a threshold index for long-term endemicity (Macdonald 1952; Aron and May 1982; Smith and McKenzie 2004).

Temporary perturbations in prevalence, such as those that occur when vectors bite relapsing hosts (Paul et al. 2004), might initiate a transitory epidemic. Note that sometimes a disease introduction that results in an endemic state, where $\mathbf{R}_0 > 1$, is referred to as an epidemic; we avoid such usage in this paper. We define an epidemic as a transitory increase in prevalence following a perturbation such that the trajectory moves away from a stable DFE ($\mathbf{R}_0 < 1$) to higher levels of prevalence in the vector or host population before eventually returning (Figure 4.1a). If this can occur then the DFE is termed ``reactive'' (Neubert and Caswell 1997). The epidemicity threshold index evaluated at the DFE, $\mathbf{E}_0$, is derived from the maximum rate of change in prevalence immediately following a perturbation such that $\mathbf{E}_0 < 1$ is equivalent to the DFE being nonreactive (Figure 4.1b), and $\mathbf{E}_0 > 1$ is equivalent to the system being reactive (see Section 4.2). Thus, a nonreactive system cannot generate epidemics, whereas a reactive system can generate epidemics.

We first investigate vector-borne disease epidemics using the standard model (4.1). A marked increase in host prevalence can occur when the threshold for epidemicity is surpassed, such that $\mathbf{E}_0 = \sqrt{\frac{a^2\left(b_x m + b_y e^{-\mu n}\right)^2}{4r\mu}} > 1$ (Table 4.1), even when $\mathbf{R}_0 < 1$ (Figure 4.2a). Clearly, some trajectories in Figure 4.2a show a marked transitory increase in host prevalence before returning to the DFE. Not all stable DFEs, however, are equivalent in epidemicity. We demonstrate that another system with identical asymptotic return rates to equilibrium (i.e., identical eigenvalues) cannot be reactive and will thus have no epidemic risk (Figure 4.2b). In this system, the DFE is again stable ($\mathbf{R}_0 < 1$), but it is not reactive ($\mathbf{E}_0 < 1$). Here, all trajectories show a monotonic decrease in the distance from the stable DFE throughout their return and no large transitory increases in prevalence are observed for either hosts or vectors. We note that an intuitive argument may suggest that epidemicity increases as the equilibrium level of prevalence goes down because of an increased proportion of susceptibles. Figure 4.2b plainly shows that this intuition is not always useful. A reduced, even zero, equilibrium level of prevalence is not a reliable estimate of epidemicity risk because some DFEs are not reactive. However, $\mathbf{E}_0$ is a useful index to identify epidemicity.

The hierarchy of parameters best suited for disease control differs between $\mathbf{R}_0$ and $\mathbf{E}_0$. Similar to the insight $\mathbf{R}_0$ gives into potential control strategies for endemicity, the threshold index for epidemicity $\mathbf{E}_0$ suggests target parameters that may reduce the risk of epidemics. The product of transmission efficiency from infected vectors to hosts and the vector-host ratio, $b_x m$, appears as a multiplicative factor with the transmission efficiency from infected hosts to vectors, b_y, and the probability of mortality during the extrinsic incubation period, $e^{-\mu n}$, under the square root in $\mathbf{R}_0$, and any of these quantities are effective targets for a control strategy aimed at reducing $\mathbf{R}_0$ (Figure 4.3a). These same parameters, however, appear as the quantity $\left(b_x m + b_y e^{-\mu n}\right)^2$ under the square root in $\mathbf{E}_0$. The transmission efficiencies and the probability of vector mortality during the extrinsic incubation period, $e^{-\mu n}$, range between 0 and 1, but m is any nonnegative number and can be much greater than

1. Thus, $\left(b_x m + b_y e^{-\mu n}\right)^2 \approx b_x^2 m^2$ as m becomes large. If the number of vectors is large relative to the number of hosts, then targeting the transmission efficiency b_x and the vector host ratio m may effectively reduce epidemicity (Figure 4.3b). Of course, if the vector-host ratio m is sufficiently small such that $0 < b_x m < 1$, then a control strategy that targets any of these parameters will have similar effects on both $\mathbf{R}_0$ and $\mathbf{E}_0$ (Figure 4.3b). In general, however, the transmission efficiency from vector to host and the vector-host ratio are much stronger candidates for a control strategy that aims to reduce epidemic increases in prevalence than is the transmission efficiency from hosts to vectors or vector mortality during the extrinsic incubation period.

4.4 Epidemics and elevated prevalence in hosts

Using phase plane analysis, we further examine epidemic behavior near the DFE. In particular, we show that the product of transmission efficiency and the vector-host ratio, $b_x m$, determines whether an epidemic elevates prevalence in hosts or in vectors. The standard model has no oscillatory solutions (nor do the models considered in Section 4.5 below). We describe the transitory behavior of trajectories following a perturbation through an analysis of eigenvectors, which describe the direction of trajectories within the phase plane, and their associated eigenvalues, which describe the trajectories' rate of change in the directions given by the eigenvectors.

For example, in Figure 4.2a-c note that the trajectories that start near the DFE initially parallel the dashed line, and later asymptotically approach the line with open circles when drawing close to the DFE. The rate of return to a stable DFE is determined by the eigenvalue with the maximum real part, which we denote λ_1 (i.e., $\lambda_1 = s(\mathbf{J}_0)$, the spectral abscissa; see Section Methods). As the time t after a perturbation goes to infinity, the prevalence in hosts and vectors will be proportional to the eigenvector associated with λ_1, denoted $\mathbf{w}^{(1)}$, that is $\lim_{t \to \infty} e^{\lambda_1 t} \left[x(t), \, y(t)\right]^T \propto \mathbf{w}^{(1)}$.

The eigenvector $\mathbf{w}^{(1)}$ is represented by the line with open circles in Figure 4.2a-c. All trajectories asymptotically approach this eigenvector as they move close to the DFE.

On the other extreme, as the time t after a perturbation goes to zero and we trace a trajectory backwards in time toward the perturbation event, the change in prevalence per time unit c will be proportional to the eigenvector associated with the eigenvalue λ_2 having the least real part. This eigenvector is denoted $\mathbf{w}^{(2)}$, and so $\lim_{t \to 0} e^{\lambda_2 t}[x(t) - x(t-c),\ y(t) - y(t-c)]^T \propto \mathbf{w}^{(2)}$. In Figure 4.2a-c, the eigenvector $\mathbf{w}^{(2)}$ is represented by the dashed line. All trajectories near the DFE initially parallel this eigenvector $\mathbf{w}^{(2)}$ before they asymptotically approach the eigenvector $\mathbf{w}^{(1)}$. Epidemics generate trajectories that not only elevate prevalence but also enable higher levels of prevalence to persist for a longer duration (Figure 4.1a) compared to trajectories within the non-reactive system (Figure 4.1b). This occurs because λ_1 gives a slow rate of return along $\mathbf{w}^{(1)}$ (relative to λ_2), and epidemics generate trajectories that approach $\mathbf{w}^{(1)}$ at a point farther from the DFE (Figure 4.2a) compared to trajectories within the non-reactive system (Figure 4.2b).

We define the shaded area of Figure 4.2a as the cone of epidemicity where reactivity is positive and trajectories are predicted to move away from the DFE such that $d\sqrt{x^2 + y^2}/dt > 0$ (Section 4.2). The epidemic occurs because a trajectory that originates near the DFE and passes through this cone of epidemicity must doubleback before returning to equilibrium: prevalence in hosts must first increase as trajectories parallel $\mathbf{w}^{(2)}$ before asymptotically approaching $\mathbf{w}^{(1)}$ and the DFE. This happens when the system is reactive and the angle θ, formed by the eigenvectors at DFE, is obtuse. The angle θ is obtuse if $b_x m > b_y e^{-\mu n}$ (Appendix F). When $b_x m = b_y e^{-\mu n}$, the eigenvectors are orthogonal and no epidemic in either hosts or vectors is possible in a system with a stable DFE (Figure 4.2b; $\mathbf{E}_0 = \mathbf{R}_0 < 1$). If $b_x m < b_y e^{-\mu n}$, then the angle θ is acute and an epidemic cannot elevate prevalence in hosts, but instead increases prevalence in vectors (Figure 4.2c). The difference between the quantities $b_x m$ and $b_y e^{-\mu n}$ therefore determines both the behavior and the presence or

absence of epidemics. As noted in Section Standard model, the range of $b_y e^{-\mu n}$ must be between 0

and 1, but $b_x m$ can be any nonnegative number. This suggests that the ratio of vectors to hosts m

might often determine whether epidemics amplify prevalence in hosts or in vectors.

4.5 Modifications to the standard model and epidemicity

The epidemicity index $\mathbf{E}_0$ gives us the ability to investigate how modifying the standard

model affects epidemicity. For example, evidence shows that vectors prefer to bite infected hosts

(Day et al. 1983, Lacroix et al. 2005), parasites increase vector biting rates (Koella et al. 1998), and

hosts have heterogeneous susceptibility to biting vectors (Woolhouse et al. 1997, Smith et al. 2005).

The effects of such variations on the endemicity of vector-borne disease have been addressed by

comparing the index $\mathbf{R}_0$ generated under the different assumptions. In this Section, we apply the

same strategy to examine epidemicity using the index $\mathbf{E}_0$.

4.5.1 Vector bias

Feeding bias by vectors may have an important effect on epidemics. Empirical evidence

suggests that the modified physiological (Rossignol et al. 1985) and behavioral (Day et al. 1983) state

of infected hosts may predispose these individuals to foraging vectors. For example, mosquitoes show

some bias for humans infected with malaria (Lacroix et al. 2005). These empirical observations have

consequences for disease transmission because more vectors are exposed to infection than in the

standard model. Bias for infected hosts by feeding vectors is described by the parameter p in the

model (Kingsolver 1987)

$$\frac{dx}{dt} = a\left[\frac{1-x}{1+(p-1)x}\right]b_x my - rx$$

$$\frac{dy}{dt} = a\left[\frac{px}{1+(p-1)x}\right]b_y\left(e^{-\mu n} - y\right) - \mu y.$$

(4.6)

Values of $p > 1$ indicate vector bias for infected hosts, values $0 < p < 1$ indicate bias for uninfected hosts, and $p = 1$ reduces to the standard model (4.1). The parameter b_y describes the transmission efficiency from hosts to vectors and is here made explicit ($b_y = 1$ in Kingsolver (1987)). As in our formulation of the standard model (4.1), in the vector bias model (4.6) we include vector mortality during the extrinsic incubation period, $e^{-\mu n}$, whereas Kingsolver (1987) implicitly assumed that infected vectors were instantly infectious, $n = 0$. Kingsolver (1987) developed this model within the context of malaria transmission and derived its basic reproduction number.

Vector bias for infected hosts affects endemicity as a linear term under the square root in $\mathbf{R}_0$ (Table 4.1). This bias, however, has a larger effect on the value of the threshold index of epidemicity, $\mathbf{E}_0$, because it is squared under the square root. Also, increasing vector bias favors increased prevalence in vectors during epidemics (Table 4.1).

4.5.2 Parasite-modified vector behavior

Behavior modification of the vector by a parasite, such as through an enhanced biting habit, may also have consequences for epidemics. For example, mosquitoes infected by the malaria parasite may have difficulty feeding (Rossignol et al. 1984), resulting in multiple feeding attempts (Rossignol et al. 1986, Koella et al. 1998). A parasite can modify the vector's biting rate a or transmission efficiency b_x by a multiplicative factor α (Dobson 1988). This factor α appears linearly under the square root of $\mathbf{R}_0$ (Table 4.1). The parasite-induced change in vector behavior, however, enters the threshold index for epidemicity $\mathbf{E}_0$ as a squared term under the square root, and so parasite-modified

vector behavior has a more important effect on epidemicity than on endemicity. In contrast to vector

bias, increasing the biting habit of infected vectors favors increases in prevalence within hosts, not

vectors, during epidemics (Table 4.1).

4.5.3 Heterogeneous host attractiveness

In the models examined above, we have assumed that the host population is homogeneous.

Evidence suggests that the majority of disease infections occur in only a fraction of the total

population (Woolhouse et al. 1997) and this may enhance the prevalence of infection in vector-borne

disease such as malaria (Smith et al. 2005). Factors promoting heterogeneity in infection among hosts

include distance from vector habitat (Ross 1911), host attractiveness (Takken and Knols 1999), and

susceptibility to infection (Smith et al. 2005). We investigate change in vector biting preference for

host subpopulations differing in susceptibility and recovery using a patch-dynamic model for

prevalence. Previous patchy transmission models for the number of infected individuals have shown

that a patchy host population leads to a basic reproduction number greater than or equal to non-patchy

models even without differences in susceptibility and recovery (Dye and Hasibeder 1986, Hasibeder

and Dye 1988). Hasibeder and Dye (1988) found that including both patchy host and vector

populations leads to a basic reproduction number greater than or equal to the patchy host model alone.

They concluded that the patchy host model is more useful in practice for addressing heterogeneous

contact between hosts and vectors. We focus on a patchy host population model for prevalence,

although the model can be extended to a patchy vector population. We derive the thresholds for

endemicity and epidemicity for vectors feeding on a host population with heterogeneous recovery and

susceptibility,

$$\frac{dx_i}{dt} = \eta_i ab_{x_i} m_i y(1 - x_i) - r_i x_i, \quad i = 1 \ldots N$$

$$\frac{dy}{dt} = ab_y \left(e^{-\mu n} - y\right)\left(\sum_{i=1}^{N} \eta_i x_i\right) - \mu y.$$

(4.7)

The parameter η_i, with $0 \le \eta_i \le 1$ and $\sum_{i=1}^{N} \eta_i = 1$, gives the preference of feeding vectors for susceptible host subpopulation i with recovery rate r_i, transmission efficiency b_i, and ratio of vectors to susceptible hosts m_i.

Just as in the standard model, Eq. (4.7) has a globally asymptotically stable DFE when $\mathbf{R}_0 < 1$. If $\mathbf{R}_0 > 1$, then the DFE is unstable and there is a single globally asymptotically stable endemic equilibrium (Appendix F). The threshold index for endemicity is

$$\mathbf{R}_0 = \sqrt{\sum_{i=1}^{N} \left(\mathbf{R}_0^{(i)}\right)^2 \eta_i^2} = \sqrt{\sum_{i=1}^{N} \frac{a^2 b_{x_i} b_y m_i e^{-\mu n}}{r_i \mu} \eta_i^2} , \tag{4.8}$$

where $\mathbf{R}_0^{(i)}$ denotes the threshold index for epidemicity of host subpopulation i in the event that vectors feed only on that subpopulation i, $(\eta_i = 1)$ (Appendix F). The threshold index for epidemicity is

$$\mathbf{E}_0 = \sqrt{\sum_{i=1}^{N} \left(\mathbf{E}_0^{(i)}\right)^2 \eta_i^2} = \sqrt{\sum_{i=1}^{N} \frac{a^2 \left(b_{x_i} m_i + b_y e^{-\mu n}\right)^2}{4 r_i \mu} \eta_i^2} , \tag{4.9}$$

where $\mathbf{E}_0^{(i)}$ denotes the threshold index for epidemicity of host subpopulation i in the event that vectors feed only on that subpopulation i, $(\eta_i = 1)$. Small fluctuations in vector feeding preference for hosts that differ in susceptibility or recovery will affect both long-term endemicity and short-term epidemicity.

Comparing the indices of $\mathbf{E}_0$ across the modified models of bias, modified behavior, and heterogeneous biting leads to 3 general conclusions. First, changes in vector bias and parasite

modified feeding behavior affect epidemicity more than endemicity. Second, vector bias favors amplified prevalence within vectors during epidemics, whereas parasite modified feeding behavior favors amplified prevalence within hosts. Third, heterogeneity in the vector feeding habit affect endemicity and epidemicity similarly and can have large effects on both. The index $\mathbf{E}_0$ allows a comparative approach that identifies how these factors increase or decrease the likelihood of an epidemic.

4.6 Discussion

Our analysis contributes two unexpected and novel concepts to vector-borne disease epidemiology. First, epidemics can occur in areas where long term transmission cannot be maintained. The index for epidemicity based on reactivity that we propose identifies the dynamics of recovery following a perturbation. These dynamics are often characterized by further increase in prevalence before eventual disappearance. Active monitoring and prompt reaction against new cases may still be required even after a disease has been eliminated locally. Second, strategies for control of epidemicity can differ from those that have been used for reducing endemicity. The parameters of the threshold index for epidemicity are the same as in the basic reproduction number because both are derived from the same model. The hierarchy of parameters, however, may differ between the two indices. The impact of a specific control campaign therefore could differ between risk of epidemicity and endemicity, and what proves efficient against one may be less so against the other. Overall, we suggest that the index of epidemicity, with its objective formality, familiar parameters, and relative ease of application, be incorporated alongside the traditional basic reproduction number in both strategic and tactical approaches to vector-borne disease control.

The threshold indices for epidemicity and endemicity are different in parameter emphasis and suggest alternative control strategies for epidemics. Vector life expectancy has long been a preferred target in reducing malaria prevalence, as exemplified by indoor residual spraying (Macdonald 1957, Gunasekaran et al. 2005). In the case of epidemics, transmission efficiency from

vectors to hosts and the vector-host ratio are also strong predictors and therefore may merit focused

targeting. The product of transmission efficiency from vectors to hosts and the vector-host ratio, $b_x m$,

is a particularly important factor in epidemicity for two reasons. First, this product can have a stronger

effect on epidemicity than the product of transmission efficiency and vector mortality during the

extrinsic incubation period, $b_y e^{-\mu n}$. Second, if $b_x m$ is greater than $b_y e^{-\mu n}$, then it is possible for an

epidemic to elevate prevalence in hosts. Vaccines are important tools for control (Girard et al. 2007),

and our findings may have implications for their role in vector-borne disease. We find that, although

both parameters are equally effective targets for reducing endemicity, if the ratio of vectors to hosts

m is large then b_x may be a more effective target parameter than b_y for targeting epidemics that

increase prevalence. In addition, decreasing b_x instead of b_y diminishes epidemics that enhance

prevalence in hosts. Thus, an immunization strategy that decreases the transmission efficiency from

vectors to hosts b_x could reduce the threat of epidemics. In malaria, for example, this could be

accomplished by administering pre-erythrocytic or erythrocytic vaccines. Similarly, and somewhat

unexpectedly, vector abundance control (e.g., Fillinger and Lindsay 2006) that targets m may be

more effective in reducing epidemicity than endemicity when vectors outnumber hosts. The above

discussion examines how a change in a parameter affects the levels of $\mathbf{R}_0$ and $\mathbf{E}_0$, but in real

applications the cost of a control strategy must also be taken into account (Killeen et al. 2002).

The indices for epidemicity and endemicity also allow predictions on how natural and human

alterations to disease systems affect disease transmission outside the context of control strategies. For

instance, the length of the extrinsic incubation period n is determined by temperature (Macdonald

1957). Climate change and land use practices may affect temperature and therefore n (Craig et al.

1999, Afrane et al. 2005). If vectors outnumber hosts, such a change in n could have a large effect on

the value of $\mathbf{R}_0$ and a negligible effect on the value of $\mathbf{E}_0$. On the other hand, both climate change

and land use practices may affect vector productivity (Munga et al. 2006, Pascual et al., 2006) and

hence m, the density of vectors relative to hosts. A substantial increase in m may have a large effect on epidemicity and a relatively small effect on endemicity.

We find that vector behavior strongly affects the epidemicity of vector-borne disease. Bias by feeding mosquitoes for infected hosts substantially increases epidemicity. Reducing bias by vectors for infected hosts, such as through the targeted administration of drugs (Lacroix *et al.*, 2005, Smith *et al.*, 2007) or insecticide treated netting, may effectively combat epidemics. Vector behavior modified by infection, such that infected vectors bite more often, also increases epidemicity more than endemicity. Heterogeneous attractiveness in hosts that differ in susceptibility or recovery can either increase or decrease both epidemicity and endemicity.

We have restricted our analysis to epidemics in the region of the DFE. The concept of reactivity also applies to the case where $\mathbf{R}_0 > 1$ and Eq. (4.1) has an endemic equilibrium. In this case, an index $\mathbf{E}^*$ similar to $\mathbf{E}_0$ can be derived (Appendix F). If $\mathbf{E}^* > 1$, then a perturbation that temporarily increases prevalence relative to the endemic equilibrium may result in a transitory epidemic. If $\mathbf{E}^* > 1$ and a perturbation temporarily decreases prevalence relative to the endemic equilibrium, however, then total levels of prevalence may dramatically decrease toward the DFE, in the short-term, before returning to the endemic equilibrium (Appendix F). Such a reverse epidemic, or hypodemic, may be of particular concern because a control strategy that temporarily decreases prevalence in areas of endemicity may initially appear more effective than it actually is. A short term control strategy, such as through the one-time administration of infection clearing drugs or insecticide treated netting, may result in a substantial but temporary reduction in prevalence before a gradual return to the original endemic state.

The above analyses define the term epidemic in a mathematical context for the prevalence within hosts and vectors (Section 4.2). We note that other linguistic, mathematic, and statistical definitions are equally useful and the best choice depends on the context of their application. Indeed, multiple definitions for an epidemic are possible even with the mathematic definition provided in Section 4.2. For example, Eq. (4.1) can be reformulated to describe the change in the prevalent

number of infected individuals. The substitutions $x = X/H$, where X is the number of infected

hosts and H is the total number of hosts, and $y = Y/V$, where Y is the number of infected vectors

and V is the total number of vectors, produce the growth equations dX/Hdt and dY/Vdt; note that

$m = V/H$. These equations, when multiplied by H and V respectively, give the change in the

prevalent number of infected hosts and vectors over time, dX/dt and dY/dt. When prevalent

number is used, instead of prevalence, $\mathbf{R}_0$ is unchanged but the index for epidemicity becomes

$$\mathbf{E}_0 = \sqrt{\frac{a^2 \left(b_x + b_y me^{-\mu n} \right)^2}{4r\mu}}$$ and the condition that epidemics elevate the number of infected hosts is

$b_x > b_y me^{-\mu n}$. Here, the nonnegative number m is multiplied by the transmission efficiency from

hosts to vectors b_y and the probability of a vector surviving the extrinsic incubation period $e^{-\mu n}$.

These latter factors assume greater importance, compared to the epidemics based on a definition of

prevalence, because m is any nonnegative number (c.f. Section 4.3). An epidemic thus defined in

terms of the prevalent number of infected hosts and vectors, instead of the prevalence of infection,

may lead to different conclusions about the nature of epidemicity, whereas the index of endemicity,

given by $\mathbf{R}_0$, remains unchanged. This highlights the importance of a precise definition for epidemic

that is suited to the problem at hand.

Although the standard model identifies the general aspects of transmission between vector

and host (Bailey, 1982, Aron and May, 1982, Smith and McKenzie, 2004), the results of this study

should be interpreted in light of the constraints and limits set by its underlying assumptions. The

standard model given by Eq. (4.1) is a general model with several assumptions that simplify the

complex interactions between host and vector. Superinfection (Aron and May, 1982, Dietz, 1988),

drug resistance (Koella and Antia, 2003, Bacaër and Sokhna, 2005), immunity (Dietz *et al.*, 1974,

Ngwa, 2004, Chitnis *et al.*, 2006), age structure (Dietz, 1988), and dynamic population sizes (Ngwa,

2004, Chitnis *et al.*, 2006) are not explicitly modeled; nor does the model include stochasticity (Lloyd

et al., 2007) or seasonal and climatic factors (Aron and May, 1982, Thomson *et al.*, 2006, Mabaso *et*

al., 2007) that affect disease transmission. Future research is needed to investigate how these complications affect epidemicity.

The threshold index of epidemicity $\mathbf{E}_0$ proposed above, like $\mathbf{R}_0$, is a complementary approach for identifying important features of disease transmission. The return of trajectories to a disease free steady state requires not only a stable disease free equilibrium ($\mathbf{R}_0 < 1$) but also depends on the absence of further perturbations. Similarly, the development of epidemics requires not only a reactive equilibrium ($\mathbf{E}_0 > 1$) but also depends on the direction of initial perturbations. Although the threshold index for epidemicity is here applied to a general vector-borne disease model, we suggest that application of the epidemicity threshold index is useful for other models of disease transmission. Taking account of the differences between epidemic and endemic threshold indices is crucial because the risk of epidemicity is always greater than or equal to the risk of endemicity (Section 4.2).

4.7 Acknowledgments

Table 4.1. Threshold indices for endemicity, $\mathbf{R}_0$, epidemicity, $\mathbf{E}_0$, and condition for epidemics to elevate prevalence in hosts. Parameters are: a biting rate; b_x, transmission efficiency from vector to host; b_y, transmission efficiency from host to vector; m, ratio of vectors to hosts; r, recovery rate of hosts; μ, mortality rate of vectors; n, duration of the extrinsic incubation period; p, feeding bias by vectors for infected hosts; α, parasite-modified vector behavior; η_i, feeding preference for host subpopulation i with susceptibility b_{x_i}, recovery rate r_i, and ratio of vectors to susceptible hosts m_i; N is the total number of host subpopulations.

Model	$\mathbf{R}_0$	$\mathbf{E}_0$	Condition for epidemics in hosts
Standard model	$\sqrt{\dfrac{a^2 b_x b_y m e^{-\mu n}}{r\mu}}$	$\sqrt{\dfrac{a^2\left(b_x m + b_y e^{-\mu n}\right)^2}{4r\mu}}$	$b_x m > b_y e^{-\mu n}$
Vector bias	$\sqrt{\dfrac{a^2 b_x b_y m p e^{-\mu n}}{r\mu}}$	$\sqrt{\dfrac{a^2\left(b_x m + b_y p e^{-\mu n}\right)^2}{4r\mu}}$	$b_x m > b_y p e^{-\mu n}$
Parasite modified vector	$\sqrt{\dfrac{\alpha a^2 b_x b_y m e^{-\mu n}}{r\mu}}$	$\sqrt{\dfrac{a^2\left(\alpha b_x m + b_y e^{-\mu n}\right)^2}{4r\mu}}$	$\alpha b_x m > b_y e^{-\mu n}$
Heterogeneous population	$\sqrt{\sum_{i=1}^{N}\dfrac{a^2 b_{x_i} b_y m_i e^{-\mu n}}{r_i \mu}\eta_i^2}$	$\sqrt{\sum_{i=1}^{N}\dfrac{a^2\left(b_{x_i} m_i + b_y e^{-\mu n}\right)^2}{4 r_i \mu}\eta_i^2}$	—
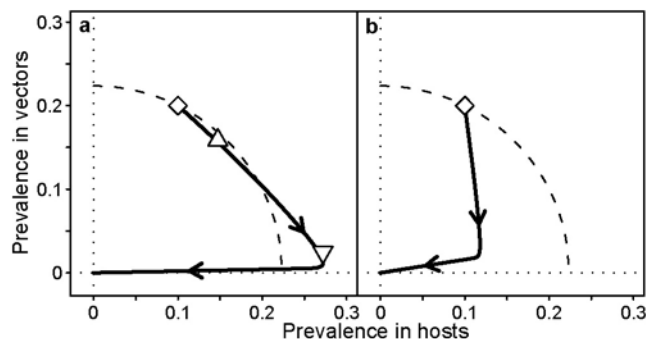
Figure 4.1. Comparison of systems with stable disease free equilibria (DFE) for the standard model ($\mathbf{R}_0 = 0.79 < 1$); the Jacobian matrices have identical sets of eigenvalues $\{\lambda_1 = -0.00366, \lambda_2 = -0.256\}$ for each system evaluated at the DFE. The open diamond ◊ denotes the initial level of prevalence immediately following a perturbation. Black solid lines are sample trajectories returning to the DFE. The dashed line marks the radius of the initial perturbation across the feasible region. In both figures, the first arrowhead marks prevalence 6 days after the perturbation and the second arrowhead marks prevalence 200 days after the perturbation. (a) A reactive system ($\mathbf{E}_0 = 3.175 > 1$). The trajectory begins to head away from the DFE at the point marked by the open triangle Δ , and returns to the DFE at the point marked by the upside down triangle ∇ . Prevalence in hosts more than doubles relative to the initial perturbation before declining. The parameter values are $a = 0.005$, $b_x = 0.5$, $b_y = 1$, $m = 125$, $r = 0.01$, $\mu = 0.25$. Susceptible vectors that bite infected hosts are assumed to become instantly infectious ($b_y = 1, n = 0$). (b) A nonreactive system ($\mathbf{E}_0 = 0.63 < 1$). The trajectory returns to the DFE with only a small increase of prevalence in hosts. The parameter values are $a = 0.0395$, $b_x = 0.1$, $b_y = 1$, $m = 10$, $r = 0.01$, $\mu = 0.25$, $n = 0$.

Figure 4.2. Comparison of systems with stable DFE with identical sets of eigenvalues. The line with open circles in each graph is the eigenvector $\mathbf{w}^{(1)}$ corresponding to $\lambda_1 = s(\mathbf{J}_0)$, the maximum eigenvalue of the Jacobian matrix of Eq. evaluated at the DFE. The dashed line in each graph is the eigenvector $\mathbf{w}^{(2)}$ corresponding to λ_2, the minimum eigenvalue at DFE. The angle θ is the angle formed by these eigenvectors. The shaded area is the cone of epidemicity where the Rayleigh quotient, which at its maximum is equivalent to reactivity, is positive and predicts increasing total levels of infection $\left(d\sqrt{x^2 + y^2} / dt > 0 \right)$. The eigenvectors and associated cone of epidemicity approximate the nonlinear system near the DFE. Black solid lines are sample trajectories returning to the DFE. (a) A reactive system ($\mathbf{E}_0 = 3.175 > 1$). The product of transmission efficiency from vectors to hosts and the ratio of vectors to hosts, $b_x m$, is greater than the transmission efficiency from hosts to vectors ($b_x m > b_y e^{-\mu n}$), and an epidemic will elevate prevalence within human hosts. The parameter values are as in Figure 1a. (b) A nonreactive system ($\mathbf{E}_0 = 0.63 < 1$) with $b_x m = b_y e^{-\mu n}$. No epidemic is possible. The parameter values are as in Figure 1b. (c) A reactive system ($\mathbf{E}_0 = 3.175 > 1$) with $b_x m < b_y e^{-\mu n}$. An epidemic elevates prevalence within vectors. The parameter values are $a = 0.3125$, $b_x = 0.01$, $b_y = 1$, $m = 1.6$, $r = 0.01$, $\mu = 0.25$, $n = 0$.
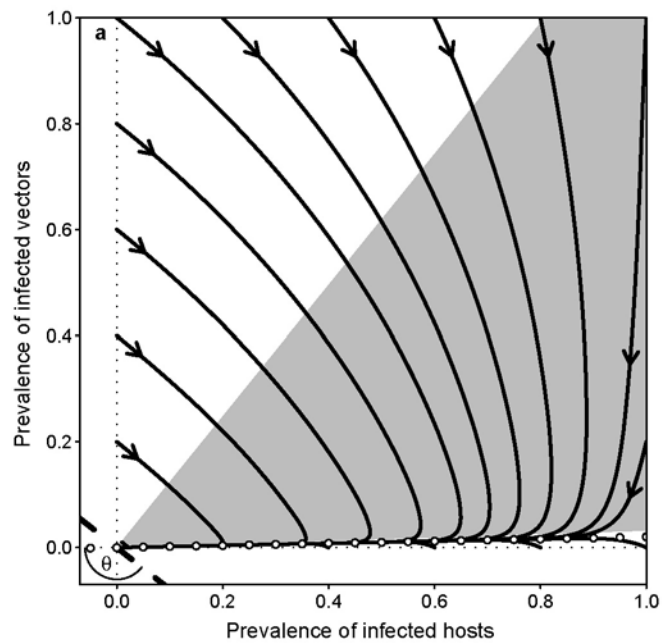
Figure 4.2a.
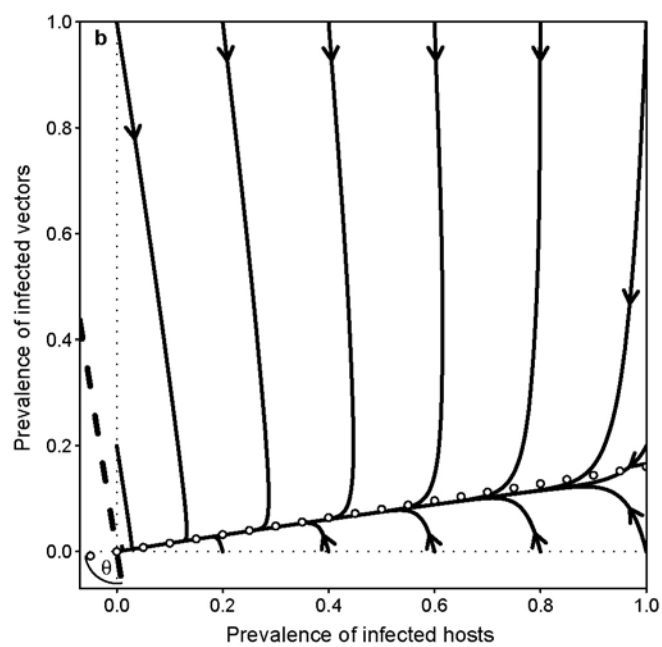
Figure 4.2b.
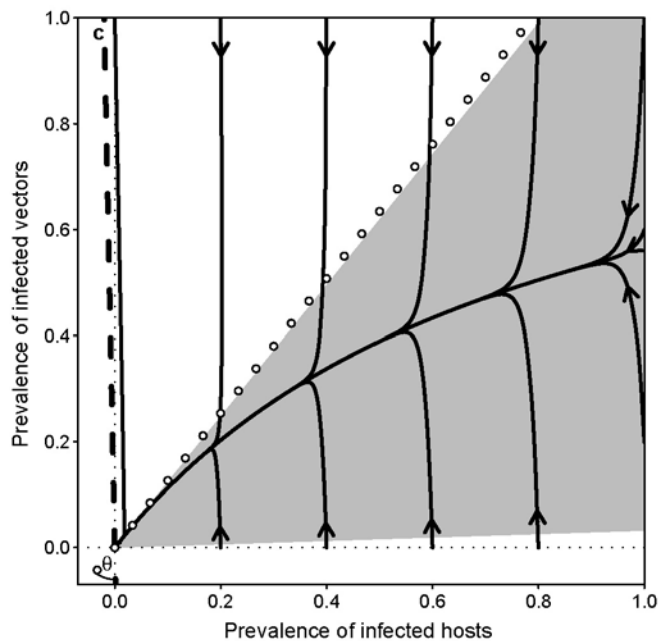
Figure 4.2c.
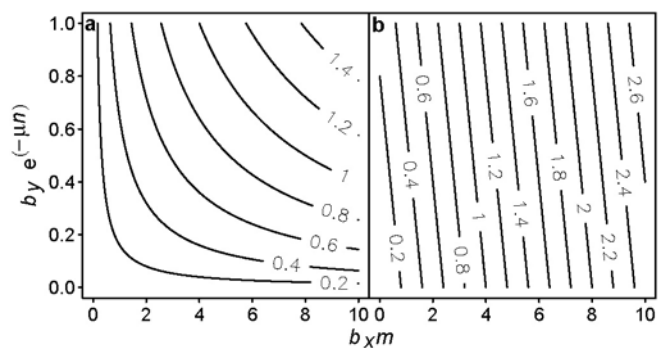
Figure 4.3. Contour graphs of $\mathbf{R}_0$ and $\mathbf{E}_0$ for combinations of $b_x m$ and $b_y e^{-\mu n}$ in the standard model (4.1). Constant parameter values are $a = 0.025$, $r = 0.01$, and $\mu = 0.25$. (a) Contours give the values of $\mathbf{R}_0$ for combinations of $b_x m$ and $b_y e^{-\mu n}$. (b) Contours give the values of $\mathbf{E}_0$ for combinations of $b_x m$ and $b_y e^{-\mu n}$. The transmission efficiency from vectors to hosts b_x and the vector-host ratio m are strong candidates for control strategies designed to reduce $\mathbf{R}_0$ and even more effective for reducing $\mathbf{E}_0$. The transmission efficiency from hosts to vectors b_y and the length of the extrinsic incubation period n have a strong effect on $\mathbf{R}_0$ but is less important for $\mathbf{E}_0$. Note that $\mathbf{E}_0 \geq \mathbf{R}_0$; this can be seen from the arithmetic-geometric means inequality applied to the threshold indices.

5 GENERAL CONCLUSIONS

Models are developed and applied to bridge the gap between existing empirical data and our need to understand and predict ecological systems. In complex communities, uncertainty is high and existing modeling techniques are unable to bridge satisfactorily this gap. New modeling tools are needed to understand and predict how these systems will react to anthropogenic and environmental pressures. In this dissertation, I addressed three forms of uncertainty associated with complex ecological systems: stability, equilibrium response, and non-equilibrium dynamics.

A graph-theoretic approach (Levins 1974, Dambacher et al. 2002) is used that enables researchers to include natural history information about the system of interest. Positive and negative feedback cycles, which enhance or dampen system response to perturbation, are identified (Chapter 2). These feedback cycles determine the stability of the ecosystem. Sensitivity analysis identifies critical links that form these feedback cycles. An algorithm based on the graph-theoretic approach provides an index that measures the relative contribution of a mechanistic link between variables to positive and negative feedback cycles. A proposed sensitivity weight index prioritizes direct effects relative to their effect on ecosystem stability. The resulting hierarchy can help guide researchers and managers to optimize resources for environmental monitoring, to explore alternative management strategies, and to formulate new testable hypotheses.

This graph-theoretic approach is developed further into a probabilistic model in Chapter 3. Here, the focus is on predicting the change in the long-term equilibrium of ecosystem variables under different perturbation scenarios. In addition, this chapter develops a theoretic method to compare alternative hypotheses for model structure. Conditional probabilities of increase and decrease are transferred from the graph-theoretic models into a Bayesian Belief Network (BBN). The BBN allows researchers to both predict how an ecosystem might change given a perturbation and also diagnose which model structure matches empirical observation.

In some ecological systems, the transitory dynamics are important. Under this scenario, management typically seeks to avoid large magnitude deviations from equilibrium. For instance, in vector-borne disease, many individuals might be exposed to a pathogen introduction, and public health will seek to minimize the risk of an epidemic. The concept of reactivity is used to derive a threshold index for epidemicity, $\mathbf{E}_0$, which gives the maximum number of new infections produced by an infective individual at a disease free equilibrium (Chapter 4). This index provides a threshold that determines whether or not major epidemics are likely. The relative importance of parameters differs between control strategies that seek to reduce endemicity and those that seek to reduce epidemicity. Vector behavior more strongly affects epidemicity than endemicity. The index $\mathbf{E}_0$ therefore is an important measure of epidemic potential that helps guide efforts to combat epidemics.

Three new theoretic approaches are presented. First, a graph-theoretic approach identifies the interconnections in a complex ecosystem that promote or diminish its stability. Second, a combined graph-theoretic and probabilistic approach evaluates the potential for long-term changes in equilibrium. Third, a threshold index predicts whether or not large-magnitude short-term transitory changes in disease prevalence can occur. Thus, each theoretic approach deals with a different facet of uncertainty and advances our understanding of the complexity and interconnectedness in ecological systems

BIBLIOGRAPHY

Afrane, Y. A., B. W. Lawson, A. K. Githeko, and G. Yan. 2005. Effects of microclimate changes caused by land use and land cover on duration of gonotrophic cycles of *Anopheles gambiae* (Diptera: Culicidae) in western Kenya highlands. Journal of Medical Entomology 42:974-980.

Aron, J. L., and R. M. May. 1982. The population dynamics of malaria. In: Anderson, R. M. (Ed.), The population dynamics of infectious diseases. Chapman and Hall, London, pp. 139-179.

Bailey, N. T. J., 1982. The biomathematics of malaria. Charles Griffin and Company, High Wycombe, UK.

Bacaër, N., and C. Sokhna. 2005. A reaction-diffusion system modeling the spread of resistance to an antimalarial drug. Mathematical Biosciences and Engineering 2:227-238.

Baxter, C. V., K. D. Fausch, M. Murakami, and P. L. Chapman. 2004. Fish invasion restructures stream and forest food webs by interrupting reciprocal prey subsidies. Ecology 85:2656-2663.

Bender, E. A., T. J. Case, and M. E. Gilpin. 1984. Perturbation experiments in community ecology: theory and practice. Ecology 65:1-13.

Berlow, E. L., A. M. Neutel, J. E. Cohen, P. C. de Ruiter, B. Ebenman, M. Emmerson, J. W. Fox, V. A. A. Jansen, J. I. Jones, G. D. Kokkoris, D. O. Logofet, A. J. McKane, J. M. Montoya, and O. Petchey. 2004. Interaction strengths in food webs: issues and opportunities. Journal of Animal Ecology 73:585-598.

Berman, A., M. Neumann, and R. J. Stern. 1989. Nonnegative matrices in dynamic systems. John Wiley and Sons, Inc., New York.

Borer, E. T., C. J. Briggs, W. W. Murdoch, and S. L. Swarbrick. 2003. Testing intraguild predation theory in a field system: does numerical dominance shift along a gradient of productivity? Ecology Letters 6:929-935.

Borer, E. T., W. W. Murdoch, and S. L. Swarbrick. 2004. Parasitoid coexistence: linking spatial field patterns with mechanism. Ecology 85:667-678.

Borusk, M. E., C. A. Stow, and K. H. Reckhow. 2004. A Bayesian network of eutrophication models for synthesis, prediction, and uncertainty analysis. Ecological Modelling 173:219-239.

Burger, J. A., and M. Gochfeld. 1997. Paradigms for ecological risk assessment. Annals of the New York Academy of Sciences 837:372-86.

Burgman, M. A. 2005. Risks and decisions for conservation and environmental management. University Press, Cambridge, UK.

Cain, J. 2001. Planning improvements in natural resource management. Centre for Ecology and Hydrology, Wallingford, UK. http://www.norsys.com/downloads/BBN%20Guidelines%20-%20Cain.pdf

Carpenter, S. R., C. E. Kraft, R. Wright, X. He, P. A. Soranno, and J. R. Hodgson. 1992. Resilience and resistance of a lake phosphorus cycle before and after a food web manipulation. American Naturalist 140:781-798.

Caswell, H. 2001. Matrix Population Models, 2nd Edition. Sinauer Associates, Inc., Sunderland, MA, USA.

Caswell, H. 2007. Sensitivity analysis of transient population dynamics. Ecology Letters 10:1-15.

Chitnis, N., J. M. Cushing, and J. M. Hyman. 2006. Bifurcation analysis of a mathematical model for malaria transmission. SIAM Journal on Applied Mathematics 67:24-45.

Cottingham, K. L., and D. E. Schindler. 2000. Effects of grazer community structure on phytoplankton response to nutrient pulses. Ecology 81:183-200.

Craig, M. H., R. W. Snow, and D. le Sueur. 1999. A climate-based distribution model of malaria transmission in sub-Saharan Africa. Parasitology Today 15:105-111.

Dambacher, J. M., D. T. Brewer, D. M. Dennis, M. Macintyre, and S. Foale. 2007. Qualitative modeling of gold mine impacts on Lihir Island's socioeconomic system and reef-edge fish community. Environmental Science and Technology 41:555-562.

Dambacher, J. M., H. W. Li, and P. A. Rossignol. 2002. Relevance of community structure in assessing indeterminacy of ecological predictions. Ecology 83:1372-1385.

Dambacher, J. M., H. W. Li, and P. A. Rossignol. 2003a. Qualitative predictions in model ecosystems. Ecological Modelling 161:79-93.

Dambacher, J. M., H.-K. Luh, H. W. Li, and P. A. Rossignol. 2003b. Qualitative stability and ambiguity in model ecosystems. American Naturalist 161:876-888.

Dambacher, J. M., R. Levins, and P. A. Rossignol. 2005. Life expectancy change in perturbed communities: derivation and qualitative analysis. Mathematical Biosciences 197:1-14.

Dambacher, J. M., and R. Ramos-Jiliberto. 2007. Understanding and predicting effects of modified interactions through a qualitative analysis of community structure. Quarterly Review of Biology 82:227-250.

Day, J. F., K. M. Ebert, and J. D. Edman. 1983. Feeding patterns of mosquitoes (Diptera:Culicidae) simultaneously exposed to malarious and healthy mice, including a method for separating blood meals from conspecific hosts. Journal of Medical Entomology 20:120-127.

Diekmann, O., and J. A.Heesterbeek, J. A. F., 2000. Mathematical epidemiology of infectious diseases: model building, analysis, and interpretation. John Wiley and Sons, Inc., New York.

Dietz, K. 1988. Mathematical models for transmission and control of malaria. In: Wernsdorfer, W. H., and McGregor, I. (Eds.), Malaria: principles and practice of malariology, vol. 2. Churchill Livingstone, London, pp. 1091-1133.

Dietz, K., L. Molineaux, and A. Thomas. 1974. A malaria model tested in the African savannah. Bulletin of the World Health Organization 50:347-357.

Dobson, A. P., 1988. The population biology of parasite-induced changes in host behavior. Quarterly Review of Biology 63:139-165.

Dojer, N., A. Gambin, A. Mizera, B. Wilczynski, and J. Tiuryn. 2006. Applying dynamic Bayesian networks to perturbed gene expression data. BMC Bioinformatics 7:249.

Dye, C., 1992. The analysis of parasite transmission by bloodsucking insects. Annual Review of Entomology. 37:1-19.

Dye, C., and G. Hasibeder. 1986. Population dynamics of mosquito-borne disease: effects of flies which bite some people more frequently than others. Trans. R. Soc. Trop. Med. Hyg. 80:69-77.

Fairbrother, A., and J. G. Turnley. 2005. Predicting risks of uncharacteristic wildfires: application of the risk assessment process. Forest Ecology and Management 211:28-35.

Feng, Z., and J. X. Velasco-Hernandez. 1997. Competitive exclusion in a vector-host model for the dengue fever. Journal of Mathematical Biology 35:523-544.

Ferson, S. 1996. What Monte Carlo methods cannot do. Human and Ecological Risk Assessment 2:990-1007.

Fillinger, U., and S. W. Lindsay. 2006. Suppression of exposure to malaria vector by an order of magnitude using microbial larvicides in rural Kenya. Tropical Medicine and International Health 11:1629-1642.

Foppa, I. M., and A. Spielman. 2007. Does reservoir host mortality enhance transmission of West Nile virus? Theoretical Biology and Medical Modelling 4:17.

Francis, R. I. C. C., and R. Shotton. 1997. "Risk" in fisheries management: a review. Canadian Journal of Fisheries and Aquatic Sciences 54:1699-1715.

Franklin, J. N. 1993. Matrix Theory. Dover Publications, Inc., Mineola, NY, USA.

Garrett-Jones, C., 1964. The human blood index of malaria vectors in relation to epidemiological assessment. Bulletin of the World Health Organization 30:241-261.

Girard, M. P., Z. H. Reed, M. Friede, and M. P. Kieny. 2007. A review of human vaccine research and development: Malaria. Vaccine 25:1567-1580.

Gunasekaran, K., S. S. Sahu, P. Jambulingam, and P. K. Das. 2005. DDT indoor residual spray, still an effective tool to control *Anopholes fluviatilis*-transmitted *Plasmodium falciparum* malaria in India. Tropical Medicine and International Health 10:160-168.

Guneralp, B. 2007. An improved formal approach to demographic loop analysis. Ecology 88:2124-2131.

Hardin, G. 1960. The competitive exclusion principle. Science 131:1292-1297.

Hasibeder, G., and C. Dye. 1988. Population dynamics of mosquito-borne disease: persistence in a completely heterogeneous environment. Theoretical Population Biology 33:31-53.

Hayes, K. R. 2002. Identifying hazards in complex ecological systems. Part 2. Infections modes and effects analysis for biological invasions. Biological Invasions 4:251-261.

Hayes, K. R., A. R. Kapuscinski, G. Dana, L. Sifa, and R. H. Devlin. 2007. Introduction to Environmental Risk Assessment for Transgenic Fish. Pages 1-28 in A. R. Kapuscinski, K. R. Hayes, S. Li, and G. Dana (editors) Environmental Risk Assessment of Genetically Modified Organisms, Volume 3: Methodologies for Transgenic Fish. CABI Publishing, Oxfordshire, UK.

Hill, M. F., J. D. Witman, and H. Caswell. 2004. Markov chain analysis of succession in a rocky subtidal community. American Naturalist 164:E46-E61.

Hoffman, E. O., and J. S. Hammonds. 1994. Propagation of uncertainty in risk assessments: the need to distinguish between uncertainty due to lack of knowledge and uncertainty due to variability. Risk Analysis 14:707-712.

Horn, R. A., and C. R. Johnson. 1985. Matrix analysis. Cambridge University Press, New York.

Hosack, G. R., K. R. Hayes, and J. M. Dambacher. 2008. Assessing model structure uncertainty through an analysis of system feedback and Bayesian networks. Ecological Applications 18(4):1070-1082.

Householder, A. S. 1964. The theory of matrices in numerical analysis, 1st edn. Blaisdell Publishing Company, New York.

Hulot, F. D., G. Lacroix, F. Lescher-Moutoue, and M. Loreau. 2000. Functional diversity governs ecosystem response to nutrient enrichment. Nature 405:340-344.

Hurwitz, A. (1895) 1964. On the conditions under which an equation has only roots with negative real parts. Translated from the German by H. G. Bergman. Pp. 77-82 in R. E. Bellman and R. Kalaba (Eds.) Selected papers on mathematical trends in control theory. Dover, New York, NY.

Ives, A. R., and S. R. Carpenter. 2007. Stability and diversity of ecosystems. Science 317:58-62.

Killeen, G. F., U. Fillinger, and B. G. J. Knols. 2002. Advantages of larval control for African malaria vectors: low mobility and behavioural responsiveness of immature mosquito stages allow high effective coverage. Malaria Journal 1:8.

Kingsolver, J. G. 1987. Mosquito host choice and the epidemiology of malaria. American Naturalist 130:811-827.

Koella, J. C., and R. Antia. 2003. Epidemiological models for the spread of anti-malarial resistance. Malaria Journal 2:3.

Koella, J. C., F. L. Sørensen, and R. Anderson. 1998. The malaria parasite *Plasmodium falciparum* increases the frequency of multiple feeding of its mosquito vector *Anopheles gambiae*. Proceedings of the Royal Society B Biological Sciences 265:763-768.

Koenker, R. 2005. Quantile regression. Cambridge University Press, New York. USA.

Koenker, R. 2006. quantreg: Quantile Regression. R package version 3.90. http://www.r-project.org

Lacroix, R., W. R. Mukabana, L. C. Gouagna, and J. C. Koella. 2005. Malaria infection increases attractiveness of humans to mosquitoes. PLoS Biology 3:1590-1593.

Lajmanovich, A., and J. A. Yorke. 1976. A deterministic model for gonorrhea in a nonhomogeneous population. Mathematical Biosciences 28:221-236.

Letellier, C., G. F. V. Amaral, and L. A. Aguirre. 2007. Insights into the algebraic structure of Lorenz-like systems using feedback analysis and piecewise affine models. Chaos 17:023104.

Levins, R. 1974. The qualitative analysis of partially specified systems. Annals of the New York Academy of Sciences 231:123-138.

Levins, R.1975. Evolution in communities near equilibrium, pp. 16-50 *in* M. L. Cody, and J. M. Diamond, eds. Ecology and Evolution of Communities. Belknap Press, Cambridge, MA, USA.

Levins, R. 1998. Qualitative mathematics for understanding, prediction, and intervention in complex ecosystems, pp. 178-204 *in* D. Rapport, R. Costanza, P. R. Epstein, C. G. Gaudet, and R. Levins, eds. Ecosystem Health. Blackwell Science, Inc., Malden, MA, USA.

Lloyd, A. L., J. Zhang, and A. M. Root. 2007. Stochasticity and heterogeneity in host-vector models. Journal of the Royal Society Interface 4:851-863.

Lotka, A. J. 1923. Contribution to the analysis of malaria epidemiology. American Journal of Hygiene 3(Suppl. 1):1-121.

Luck, R. F., and H. Podoler. 1985. Competitive exclusion of *Aphytis lingnanensis* by *A. melinus*: potential role of host size. Ecology 66:904-913.

Mabaso, M. L. H., M. Craig, A. Ross, and T. Smith. 2007. Environmental predictors of the seasonality of malaria transmission in Africa: the challenge. American Journal of Tropical Medicine and Hygiene 76:33-38.

Macdonald, G. 1952. The analysis of equilibrium in malaria. Tropical Diseases Bulletin 49:813-828.

Macdonald, G. 1957. The epidemiology and control of malaria. Oxford University Press, London.

Marcot, B. G., R. S. Holthausen, M. G. Raphael, M. M. Rowland, and M. J. Wisdom. 2001. Using Bayesian belief networks to evaluate fish and wildlife population viability under land management alternatives from an environmental impact statement. Forest Ecology and Management 153:29-42.

May, R. M. 1974. Stability and Complexity in Model Ecosystems, 2nd Edition. Princeton University Press, Princeton, NJ, USA.

McDermott, J. J., and P. G. Coleman. 2001. Comparing apples and oranges - model-based assessment of different tsetse-transmitted trypanosomosis control strategies. International Journal for Parasitology 31:603-609.

Metropolis, N., and S. Ulam. 1949. The Monte Carlo method. Journal of the American Statistical Association 44:335-341.

Minc, H. 1978. Permanents. Encyclopedia of Mathematics and Its Applications. Vol. 6. Addison-Wesley Publishing Company, Reading, UK.

Morgan, M. G., and M. Henrion. 1990. Uncertainty: a guide to dealing with uncertainty in quantitative risk and policy analysis. Cambridge University Press, Melbourne, Victoria, Australia.

Mortera, J., A. P. Dawid, and S.L. Lauritzen. 2003. Probabilistic expert systems for DNA mixture profiling. Theoretical Population Biology 63:191-205.

Munga, S., N. Minakawa, G. Zhou, E. Mushinzimana, O.-O. J. Barrack, A. K. Githeko, and G. Yan. 2006. Association between land cover and habitat productivity of malaria vectors in western Kenyan highlands. American Journal of Tropical Medicine and Hygiene 74:69-75.

Murdoch, W., C. J. Briggs, and S. Swarbrick. 2005. Host suppression and stability in a parasitioid-host system: experimental demonstration. Science 309:610-613.

Nakajima, H. 1992. Sensitivity and stability of flow networks. Ecological Modelling 62:123-133.

Neubert, M. G., and H. Caswell. 1997. Alternatives to resilience for measuring the responses of ecological systems to perturbations. Ecology 78:653-665.

Ngwa, G. A. 2004. Modelling the dynamics of endemic malaria in growing populations. Discrete and Continuous Dynamical Systems B 4:1173-1202.

Norsys. 2006. Netica. www.norsys.com

OGTR (Office of the Gene Technology Regulator). 2005. Risk analysis framework. Department of Health and Ageing, Australian Government. Canberra, Australian Capital Territory.

Ong, I. M., J. D. Glasner, and D. Page. 2002. Modelling regulatory pathways in *E. coli* from time series expression profiles. Bioinformatics 18(S1):S241-S248.

Pascual, M., J. A. Ahumada, L. F. Chaves, X. Rodo, and M. Bouma. 2006. Malaria resurgence in the East African highlands: temperature trends revisited. Proceedings of the National Academy of Sciences USA 103:5829-5834.

Paul, R. E. L., M. Diallo, and P. T. Brey. 2004. Mosquitoes and transmission of malaria parasites - not just vectors. Malaria Journal 3:39.

Pearl, J. 2000. Causality: models, reasoning, and inference. Cambridge University Press, New York, New York, USA.

Pollino, C. A., O. Woodberry, A. Nicholson, K. Korb, and B. T. Hart. 2007. Parameterisation and evaluation of a Bayesian network for use in an ecological risk assessment. Environmental Modelling and Software 22:1140-1152.

Puccia, C. J., and R. Levins. 1985. Qualitative modeling of complex systems. Harvard University Press, Cambridge, MA.

Punt, A. E., and R. Hilborn. 1997. Fisheries stock assessment and decision analysis: the Bayesian approach. Reviews in Fish Biology and Fisheries 7:35-63.

RCDT (R Core Development Team). 2005. R: A language and environment for statistical computing. R Foundation for Statistical Computing, Vienna, Austria. www.R-project.org

Reckhow, K. H. 1994. Water quality simulation modelling and uncertainty analysis for risk assessment and decision making. Ecological Modelling 72:1-20.

Regan, H. M., M. Colyvan, and M. A. Burgman. 2002. A taxonomy and treatment of uncertainty for ecology and conservation biology. Ecological Applications 12:618-628.

Ross, R. 1911. The Prevention of Malaria. Murray, London, 2nd ed.

Rossignol, P. A., J. M. C. Ribeiro, M. Jungery, M. J. Turell, A. Spielman, and C. L. Bailey. 1985. Enhanced mosquito blood-finding success on parasitemic hosts: evidence for vector-parasite mutualism. Proceedings of the National Academy of Sciences USA 82:7725-7727.

Rossignol, P. A., J. M. C. Ribeiro, and A. Spielman, A., 1984. Increased intradermal probing time in sporozoite-infected mosquitoes. American Journal of Tropical Medicine and Hygiene 33:17-20.

Rossignol, P. A., and J. M. C. Ribeiro, and A. Spielman. 1986. Increased biting rate and reduced fertility in sporozoite-infected mosquitoes. American Journal of Tropical Medicine and Hygiene 35, 277-279.

Ruan, S., D. Xiao, and J. C. Beier. 2008. On the delayed Ross-Macdonald model for malaria transmission. Bulletin of Mathematical Biology 70:1098-1114.

Ruckelshaus, M. H., P. Levin, J. B. Johnson, and P. M. Kareiva. 2002. The Pacific salmon wars: what science brings to the challenge of recovering species. Annual Review of Ecology and Systematics 33:66-706.

Scheffer, M., S. Carpenter, J. A. Foley, and B. Walker. 2001. Catastrophic shifts in ecosystems. Nature 413:591-596.

Scheffer, M., S. H. Hosper, M. L. Meijer, and B. Moss. 1993. Alternative equilibria in shallow lakes. Trends in Ecology and Evolution 8:275-279.

Schmitz, O. J. 1997. Press perturbations and the predictability of ecological interactions in a food web. Ecology 78:55-69.

Shipley, B. 2000. Cause and correlation in biology. Cambridge University Press, Cambridge, UK.

Sibly, R. M., D. Barker, J. Hone, and M. Pagel. 2007. On the stability of populations of mammals, birds, fish, and insects. Ecology Letters 10:970-976.

Sih, A., P. Crowley, M. McPeek, J. Petranka, and K. Strohmeier. 1985. Predation, competition, and prey communities: a review of field experiments. Annual Review of Ecology and Systematics 16:269-311.

Smith, D. L., J. Dushoff, R. W. Snow, and S. I. Hay. 2005. The entomological inoculation rate and *Plasmodium falciparum* infection in African children. Nature 438:492-495.

Smith, D. L., and F. E. McKenzie. 2004. Statics and dynamics of malaria infection in Anopheles mosquitoes. Malaria Journal 3:13.

Smith, D. L., F. E. McKenzie, R. W. Snow, and S. I. Hay. 2007. Revisiting the basic reproductive number for malaria and its implications for malaria control. PLoS Biology 5:e42.

Soule, C. 2003. Graphic requirements for multistationarity. Complexus 1:123-133.

Stiber, N. A., M. J. Small, and M. Pantazidou. 2004. Site-specific updating and aggregation of Bayesian Belief Network models for multiple experts. Risk Analysis 24:1529-1538.

Takken, W., and B. G. J. Knols. 1999. Odor-mediated behavior of afrotropical malaria mosquitoes. Annual Review of Entomology 44:131-157.

Tanner, J. E., T. P. Hughes, and J. H. Connell. 1994. Species coexistence, keystone species, and succession: a sensitivity analysis. Ecology 75:2204-2219.

Ticehurst, J. L., L. T. H. Newham, D. Rissik, R. A. Letcher, and A. J. Jakeman. 2007. A Bayesian network approach for assessing the sustainability of coastal lakes in New South Wales, Australia. Environmental Modelling and Software 22:1129-1139.

Thieme, H. R. 2003. Mathematics in population biology. Princeton University Press, Princeton, New Jersey.

Thomas, R., and M. Kaufman. 2005. Frontier diagrams: partition of phase space according to the signs of eigenvalues or sign patterns of the circuits. International Journal of Bifurcation and Chaos 15:3051-3074.

Thomson, M. C., F. J. Doblas-Reyes, S. J. Mason, R. Hagedorn, S. J. Connor, T. Phindela, A. P. Morse, and T. N. Palmer. 2006. Malaria early warnings based on seasonal climate forecasts from multi-model ensembles. Nature 439:576-579.

USEPA (U. S. Environmental Protection Agency). 1992. Framework for ecological risk assessment, EPA/630/R-92/001. Risk Assessment Forum, Washington, DC, USA.

Vance, R. R. 1978. Predation and resource partitioning in one predator - two prey model communities. American Naturalist 112:797-813.

van den Driessche, P., and J. Watmough. 2002. Reproduction numbers and sub-threshold endemic equilibria for compartmental models of disease transmission. Mathematical Biosciences 180:29-48.

Venables, W. N., and B. D. Ripley. 2002. Modern Applied Statistics with S. 4th Edition. Springer-Verlag, New York, USA.

Woolhouse, M. E. J., C. Dye, J.-F. Etard, T. Smith, J. D. Charlwood, G. P. Garnett, P. Hagan, J. L. K. Hii, P. D. Ndhlovu, R. J. Quinnell, C. H. Watts, S. K. Chandiwana, and R. M. Anderson. 1997. Heterogeneous host-vector contact rates and the control of vector-borne diseases. Proceedings of the National Academy of Sciences USA 94:338-342.

Wootton, J. T. 1994. The nature and consequences of indirect effects. Annual Review of Ecology and Systematics 25:443-466.

Wootton, J. T. 2001. Prediction in complex communities: analysis of empirically derived Markov models. Ecology 82:580-598.

Wootton, J. T., and M. Emmerson. 2005. Measurement of interaction strength in nature. Annual Review of Ecology, Evolution, and Systematics 36:419-444.

World Health Organization, 1975. Manual on practical entomology in malaria, part 1. Geneva, Switzerland.

Varis, O., and S. Kuikka. 1999. Learning Bayesian decision analysis by doing: lessons from environmental and natural resources management. Ecological Modelling 119:177-195.

Yodzis, P. 1988. The indeterminacy of ecological interactions as perceived through perturbation experiments. Ecology 69:508-515.

Yonow, T., C. C. Brewster, J. C. Allen, and M. I. Meltzer. 1998. Models for heartwater epidemiology: practical implications and suggestions for future research. Onderstepoort Journal of Veterinary Research 65, 263-273.

Yu, D. S., R. F. Luck, and W. W. Murdoch. 1990. Competition, resource partitioning and coexistence of an endoparasitoid *Encarsia perniciosi* and an ectoparasitoid *Aphytis melinus* of the California red scale. Ecological Entomology 15:469-480.

APPENDICES

APPENDIX A. MATHEMATICAL DERIVATION OF SENSITIVITY MATRICES

A.1 Stability criteria

The direct effects of a signed digraph translate into the entries within the signed digraph's corresponding Jacobian matrix $\mathbf{A}$ (Figure 2.1). The matrix entry in the ith row and the jth column shows the magnitude (a_{ij}), and the sign ($+$, $-$) of the direct effect of species j on species i near a steady state. The a_{ij}, and their associated signs, describe the direct effect of species j on species i and incorporate parameters such as species interaction magnitudes and rates of growth and decay at a steady state (May 1974). The eigenvalues of $\mathbf{A}$ determine whether or not a community is stable and are derived from the characteristic equation

$$\det(\mathbf{A} - \lambda) = \sum_{k=0}^{n} F_k \lambda^{n-k} = F_0 \lambda^n + F_1 \lambda^{n-1} + \cdots + F_n = 0, \tag{A.1}$$

where F_k are the polynomial coefficients, k denotes the feedback level, $F_0 = -1$ by convention, and n is the number of species within the community. The polynomial coefficients F_k are sums of cycle products that include k variables. The n roots of Equation (A.1) are the eigenvalues of $\mathbf{A}$.

A negative real part for all eigenvalues implies that the equilibrium is stable. There are two criteria for all eigenvalues of Equation (A.1) to have negative real parts:

1) The coefficients F_k, $k = 0 \ldots n$, of the characteristic polynomial must all have the same sign. Since we adopt the convention that $F_0 = -1$, this means that all coefficients F_k must be negative.

2) All n Hurwitz determinants, Δ_k, $k = 1 \ldots n$, must be positive. The signs of the F_k as specified above are reversed to conform with the convention of Hurwitz ([1895] 1964). The second criterion thus takes the form

$$\Delta_k = \det \begin{bmatrix} -F_1 & -F_3 & -F_5 & \cdots & -F_{2k-1} \\ -F_0 & -F_2 & -F_4 & \cdots & -F_{2k-2} \\ 0 & -F_1 & -F_3 & \cdots & -F_{2k-3} \\ \vdots & \vdots & \vdots & \ddots & \vdots \\ 0 & . & . & . & -F_k \end{bmatrix} > 0, \quad k = 1 \ldots n, \tag{A.2}$$

where the $-F_h$ with $h < 0$ or $h > n$ evaluate to zero.

The first criterion is a necessary condition for stability. The second criterion is both necessary and sufficient (Hurwitz [1895] 1964). Further, the condition in the second criterion that $\Delta_{n-1} > 0$ and $\Delta_n > 0$ is equivalent to the condition that $\Delta_{n-1} > 0$ and $F_n < 0$, that is, the condition that $\Delta_n > 0$ is redundant (Hurwitz [1895] 1964).

A.2 Structural stability

The community structure is given a matrix representation. The entries of the matrix $°\mathbf{A}$ take the values 0, $+1$, or 1 depending on the sign associated with the a_{ij} in the matrix $\mathbf{A}$. The matrix $°\mathbf{A}$ can be formally defined as the transposed signed adjacency matrix of the signed digraph. The following calculations provide qualitative measures of structural stability (see Dambacher *et al.* 2003 for details).

The net number of cycle products at each feedback level, that is, the net number of positive and negative monomial terms within each F_k, is denoted $°F_k$ and is calculated by substituting the matrix $°\mathbf{A}$ for the symbolic matrix $\mathbf{A}$ in Equation (A.1). The total number of cycle products within each coefficient, denoted $^\bullet F_k$, is calculated using the matrix permanent (Minc 1978) and the matrix $^\bullet\mathbf{A}$. The matrix $^\bullet\mathbf{A}$ is defined by the absolute value of the entries within $°\mathbf{A}$ and is equivalent to the (unsigned) transposed adjacency matrix of the signed digraph. The $^\bullet F_k$ are calculated using the equation

$$\text{per}\left(\left|\vec{\mathbf{A}}\right|+\lambda\right)=\sum_{k=0}^{n}F_{k}^{'}\lambda^{n-k}=F_{0}^{'}\lambda^{n}+F_{1}^{'}\lambda^{n-1}+\cdots+F_{n}^{'}=0, \qquad (A.3)$$

where $\left|\vec{\mathbf{A}}\right|$ denotes the absolute value of the entries within the symbolic matrix $\mathbf{A}$, and per refers to

the matrix permanent. The matrix $^{\bullet}\mathbf{A}$ is substituted for $\mathbf{A}$ in Equation (A.3) to obtain the $^{\bullet}F_{k}$.

Weighted feedback is defined as $wF_{k}={}^{\circ}F_{k}/{}^{\bullet}F_{k}$, for $k=1\ldots n$. The measure wF_{k} is the

ratio of the net number of cycle products to the total number of cycle products appearing within the

k^{th} coefficient. Weighted feedback of -1.0 ($+1.0$) indicates that a coefficient is composed entirely

of negative (positive) cycle products. Weighted feedback is 0 if an equal number of negative and

positive cycle products are present. Weighted feedback between 0 and -1.0 ($+1.0$) indicates more

negative (positive) cycle products are present than positive (negative) cycle products.

The net number of addends in each Hurwitz determinant, $^{\circ}\Delta_{k}$, $k=1\ldots n$, are derived by

substituting the net polynomial coefficients, $^{\circ}F_{k}$, for the symbolic coefficients, F_{k}, in Equation (A.2).

The absolute number of terms in each Hurwitz determinant, $^{\bullet}\Delta_{k}$, $k=1\ldots n$, are derived from the

equation

$$\Delta_{k}^{'}=\text{per}\begin{bmatrix} F_{1}^{'} & F_{3}^{'} & F_{5}^{'} & \cdots & F_{2k-1}^{'} \\ F_{0}^{'} & F_{2}^{'} & F_{4}^{'} & \cdots & F_{2k-2}^{'} \\ 0 & F_{1}^{'} & F_{3}^{'} & \cdots & F_{2k-3}^{'} \\ \vdots & \vdots & \vdots & \ddots & \vdots \\ 0 & . & . & . & F_{k}^{'} \end{bmatrix}, \qquad (A.4)$$

by substituting the $^{\bullet}F_{k}$ for $F_{k}^{'}$ in Equation (A.4).

Weighted Hurwitz determinants compare the relative magnitudes of different level of

feedback and are computed as $w\Delta_{k}={}^{\circ}\Delta_{k}/{}^{\bullet}\Delta_{k}$. The measure $w\Delta_{k}$ is the ratio of the net number of

addends to the total number of addends appearing within the kth Hurwitz determinant (Dambacher *et*

al. 2003). A weighted Hurwitz determinant of $+1.0$ (-1.0) indicates that the Hurwitz determinant is

composed entirely of positive (negative) addends. A weighted Hurwitz determinant is 0 if an equal number of positive and negative addends are present. A weighted Hurwitz determinant between 0 and $+1.0$ (-1.0) indicates that more positive (negative) addends are present than negative (positive) addends. The $w\Delta_n$ provide a measure of structural stability (see Dambacher *et al.* 2003).

A.3 Stability sensitivity

A.3.1 Partial derivatives of determinants and permanents

We use partial derivatives of determinants and permanents to determine how the direct effects affect feedback in a community. The direct effects that compose the entries in the matrix $\mathbf{A}$ usually consist of a combination of parameters that describe rates of birth and death. Let γ represent one such parameter, and assume that the entries in $\mathbf{A}(\gamma)$ are differentiable functions of γ. The partial derivative of the determinant of this matrix with respect to γ is calculated using the equation

$$\frac{\partial \det \mathbf{A}(\gamma)}{\partial \gamma} = \sum_{q=1}^{n} \det \mathbf{A}(\gamma)_q, \tag{A.5}$$

where $\det \mathbf{A}(\gamma)_q$ is the determinant formed by replacing the qth row of $\mathbf{A}(\gamma)$ with the row of partial derivatives $\frac{\partial \mathbf{A}(\gamma)_{qj}}{\partial \gamma}$, $j = 1 \ldots n$ (Franklin 1993). It can easily be shown that the partial derivative of the permanent of this same matrix with respect to γ is

$$\frac{\partial \operatorname{per} \mathbf{A}(\gamma)}{\partial \gamma} = \sum_{q=1}^{n} \operatorname{per} \mathbf{A}(\gamma)_q, \tag{A.6}$$

where per $\mathbf{A}(\gamma)_q$ is the permanent formed by replacing the qth row of $\mathbf{A}(\gamma)$ with the row of partial derivatives $\frac{\partial \mathbf{A}(\gamma)_{qj}}{\partial \gamma}$, $j = 1 \ldots n$.

A.3.2 Sensitivity matrices for the feedback levels

For each of the k polynomial coefficients, we define a net sensitivity matrix, $\mathbf{N}^{F_k}$, that gives the net number of cycle products containing each of the direct effects. The $n \times n$ net sensitivity matrix for each polynomial coefficient is calculated by differentiating the characteristic polynomial in Equation (A.1) with respect to each a_{ij}. This is accomplished by substituting the matrix $\mathbf{A}(\gamma) - \lambda$ for $\mathbf{A}(\gamma)$ and substituting a_{ij} for γ in Equation (A.5). Each such differentiated equation is evaluated with the entries of the matrix $^\circ\mathbf{A}$ substituted for those of $\mathbf{A}$ to derive the equation

$$\frac{\partial \det\left(\mathbf{A}(a_{ij}) - \lambda\right)}{\partial a_{ij}}\bigg|_{\mathbf{A} = ^\circ\mathbf{A}} = \sum_{k=0}^{n} \frac{\partial F_k}{\partial a_{ij}} \lambda^{n-k}\bigg|_{\mathbf{A} = ^\circ\mathbf{A}} = \sum_{k=1}^{n} \frac{\partial F_k}{\partial a_{ij}} \lambda^{n-k}\bigg|_{\mathbf{A} = ^\circ\mathbf{A}}$$

$$= \sum_{k=1}^{n} \mathbf{N}_{ij}^{F_k} \lambda^{n-k}. \tag{A.7}$$

The last equality in Equation (A.7) occurs because the direct effects do not affect the value of F_0, which by convention is always -1. An array of n net sensitivity matrices, with one net sensitivity matrix for each level of feedback $k = 1 \ldots n$, is constructed from Equation (A.7):

$$\mathbf{N}^{F_k} = \left[\mathbf{N}_{ij}^{F_k}\right], \quad i, j = 1 \ldots n. \tag{A.8}$$

Similarly, the $n \times n$ total sensitivity matrix for each polynomial coefficient, $\mathbf{T}^{F_k}$, is calculated by differentiating the absolute characteristic polynomial in Equation (A.3) with respect to each a_{ij}. The matrix $\left|\overrightarrow{\mathbf{A}(\gamma)}\right| + \lambda$ is substituted for $\mathbf{A}(\gamma)$ and a_{ij} is substituted for γ into Equation (A.6). Each such

differentiated equation is evaluated with the entries of matrix $^{\bullet}\mathbf{A}$ substituted for those of $\mathbf{A}$ to derive

the equation

$$\frac{\partial \operatorname{per}\left(\left|\mathbf{A}(\overrightarrow{a_{ij}})\right| + \lambda\right)}{\partial a_{ij}}\Bigg|_{\mathbf{A}=^{\bullet}\mathbf{A}} = \sum_{k=1}^{n} \mathbf{T}_{ij}^{F_k} \lambda^{n-k}. \tag{A.9}$$

An array of n total sensitivity matrices, with one total sensitivity matrix for each level of feedback

$k = 1 \ldots n$, is constructed from Equation (A.9):

$$\mathbf{T}^{F_k} = \left[\mathbf{T}_{ij}^{F_k}\right] \quad i, j = 1 \ldots n. \tag{A.10}$$

The total sensitivity matrix for the kth polynomial coefficient gives the total number of cycle

products that contain each a_{ij} for the kth feedback level.

The $n \times n$ weighted sensitivity matrix for the kth polynomial coefficient is defined as

$$\mathbf{W}_{ij}^{F_k} = \begin{cases} \frac{\mathbf{N}_{ij}^{F_k}}{\mathbf{T}_{ij}^{F_k}}, & \text{if } \mathbf{T}_{ij}^{F_k} > 0 \\ \{ \}, & \text{if } \mathbf{T}_{ij}^{F_k} = 0 \end{cases}, \tag{A.11}$$

where $\{ \}$ is the empty set. This weighted sensitivity matrix gives the ratio of the net number to the

total number of cycle products containing each a_{ij} at the kth feedback level.

A.3.3 Sensitivity matrices for the Hurwitz determinants

The net sensitivity for an a_{ij} in a Hurwitz determinant provides the net number of positive

and negative occurrences of a_{ij} in Δ_k. A $n \times n$ net sensitivity matrix is defined for each Hurwitz

determinant, $\mathbf{N}^{\Delta_k}$, by differentiating the Equation (A.2) with respect to each a_{ij} and substituting the

matrix $°\mathbf{A}$ for $\mathbf{A}$. This is accomplished by substituting the Hurwitz determinant $\Delta_k(\gamma)$ for $\det \mathbf{A}(\gamma)$

and substituting a_{ij} for γ in Equation (A.5), and evaluating with the matrix $°\mathbf{A}$ to derive the net

sensitivity matrix for each Hurwitz determinant, $k = 1\ldots n$:

$$\mathbf{N}_{ij}^{\Delta_k} = \left[\left. \frac{\partial \Delta_k(a_{ij})}{\partial a_{ij}} \right|_{\mathbf{A}=°\mathbf{A}} \right], \quad i, j = 1\ldots n. \tag{A.12}$$

Equation (A.12) is, for each partial derivative taken with respect to a particular a_{ij}, a sum of k

determinants following from Equation (A.5). The undifferentiated rows within each of these

determinants are, when evaluated, constructed from the net polynomial coefficients $°F_k$, as derived

from Equation (A.1), but reversed in sign as with the F_k in Equation (A.2). The differentiated rows

are constructed from the net sensitivities of these polynomial coefficients $\mathbf{N}_{ij}^{F_k}$, as defined by

Equation (A.7), also reversed in sign.

The total sensitivity for an a_{ij} in a Hurwitz determinant provides the total number of

occurences for a_{ij} in Δ_k. The $n \times n$ total sensitivity matrix for each Hurwitz determinant, $\mathbf{T}^{\Delta_k}$, is

calculated by differentiating the Equation (A.4) with respect to each a_{ij} and substituting the matrix

$•\mathbf{A}$ for $\mathbf{A}$. The permanent $\Delta'_k(\gamma) + \lambda$ is substituted for per $\mathbf{A}(\gamma)$ and a_{ij} is substituted for γ in

Equation (A.6), and the matrix $•\mathbf{A}$ is substituted for $\mathbf{A}$ to derive the net sensitivity matrix for each

Hurwitz determinant, $k = 1\ldots n$:

$$\mathbf{T}_{ij}^{\Delta_k} = \left[\left. \frac{\partial \Delta'_k(a_{ij})}{\partial a_{ij}} \right|_{\mathbf{A}=•\mathbf{A}} \right], \quad i, j = 1\ldots n. \tag{A.13}$$

The undifferentiated rows within the partial derivative of Equation (A.13) are constructed from the

total polynomial coefficients $•F_k$, derived from Equation (A.3), and the differentiated rows are

constructed from the net sensitivities of these polynomial coefficients $\mathbf{T}_{ij}^{F_k}$, as defined by Equation (A.9).

As in the above weighted sensitivity matrix for the kth polynomial coefficient $\mathbf{W}^{F_k}$, the $n \times n$ weighted sensitivity matrix for the kth Hurwitz determinant is defined as

$$\mathbf{W}_{ij}^{\Delta_k} = \begin{cases} \frac{\mathbf{N}_{ij}^{\Delta_k}}{\mathbf{T}_{ij}^{\Delta_k}}, & \text{if } \mathbf{T}_{ij}^{\Delta_k} > 0 \\ \{\,\}, & \text{if } \mathbf{T}_{ij}^{\Delta_k} = 0 \end{cases}. \tag{A.14}$$

APPENDIX B. MAPLE CODE FOR SENSITIVITY ANALYSIS

```
> restart;with(LinearAlgebra):
```
Provide the signs of the entries within the matrix **A**; then hit the above *!!!* button.
```
> sA := Matrix([ [-1,-1,1],[1,0,-1],[0,1,0] ]);
interface(rtablesize=RowDimension(sA)):
```
A free graphical editor that constructs the transposed signed adjacency matrix of a signed digraph is available at Ecological Archives E083-022-S1-R1 on the web:
 http://www.esapubs.org/archive/ecol/E083/022/suppl-1.htm#anchorDownload2

Procedures

Procedure taking partial derivative of polynomial coefficients with respect to Aij.
```
> pcoeffs := proc(A,M,N)
local j, k, l, Msil, Mabl, Fd, Fp, CMd, CMp, Fw, S;
S := RowDimension(A);
Fd := Vector(S);
Fp := Vector(S);
Fw := Vector(S);
Msil := DiagonalMatrix(Vector(S,fill=lambda))-A;
Mabl := DiagonalMatrix(Vector(S,fill=lambda))+abs(A);
for j from 1 to S do
 if j = N then
  Msil[M,j] := A[M,j];
  Mabl[M,j] := abs(A[M,j]);
 else
  Msil[M,j] := 0;
  Mabl[M,j] := 0;
 fi;
od;
CMd := Determinant(Msil);
if coeff(CMd,lambda,S) > 0 then
 CMd := CMd*(-1);
fi;
CMp := Permanent(Mabl);
for k from 1 to S do
 Fd[k] := coeff(CMd,lambda,S-k);
 Fp[k] := coeff(CMp,lambda,S-k);
od;
for l from 1 to S do
 if Fp[l] > 0 then
  if Fd[l] = Fp[l] then
   Fw[l] := 1;
  elif (-1)*Fd[l] = Fp[l] then
   Fw[l] := -1;
  else
   Fw[l] := evalf[3](Fd[l]/Fp[l]);
  fi;
 else
  Fw[l] := {};
 fi;
od;
```

```
Fd,Fp,Fw;
end:
```

Procedure taking partial derivative of Hurwitz determinants with respect to Aij.

```
> hdets := proc(Cd,Cp,A)
local Harrd, Harrp, Hd, Hp, i, j, k, Hnpd, Hnpp, o, p, CPd, CPp, S,
l, m, n, arrd, arrp, oldd, oldp, Matd, Matp, q, arrw;
S := Dimension(Cd);
Hd := Matrix(S);
Hp := Matrix(S);
Hnpd := Matrix(S);
Hnpp := Matrix(S);
arrd := Array(1..S);
arrp := Array(1..S);
arrw := Array(1..S);
CPd := Determinant(DiagonalMatrix(Vector(S,fill=lambda))-A);
if coeff(CPd,lambda,S) < 0 then
 CPd := CPd*(-1);
fi;
CPp := Permanent(DiagonalMatrix(Vector(S,fill=lambda))+abs(A));
for i from 1 to S do
 for j from 1 to S do
  if 2*j-i > S then
   Hd[i,j] := 0;
   Hp[i,j] := 0;
   Hnpd[i,j] := 0;
   Hnpp[i,j] := 0;
  else
   if 2*j-i > 0 then
    Hd[i,j] := Cd[2*j-i]*(-1);
    Hp[i,j] := Cp[2*j-i];
    Hnpd[i,j] := coeff(CPd,lambda,S-(2*j-i));
    Hnpp[i,j] := coeff(CPp,lambda,S-(2*j-i));
   elif 2*j-i = 0 then
    Hnpd[i,j] := coeff(CPd,lambda,S-(2*j-i));
    Hnpp[i,j] := coeff(CPp,lambda,S-(2*j-i));
   else
    Hd[i,j] := 0;
    Hp[i,j] := 0;
    Hnpd[i,j] := 0;
    Hnpp[i,j] := 0;
   fi;
  fi;
 od;
od;
for k from 1 to S do
 arrd[k] := 0;
 arrp[k] := 0;
 oldd := 0;
 oldp := 0;
 Matd := Matrix(k);
 Matp := Matrix(k);
 for l from 1 to k do
  for m from 1 to k do
   for n from 1 to k do
```

```
    if m = 1 then
     Matd[m,n] := Hd[m,n];
     Matp[m,n] := Hp[m,n];
     else
     Matd[m,n] := Hnpd[m,n];
     Matp[m,n] := Hnpp[m,n];
    fi;
   od;
  od;
  arrd[k] := Determinant(Matd) + oldd;
  oldd := arrd[k];
  arrp[k] := Permanent(Matp) + oldp;
  oldp := arrp[k];
 od;
od;
for q from 1 to S do
 if arrp[q] > 0 then
  if arrd[q] = arrp[q] then
   arrw[q] := 1;
  elif (-1)*arrd[q] = arrp[q] then
   arrw[q] := -1;
  else
   arrw[q] := evalf[3](arrd[q]/arrp[q]);
  fi;
 else
  arrw[q] := {};
 fi;
od;
arrd, arrp, arrw;
end:
```

Procedure constructing arrays of senstivity matrices for the polynomial coefficients and the Hurwitz determinants.

```
> coeff_hrtz := proc(Q)
local i, j, Y, Z, pnet, ptot, pwts, hrtn, hrtt, hrtw, m, pwtt,hwtt;
pnet := Array(1..RowDimension(Q));
ptot := Array(1..RowDimension(Q));
pwts := Array(1..RowDimension(Q));
hrtn := Array(1..RowDimension(Q));
hrtt := Array(1..RowDimension(Q));
hrtw := Array(1..RowDimension(Q));
for m from 1 to RowDimension(Q) do
 pnet[m] := Matrix(RowDimension(Q));
 ptot[m] := Matrix(RowDimension(Q));
 pwts[m] := Matrix(RowDimension(Q));
 hrtn[m] := Matrix(RowDimension(Q));
 hrtt[m] := Matrix(RowDimension(Q));
 hrtw[m] := Matrix(RowDimension(Q));
 for i from 1 to RowDimension(Q) do
  for j from 1 to RowDimension(Q) do
   if Q[i,j] = 0 then
    pnet[m][i,j] := `.`;
    ptot[m][i,j] := `.`;
    pwts[m][i,j] := `.`;
    hrtn[m][i,j] := `.`;
```

```
      hrtt[m][i,j] := `.`;
      hrtw[m][i,j] := `.`;
    else
     Y := pcoeffs(Q,i,j);
     Z := hdets(Y[1],Y[2],Q);
     pnet[m][i,j] := Y[1][m];
     ptot[m][i,j] := Y[2][m];
     if Y[3][m] = 0 then
      pwts[m][i,j] := 0;
     else
      pwts[m][i,j] := Y[3][m];
     fi;
     hrtn[m][i,j] := Z[1][m];
     hrtt[m][i,j] := Z[2][m];
     if Z[3][m] = 0 then
      hrtw[m][i,j] := 0;
     else
      hrtw[m][i,j] := Z[3][m];
     fi;
    fi;
   od;
  od;
od;
Array([pnet,ptot,pwts,hrtn,hrtt,hrtw]);
end:
```

Procedure displaying results of the sensitivity analysis for the polynomial coefficients

```
> res_coeff := proc(A, out)
local t;
`print`('``');
for t from 1 to RowDimension(A) do
 print('`FEEDBACK LEVEL`');
 `print`(t);
 `print`('``');
 `print`(N^F[t]);
 `print`(out[1][t]);
 `print`('``');
 `print`(T^F[t]);
 `print`(out[2][t]);
 `print`('``');
 `print`(W^F[t]);
 `print`(out[3][t]);
 `print`('``');
od;
end:
```

Procedure displaying results of the sensitivity analysis for the Hurwitz determinants

```
> res_hurtz := proc(A, out)
local t;
`print`('``');
for t from 1 to RowDimension(A) do
 print('`HURWITZ DETERMINANT`');
 `print`(t);
 `print`('``');
 `print`(N^Delta[t]);
 `print`(out[4][t]);
```

```
 `print`('``');
 `print`(T^Delta[t]);
 `print`(out[5][t]);
 `print`('``');
 `print`(W^Delta[t]);
 `print`(out[6][t]);
 `print`('``');
od;
end:
```

Partial derivatives of polynomial coefficients and Hurwitz determinants with respect to all elements
aij
```
> PH := coeff_hrtz(sA):
```
See Appendix A for definition of sensitivity matrices.

Sensitivity matrices for the polynomial coefficients

```
> res_coeff(sA,PH);
```

Sensitivity matrices for the Hurwitz determinants

```
> res_hurtz(sA,PH);
>
```

APPENDIX C. METHODS AND RESULTS FOR SECOND-ORDER MONTE CARLO SIMULATION

This appendix details the methods and results of a second-order Monte Carlo simulation (MCS) that explores the effects of different model structures, dependence, and interaction strength on the prediction weights of a qualitative model. For consistency with previous research, we have used an array of models investigated in prior simulations (Dambacher et al. 2003a). In that study, it was assumed that matrix elements were independently, identically, and uniformly distributed. All simulations discussed here used 500 replicate stable matrices, i.e. $\max(\mathrm{Re}(\lambda(\mathbf{A}))) < 0$, of 18 different models.

In the MCS we varied the distribution shape of elements of matrix $^{\#}\mathbf{A}$ to compare how the proportion of strong and weak links affect the predictive ability of SDGs. The magnitudes of $^{\#}a_{ij}$ were drawn from four different distributions (Fig. 3.3(a) from top):

(1) Uniform($\mu = 0$, $\sigma^2 = 1$) distribution;

(2) Normal($\mu = 0$, $\sigma^2 = 1/9$) distribution doubly truncated at $^{\#}a_{ij} = 0$ and $^{\#}a_{ij} = 1$;

(3) Normal($\mu = 1$, $\sigma^2 = 1/9$) distribution doubly truncated at $^{\#}a_{ij} = 0$ and $^{\#}a_{ij} = 1$;

(4) Normal($\mu = 1/2$, $\sigma^2 = 1/36$) distribution doubly truncated at $^{\#}a_{ij} = 0$ and $^{\#}a_{ij} = $

   1.

All matrix elements were drawn independently from the chosen distribution. Each distribution ranges from 0 to 1; simulations which drew matrix elements using distributions with supports from 0 to ∞, for example an Exponential(1) or Gamma(scale = 2, shape = 3), produced qualitatively similar results. We fit a nonlinear least-squares function, Eq. 3.5, to each of the four distributions of interaction strength (Fig. 3.3a) using `nls` (Venables and Ripley 2002) in R (RDCT 2005). All of the parameter fits were highly significant ($p < 0.001$; Table C.1).

An infinite number of assumptions on the dependence relationships between matrix elements are possible. We limited our investigations to the effect of dependence conferred through trophic relationships. Trophic relationships occur when a variable X_2 consumes another and thus has a

negative direct effect, - $a_{1,2}$, on the prey X_1. The prey X_1 provides a positive direct effect $a_{2,1}$ on the predator. However, $|a_{2,1}| < |- a_{1,2}|$ because of energetic costs resulting from the metabolization of ingested matter and the typically pyramidal distribution of predator and prey population abundances.

In the MCS summarized in Figure 3 we assumed that the ecological efficiency ranges uniformly from 0 to 0.1 and that the equilibrium density of the predator is one order of magnitude less than the prey equilibrium density. We assume that the simulated matrices represent Jacobian matrices (Eq. 3.2) of generalized Lotka-Volterra systems of equations with feasible interior equilibrium points. Dependence between $^{\#}a_{1,2}$ and $^{\#}a_{2,1}$ is invoked by first drawing the magnitude of the direct effect of predator on prey, $|^{\#}a_{1,2}|$, from its respective distribution (Fig 3.3a). This value of $|^{\#}a_{1,2}|$ is then multiplied by a random variable drawn from a Uniform(0, 0.01) distribution to produce the magnitude of $^{\#}a_{2,1}$, reflecting the assumptions on ecological efficiency and difference in densities above. Thus the maximum possible magnitude of $^{\#}a_{2,1}$ is equal to one hundredth of the magnitude of $^{\#}a_{1,2}$.

The results from these simulations are in Table C.1. Introducing dependence results in very weak direct effects of prey on predator. This non-random patterning of very weak direct effects erodes the sign determinancy associated with prediction weights relative to the scenario where all interactions are drawn independently. The fits for all parameters were highly significant in all cases, however, and prediction weights were informative even when dependence was introduced.

The assumptions on the rates of ecological efficiency and trophic structure above may be overly restrictive, and we compared results to a less restrictive scenario where the value of $|^{\#}a_{1,2}|$ is multiplied by a random variable drawn from a Uniform(0, 0.1) distribution to produce the magnitude of $^{\#}a_{2,1}$. Further scenarios explored the effect of weak non-trophic effects, with maximum magnitudes set to 1/100th of the maximum magnitude of the negative direct effect of predator on prey, and strong non-trophic effects, with maximum magnitudes equal to the maximum magnitude of the negative direct effect of predator on prey. Weak non-trophic effects were created by drawing a magnitude from the appropriate distribution (1-4 above) and multiplying by 0.1 or 0.01, matching the level of dependence introduced into the trophic relationships. Table C.2 summarizes the effects of varying the assumptions of dependence on prediction weights. Strong non-trophic effects reduced the value of β_W.

Alternatives to Eq. 3.5 may be applied to modify the robustness of probabilities of increase, decrease, and weak response given a particular value of prediction weight. Eq. 3.5 fits the expected proportion of correct sign (excluding occurrences where an element of adj$(-\,^{\circ}\mathbf{A})_{hij} = 0$). It was assumed that the proportion of correct sign when $\mathbf{W}_{hij} = 0$ was 0.50, that is, there is a 50/50 chance that the numeric sign of adj$(-\#\mathbf{A})_{hij}$ equals the sign of adj$(-\,^{\circ}\mathbf{A})_{hij}$ when weights are uninformative. An alternative approach may seek to bound numeric simulations such that 95% of the points are above the fitted line. Some points drop below a 0.50 proportion of correct sign (Fig. 3.3c), therefore Eq. 3.5 is modified to allow a varying intercept, β_0,

$$\Pr\!\left[\mathrm{sgn}\!\left(\mathrm{adj}\!\left(-\,^{\circ}\mathbf{A}\right)_{ij}\right) = \mathrm{sgn}\!\left(\mathrm{adj}\!\left(-\,^{\#}\mathbf{A}\right)_{ij}\right)\right] = \frac{\exp\!\left(\beta_W \mathbf{W}_{ij} + \beta_{WT}\mathbf{W}_{ij}\mathbf{T}_{ij}\right)}{\beta_0 + \exp\!\left(\beta_W \mathbf{W}_{ij} + \beta_{WT}\mathbf{W}_{ij}\mathbf{T}_{ij}\right)}. \tag{C.1}$$

Here we use quantile regression (Koenker 2005, Koenker 2006) to provide a 95% lower bound on the fit of Eq. C.1 to the simulation results (Fig. C.1). Unlike the expected proportion of correct sign (Eq. 3.5, Figs. 3.4b, 3.4c), the 95% bound on the proportion of correct sign fitted to Eq. C.1 drops below 0.50. Weights are either informative or uninformative, therefore, a lower limit of 1/3 is set to the respective probabilities of the three categories of increase, decrease, and weak response. Eq. C.2 is substituted for Eq. 6 to account for this lower threshold on probabilities

$$\Pr(Increase) = \begin{cases} \dfrac{1}{3}; & 0 \le g\!\left(\mathbf{W}_{ij},\mathbf{T}_{ij}\right) < 0.5 \\[2ex] \dfrac{4}{3}h\!\left(\mathbf{W}_{ij},\mathbf{T}_{ij}\right) - \dfrac{1}{3}; & 0.5 \le g\!\left(\mathbf{W}_{ij},\mathbf{T}_{ij}\right) \le 1.0 \end{cases}, \tag{C.2}$$

where $h(\mathbf{W}_{ij}, \mathbf{T}_{ij})$ refers to Eq. C.1 evaluated at particular values of prediction weight $\mathbf{W}_{ij}$ and total feedback $\mathbf{T}_{ij}$. Probabilities of increase, decrease, and weak response are calculated as described in the methods with Eqs. C.1 and C.2 substituted for Eqs. 3.5 and 3.6, respectively.

Table C.1. Results from the nonlinear least-squares fits shown in Figure 3.3b,c. Distribution types are those in Fig. 3.3a, numbered from top to bottom respectively.

Distribution	Dependence	β_W	SE	P-value	β_{WT}	SE	P-value
1	No	4.04151	0.05876	<0.0001	0.02614	0.00086	<0.0001
2	No	3.77860	0.05564	<0.0001	0.02240	0.00083	<0.0001
3	No	6.96539	0.11434	<0.0001	0.06148	0.00164	<0.0001
4	No	8.13840	0.13976	<0.0001	0.07910	0.00217	<0.0001
1	Yes	3.45962	0.17286	<0.0001	0.03417	0.00348	<0.0001
2	Yes	3.44285	0.16548	<0.0001	0.03254	0.00326	<0.0001
3	Yes	3.51374	0.19870	<0.0001	0.03962	0.00429	<0.0001
4	Yes	3.51746	0.20164	<0.0001	0.04175	0.00449	<0.0001

Table C.2. Parameter estimates and standard errors using a nonlinear least squares fit for the function
$$\Pr\left[\text{sgn}\left(\text{adj}\left(-{}^{\circ}\mathbf{A}\right)_{ij}\right) = \text{sgn}\left(\text{adj}\left(-{}^{\#}\mathbf{A}\right)_{ij}\right)\right] = \frac{\exp\left(\beta_W \mathbf{W}_{ij} + \beta_{WT} \mathbf{W}_{ij} \mathbf{T}_{ij}\right)}{1 + \exp\left(\beta_W \mathbf{W}_{ij} + \beta_{WT} \mathbf{W}_{ij} \mathbf{T}_{ij}\right)}$$ under different assumptions of
dependence and uniformly distributed interaction strength magnitudes. Within pairwise predator-prey relationships, PN denotes the negative direct effect of predator on prey, PP denotes the positive direct effect of prey on predator, and NT denotes non-trophic relationships. The inequalities denote the maximum values of a_{ij} depending on whether they are part of trophic or non-trophic relationships. The inequalities were compared for three scenarios: zero, one, and two orders of magnitude difference between maximum values for the categories PN, PP, or NT.

Scenario	Order	β_W	SE	P-value	β_{WT}	SE	P-value
PN = NT = PP	-	4.0415	0.0588	<0.0001	0.0261	0.0009	<0.0001
PN > PP = NT	1	3.8921	0.1353	<0.0001	0.0318	0.0023	<0.0001
PN > PP = NT	2	4.0617	0.1847	<0.0001	0.0339	0.0031	<0.0001
PN = NT > PP	1	3.4744	0.1348	<0.0001	0.0321	0.0026	<0.0001
PN = NT > PP	2	3.4596	0.1729	<0.0001	0.0342	0.0035	<0.0001

Table C.3. Fitted parameters for the 95% lower bound on the numeric simulations of Appendix C for different values of $\mathbf{W}_{ij}$ and $\mathbf{T}_{ij}$. Simulated data are those of Fig. 3.4c for uniform ${}^{\#}a_{ij}$.

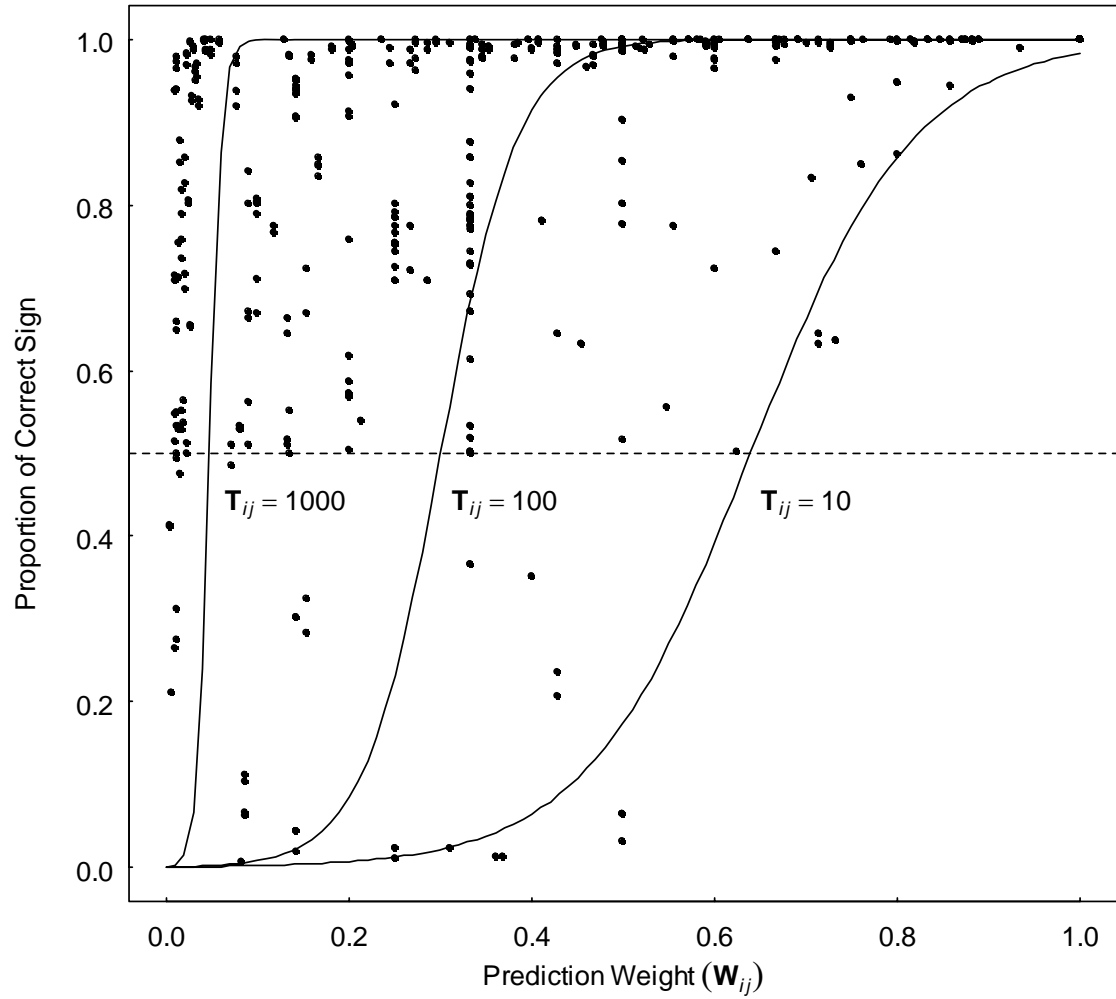| Parameter	Estimate
β_0	1253.992
β_W	9.766
β_{WT}	0.139

Figure C.1. 95% lower bound on the numeric simulations of Appendix C for different values of $\mathbf{W}_{hij}$ and $\mathbf{T}_{hij}$. Simulated data are those of Fig. 3.4c for uniform ${}^{\#}a_{ij}$.

APPENDIX D. INSTRUCTION GUIDE FOR BUILDING CONDITIONAL PROBABILITY TABLES

This instruction guide describes in detail the transition from a signed directed graph (SDG) to a Bayesian Belief Network (BBN). Required software includes:

`CPT Builder.mws` (Maple file; code in Appendix D), used to create the conditional probabilities

`Netica`, BBN software, available at www.norsys.com

`SDG Graphical Editor`, used to create the matrix °**A** (available on the web at http://www.ent.orst.edu/loop/download.aspx)

We start with the qualitative mathematics underlying the red scale *Aonidiella aurantii* example. The system of equations for unparasitized hosts (X_1), hosts parasitized by *Encarsia perniciosi* (X_2), and hosts parasitized by *Aphytis melinus* (X_3) are:

$$\frac{\mathrm{d}X_1}{\mathrm{d}t} = X_1\left(r_1 - \alpha_{1,1}X_1 - \alpha_{1,2}X_2 - \alpha_{1,3}X_3\right)$$

$$\frac{\mathrm{d}X_2}{\mathrm{d}t} = X_2\left(-r_2 + \alpha_{2,1}X_1 - \alpha_{2,2}X_2 - \alpha_{2,3}X_3\right) \qquad \text{(D.1)}$$

$$\frac{\mathrm{d}X_3}{\mathrm{d}t} = X_3\left(-r_3 + \alpha_{3,1}X_1 + \alpha_{3,2}X_2 - \alpha_{3,3}X_3\right)$$

Here r_i describes the number of per capita *births – deaths* experienced by the scale insect under the different states of parasitism. The α_{ij}, $i \neq j$, represent the coefficient of transfer between parasitism states due to interaction with scale insects. The α_{ij}, $i = j$, correspond to self-regulation through competition for resources by unparasitized scale insects or reattack by wasps on scale hosts previously parasitized by their own species. Rates of parsitization are assumed to be linearly proportional to the number of hosts parasitized.

The matrix of first partials of the above system of equations evaluated at equilibrium (*) is

$$\begin{bmatrix} -\alpha_{1,1}X_1^* & -\alpha_{1,2}X_1^* & -\alpha_{1,3}X_1^* \\ \alpha_{2,1}X_2^* & -\alpha_{2,2}X_2^* & -\alpha_{2,3}X_2^* \\ \alpha_{3,1}X_3^* & \alpha_{3,2}X_3^* & -\alpha_{3,3}X_3^* \end{bmatrix} \tag{D.2}$$

which is represented symbolically with the matrix

$$\mathbf{A} = \begin{bmatrix} -a_{1,1} & -a_{1,2} & -a_{1,3} \\ a_{2,1} & -a_{2,2} & -a_{2,3} \\ a_{3,1} & a_{3,2} & -a_{3,3} \end{bmatrix}. \tag{D.3}$$

The classical adjoint of $-\mathbf{A}$ is then

$$\begin{bmatrix} a_{2,2}a_{3,3} + a_{2,3}a_{3,2} & -a_{1,2}a_{3,3} - a_{1,3}a_{3,2} & a_{1,2}a_{2,3} - a_{1,3}a_{2,2} \\ a_{2,1}a_{3,3} - a_{2,3}a_{3,1} & a_{1,1}a_{3,3} + a_{1,3}a_{3,1} & -a_{1,1}a_{2,3} - a_{1,3}a_{2,1} \\ a_{2,1}a_{3,2} + a_{2,2}a_{3,1} & a_{1,1}a_{3,2} - a_{1,2}a_{3,1} & a_{1,1}a_{2,2} + a_{1,2}a_{2,1} \end{bmatrix}. \tag{D.4}$$

A positive press perturbation to the intrinsic growth rate of the unparasitized host X_1, such as through increasing fecundity due to enhanced resource availability, is read down the first column of adj($-\mathbf{A}$). The qualitative response (increase, decrease, or weak response) is registered along the rows. Therefore, the qualitative response of X_1 and X_3 is unambiguously positive, whereas the qualitative response of X_2 depends on the magnitudes of the elements occurring in adj($-\mathbf{A}$)$_{2,1}$. Puccia and Levins (1985) discuss the interpretation of such inequalities within small systems based on empirical data. Here we employ weighted feedback to provide probabilities of qualitative change in the absence of the natural history information necessary to establish the sign of adj($-\mathbf{A}$)$_{2,1}$.

D.1 Application

D.1.1 Creating the model ecosystem

Open the SDG Graphical Editor. Variables are created by clicking on the button ① and then left-clicking at the location where you wish it to be placed. Connecting arrows are drawn by first

clicking either the ⟶• button or ⟶ button at the top of the screen, then clicking on the originating variable. While holding the button down, drag the arrow to the receiving variable and release. Self-regulating loops are added by selecting the negative arrow, then clicking and releasing on the chosen variable. Variable names may be entered by right-clicking on a variable and selecting "Edit". Mistakes can be corrected by clicking first on the trashcan icon followed by the problem variable or arrow.

To build Fig. 3.1, begin by entering the variables X1, X2, and X3 in sequence, then draw the connecting arrows and self-regulation loops. After recreating Fig. 3.1, click on "DataTools" in the upper left, and then select "Show Matrix View" from the options provided. The matrix is described in four ways: (1) the matrix ºA and variable names; (2) the variable names numbered in the order they were entered into the SDG editor; (3) a list of the rows of matrix ºA; and (4) a Maple command for creating an array that corresponds to ºA. Make sure that the matrix ºA listed (#1 above) has the same sign structure as matrix A listed above. Doubleclick on the second row from the bottom (#3 above), select all the contents, and copy to the clipboard.

D.1.2 Building conditional probabilities

Open the Maple file `CPT Builder.mws`. Place the cursor on the first line and hit the enter key. Then hit the enter key once more to execute the procedures; these may then be hidden from view by scrolling back up to the text "**Procedures**" and clicking on the downward pointing grey arrow.

Next, enter the variable names into the "**Namevec**" vector between the brackets **[]** after clearing out any previous contents that may be there. These variable names should be listed in the same order as they were entered into the SDG editor, i.e. the sequence listed in #2 above (see description of "Show Matrix View" function of the SDG editor). For this example, the **Namevec** vector will look like:

```
> Namevec := Vector([X1,X2,X3]);                                        (D.5)
```

After typing in the change in contents, hit enter to execute. You should see Maple rewrite the vector

in blue immediately below the command line.

Next the model matrices are specified. In this example we will compare the H-PC model of

Fig. 3.1 to the null model. The H-PC model has just been created using the SDG editor, and the

associated matrix °**A** is currently on the clipboard. Take the existing command naming a matrix **M1**

and delete the contents (a list of matrix rows) located between the outermost brackets **[]** occurring on

the right hand side of the assignment operator **:=**. Paste the rows copied from the SDG between the

outermost brackets. Then rename the model matrix to "HPC" so that the command appears as follows:

```
> HPC := Matrix([[-1,-1,-1],[1,-1,-1],[1,1,-1]]);                    (D.6)
```

Then, while holding down the "Shift" key, press the "Enter" key. The cursor will now be blinking

below the above command line. This is where we will place the command line that will create the null

model.

The null model may be created in one of two ways:

1) Use the SDG editor to create a fully connected three-variable system, including self-regulation,

then use the "Show Matrix View" function of the SDG editor to copy the resulting matrix rows of °**A**.

This will be use to paste a second model matrix into the Maple file. This matrix will be a 3x3 matrix

full on 1's. The resulting command line should look like:

```
> HPC := Matrix([[-1,-1,-1],[1,-1,-1],[1,1,-1]]);                    (D.7)
 Null := Matrix([[1,1,1],[1,1,1],[1,1,1]]);
```

2) A better option is to use the shortcut command **Matrix(3,fill=1)** which creates a 3x3 matrix

filled with one's. The command line in this case should look like this:

```
> HPC := Matrix([[-1,-1,-1],[1,-1,-1],[1,1,-1]]);                    (D.8)
 Null := Matrix(3,fill=1);
```

After specifying the null model using method 1 (Eq. D.7) or 2 (Eq. D.8), hit enter and verify

that Maple received the commands. The H-PC and null model matrices should be written in blue font

immediately below the command line. It should be noted that a null model is not essential for running the program.

The alternative models will now be placed within a single vector. Again, first delete any existing contents between the outermost brackets **[]** of the **Modelvec** command. Then enter the names of the alternative model matrices; in this case the command line will appear as follows:

> **Modelvec := Array([HPC, Null]);**   (D.9)

Then hit enter and verify the command execution.

The **Inputvec** command declares the variables which receive a press perturbation. These should be entered in an order reflecting their introduction into the SDG editor and the **Namevec** command (Eq. D.5). For this example, if press perturbations occur in both X1 and X3, then X1 should precede X3 and not vice versa. This procedure will later make pasting conditional probabilities into Netica much simpler. Here, though, as in the Results, we will limit the investigation to a press perturbation on a single variable, X1. The **Inputvec** command will then look like:

> **Inputvec := Vector([X1]);**   (D.10)

which should be entered and the execution verified.

Next, hit enter to execute the command:

> **Checkinputs(Namevec,Inputvec);**   (D.11)

The **Checkinputs** command will doublecheck whether the **Inputvec** statement was correctly set relative to **Namevec**. If so, a vector of "Ok" entries will appear, with a length equal to the number of input variables requested. Otherwise, an error message will appear.

Now choose a transformation specifying the relationship between prediction weights and probabilities. Two choices are given. Method 1 corresponds to the expected response shown using the uniform distribution in Fig 4c, and was used in the construction of the BBN models presented in the Results. Method 2 uses a 95% lower bound on these points instead (Appendix C). Select method 1 to compare this BBN with that presented in Results. After selecting an option, hit enter to execute the appropriate **trans** command. No blue verification will be issued in this instance.

At this point, move the cursor so that it is blinking by the **X** on the last line of code:

```
> X := CPTconstruct(Namevec,Modelvec,Inputvec,trans,NoFBtrans,no);
```
$$(D.12)$$

This is the object that will be created using the above information provided by the user. Hit enter and the conditional probabilities will be evaluated. The resulting matrix of conditional probabilities is assigned to the name X and appears in blue font. Rightclick on the blue placeholder for the matrix, select the option "Export As", and choose "Tab Delimited". Save the file in an appropriate directory. Saving the file with a ".txt" extension will allow it to later be opened with Excel. For this example, save the file under the name "HPCcpts.txt". The conditional probabilities derived from the SDG models are now stored in this tab-delimited text file.

D.1.3 Constructing the Bayesian Belief Network

Construction of the BBN begins with drawing its graph structure (e.g., Fig. 3.4). Open the program Netica, select "File", then "New Network". First we will enter the "Structure" node containing the alternative models (refer to Fig. 3.4). Click on the yellow ellipse ⬭ located on the top toolbar. Then click within the white blank space to place the node. To rename the title of the node from the default "A", first doubleclick on the node, then type in the appropriate name in the "Name" field. Likewise, in the "State" field enter the first model matrix name entered into the Maple worksheet (in this case, "H_PC"). Enter the next alternative model name ("Null" in this example) into a second state. States can be added by clicking "New". Then hit "Okay". The Netica help file is a good resource for guiding the BBN construction if there are questions.

Next, create the row(s) of "observation nodes" below the structure node (see Fig. 3.4). In this example, we have three variables and therefore three nodes. Again click on the yellow ellipse ⬭ and place three nodes into the network. It is convenient to name these in sequence, from left to right, just as they were first entered into the SDG editor and the vector **Namevec** in the Maple file. Title the first node "X1". In the "State" field enter "Increase", and then add the states "No_Obs_Response" and

"Decrease". Again, new states can be added by clicking "New". Complete by hitting "Okay". Repeat this process for the two remaining observation nodes, X2 and X3.

Now construct the "Input nodes" (Fig. 3.3). Click on the yellow ellipse icon, and click on the location where the node is to be placed. If there are multiple nodes, place these in the same order (from left to right) as their names appeared in the vector **Inputvec** in the Maple file. In this example, with the single input to X1, doubleclick on the single node and change the name to "Input_to_X1". Change the state names to Positive, None, and Negative.

The nodes are now all in place and they just require connections. While holding down the "Ctrl" key, click on all of the observations nodes so that they are all highlighted. Click on Netica's arrow icon. Place the mouse pointer over the structure node and press the left mouse button. While holding down the left button, guide the pointer over an observation node and then release. Arrows will now connect the structure node to all of the observation nodes.

After connecting the structure node, check to make sure all observation nodes are still highlighted. If so, click on the arrow icon and place the pointer over the input node farthest to the left (if there is more than one). Then, as above, click the left mouse button and drag an arrow up to an observation node and release. Repeat for all input nodes, moving from left to right, so that all input nodes connect to every observation node.

The network structure is now set and we can begin entering conditional probabilities. First, navigate to the CPT output file, in this example saved under the name "HPCcpts.txt". Open with Excel (change the file extension to ".txt" if necessary) to view the calculated conditional probabilities which will be transferred into the BBN Netica file. Select all cells containing the probabilities and click on "Format" → "Cells". Select the "Number" tab, then highlight the Category "Numbers". Increase the number of decimal places to 10 and click "Ok". The conditional probabilities are now ready to be pasted into Netica.

The format of the data file is as follows. The first column lists all possible models in the order that they were entered into the Maple file. This column is followed by m columns, where m is the number of input nodes, listed in the sequence that they were entered into the vector **Inputvec**.

These input columns, together with the "Model" column, describe all possible permutations of conditions within the BBN. Following the input columns are the conditional probabilities. These are listed in groups of three, where each observation node (variable) has three adjacent columns giving probabilities of increase, unchanged, and decrease. These sets of observational node columns are listed in the order that their respective variable names were entered into the vector **Namevec**.

Select and copy the conditional probabilities belonging to all three columns of the observational node X1 (just the numeric cells). Go to Netica and click on the observation node X1 so that it is highlighted. Select the command "Table" → "View/Edit". Make sure that probabilities, and not percentages, are selected from the options tab above the table. Select the entire Conditional Probability Table (CPT). (The easiest way to do this is to press "Ctrl" and "A" simultaneously). Then paste the content clipboards into the CPT. Note that the columns denoting the conditions in the CPT, on the left hand side of the double line, appear in the same sequence as in the data file. The conditional probabilities should be matched with their conditions in the CPT, just as they are in the datafile. Hit "Okay", and return to the datafile to select the next three columns of conditional probabilities to paste into observation node X2. Repeat the process until the CPT's for all observation nodes have been entered.

Click and highlight the input node, then select "Table" → "View/Edit". The CPT for this node has a different appearance then the observation nodes because this node has no parents. We will begin with equal probabilities of a press perturbation having an input effect of increase, weak response, or decrease on variable X1. Select "Table" → "Uniform Probabilities" to specify equal probabilities of increase, weak response, and decrease and hit "Okay". Repeat this process again for the structure node to allocate equal prior probabilities for each alternative model being true.

The network structure and conditional probabilities have now all been added, and the net is ready to be compiled. Select "Network" → "Compile" and the BBN is ready for use. Consult the Netica help files to learn how to enter findings (observation likelihoods), interpret BBN predictions, and conduct sensitivity analyses.

APPENDIX E. MAPLE CODE FOR BUILDING CONDITIONAL PROBABILITY TABLES

```
> restart: with(LinearAlgebra):
```

See Appendix D for instructions.

Procedures

Hit enter to execute, then click upper left grey arrow to hide code:

```
> Checkinputs := proc(Names,Ins)
local i, test, j, entrs, k;
test := Vector(Dimension(Ins));
entrs := Vector(Dimension(Ins));
for i from 1 to Dimension(Ins) do
 test[i] := 0;
 for j from 1 to Dimension(Names) do
  if Ins[i] = Names[j] then
   test[i] := 'Ok':
   entrs[i] := j;
  fi;
  if test[i] = 0 then
   test[i] := 'Input <> Name':
   entrs[i] := -9;
  fi;
 od;
od;
for k from 2 to Dimension(Ins) do
 if (entrs[k] <> -9) and (entrs[k-1] <> -9) then
  if entrs[k] < entrs[k-1] then
   test := "Inputvec Sequence Out of Order";
  fi;
 fi;
od;
if nops(convert(entrs,set)) <> Dimension(Ins) then
 test := "Duplicate Name in Inputvec";
fi;
test;
end:


CPTconstruct := proc(Nvec,Mods::Array,Ins,f,NFT,Other)
local i, j, k, N, Ads, M, Nrows, Ncols, counter, Ind, ModV;
N := op(ArrayDims(Mods))[2];
Ads := Array(1..N);
Ncols := Dimension(Ins)+1+3*Dimension(Nvec);
if Other = 'no' then
 Nrows := N*3^Dimension(Ins);
elif Other = 'yes' then
 Nrows := (N+1)*3^Dimension(Ins);
```

```
else
 print(Other, yes or no);
 break;
fi;
Ind := Array(1..Dimension(Ins));
M := Matrix(Nrows+1, Ncols);
for i from 1 to N do
 Ads[i] := Adjoint((-1)*Mods[i]);
od;
for j from 1 to Ncols do
 for k from 1 to Nrows do
  if j = 1 then
   M[1,j] := Model;
   if Other = 'no' then
    ModV := [seq(op([seq(z,y=1..Nrows/N)]),z=1..N)];
    M[k+1,j] := ModV[k];
   elif Other = 'yes' then
    ModV := [seq(op([seq(z,y=1..Nrows/(N+1))]),z=1..N)];
    if k+1 < Nrows-(3^Dimension(Ins))+2 then
     M[k+1,j] := ModV[k];
    else
     M[k+1,j] := 'other';
    fi;
   fi;
  elif (j > 1) and (j < (2 + Dimension(Ins))) then
   M[1,j] := In||op(Ins[j-1]);
   if Other = 'no' then
    Ind[j-1] := [seq(op([seq(Incr,zz=1..3^(Dimension(Ins)-(j-1))),
              seq(Unch,zz=1..3^(Dimension(Ins)-(j-1))),
              seq(Decr,zz=1..3^(Dimension(Ins)-(j-1)))]),
         y=1..N*3^(j-2))];
   elif Other = 'yes' then
    Ind[j-1] := [seq(op([seq(Incr,zz=1..3^(Dimension(Ins)-(j-1))),
              seq(Unch,zz=1..3^(Dimension(Ins)-(j-1))),
              seq(Decr,zz=1..3^(Dimension(Ins)-(j-1)))]),
         y=1..(N+1)*3^(j-2))];
   fi;
   M[k+1,j] := Ind[j-1][k];
  elif j > 1 + Dimension(Ins) then
   counter := j-(1+Dimension(Ins));
   if frac(counter/3) = 1/3 then
    M[1,j] := Incr||op(Nvec[trunc(counter/3+2/3)]);
    if Other = 'no' then
     M[k+1,j] :=
Avg_SpR_IUD(N,Ins,Incr,trunc(counter/3+2/3),k+1,M,Ads,trans,Nvec,NFT
,Mods);
    elif Other = 'yes' then
     if k < Nrows-(3^Dimension(Ins))+1 then
      M[k+1,j] :=
Avg_SpR_IUD(N,Ins,Incr,trunc(counter/3+2/3),k+1,M,Ads,trans,Nvec,NFT
,Mods);
     else
      M[k+1,j] := evalf(1/3);
     fi;
```

```
      fi;
    elif frac(counter/3) = 2/3 then
     M[1,j] := Unch||op(Nvec[trunc(counter/3+2/3)]);
     if Other = 'no' then
      M[k+1,j] :=
Avg_SpR_IUD(N,Ins,Unch,trunc(counter/3+2/3),k+1,M,Ads,trans,Nvec,NFT
,Mods);
     elif Other = 'yes' then
      if k < Nrows-(3^Dimension(Ins))+1 then
       M[k+1,j] :=
Avg_SpR_IUD(N,Ins,Unch,trunc(counter/3+2/3),k+1,M,Ads,trans,Nvec,NFT
,Mods);
      else
       M[k+1,j] := evalf(1/3);
      fi;
     fi;
    else
     M[1,j] := Decr||op(Nvec[trunc(counter/3+2/3)]);
     if Other = 'no' then
      M[k+1,j] :=
Avg_SpR_IUD(N,Ins,Decr,trunc(counter/3+2/3),k+1,M,Ads,trans,Nvec,NFT
,Mods);
     elif Other = 'yes' then
      if k < Nrows-(3^Dimension(Ins))+1 then
       M[k+1,j] :=
Avg_SpR_IUD(N,Ins,Decr,trunc(counter/3+2/3),k+1,M,Ads,trans,Nvec,NFT
,Mods);
      else
       M[k+1,j] := evalf(1/3);
      fi;
     fi;
    fi;
   fi;
  od;
 od;
 M;
end:

Avg_SpR_IUD := proc(N,Ins,SpRIUD,SpR,row,M,Ads,f,Nms,NFT,Mods)
local k, j, AvgPr, NetVec, SumIns, Prb, Nelem, counts, TotVec,
SumTot;
NetVec := Vector(N);
TotVec := Vector(N);
NetVec := Vector(Dimension(Ins));
TotVec := Vector(Dimension(Ins));
for k from 1 to Dimension(Ins) do
 if M[row,1+k] = 'Incr' then
  NetVec[k] := Ads[M[row,1]][SpR,GetEntryIndex(Ins[k],Nms)];
  TotVec[k] :=
Permanent(Minor(map(abs,Mods[M[row,1]]),GetEntryIndex(Ins[k],Nms),Sp
R,output='matrix'));
 elif M[row,1+k] = 'Decr' then
  NetVec[k] := (-1)*Ads[M[row,1]][SpR,GetEntryIndex(Ins[k],Nms)];
```

```
   TotVec[k] :=
Permanent(Minor(map(abs,Mods[M[row,1]]),GetEntryIndex(Ins[k],Nms),Sp
R,output='matrix'));
 elif M[row,N+k] = 'Unch' then
  NetVec[k] := 0;
  TotVec[k] := 0;
 fi;
od;
SumIns := add(NetVec[cc],cc=1..Dimension(Ins));
SumTot := add(TotVec[cc],cc=1..Dimension(Ins));
if SumTot = 0 then
 if SpRIUD = 'Unch' then
  Prb := NFT;
 else
  Prb := (1-NFT)/2;
 fi;
else
 Prb := ProbTransform(SumIns,abs(SumIns/SumTot),SumTot,SpRIUD,f);
fi;
Prb;
end:


ProbTransform := proc(AdjElem,WtElem,TotElem,SpRIUD,f)
local P;
if (AdjElem = 0) then
  P := evalf(1/3);
elif sign(AdjElem) > 0 then
 if SpRIUD = 'Incr' then
  P := f(WtElem,TotElem);
 else
  P := (1-f(WtElem,TotElem))/2;
 fi;
elif sign(AdjElem) < 0 then
 if SpRIUD = 'Decr' then
  P := f(WtElem,TotElem);
 else
  P := (1-f(WtElem,TotElem))/2;
 fi;
fi;
eval(P);
end:


GetEntryIndex := proc(inp,nms)
local i, x;
for i from 1 to Dimension(nms) do
 if inp = nms[i] then
  x := i;
 fi;
od;
eval(x);
end:
```

Enter variable names in same order as qualitative matrix

```
> NamevecFC := Vector([P,A,H,C]);
NamevecFG := Vector([P,A1,A2,Ap,H1,H2,C1,C2]);
```

Specify model matrices:

```
> PD:=Matrix([[-1,-1,0,0],[1,0,-1,0],[0,1,0,-1],[0,0,1,0]]);
PR:=Matrix([[-1,-1,0,0],[1,-1,-1,0],[0,1,-1,-1],[0,0,1,-1]]);
NullFC := Matrix(4,fill=1);
FG := Matrix([[-1,-1,-1,-1,0,0,0,0],[1,0,0,0,-1,-1,0,0],[1,0,0,0,0,-
1,0,0],[1,0,0,-1,0,0,0,0],[0,1,0,0,0,0,-1,-1],[0,1,1,0,0,0,0,-
1],[0,0,0,0,1,0,0,-1],[0,0,0,0,1,1,1,-1]]);
NullFG := Matrix(8,fill=1);
```

Place alternative models into single array:

```
> ModelvecFC := Array([PD,PR,NullFC]);
ModelvecFG := Array([FG,NullFG]);
```

Specify vector of inputs:

```
> Inputvec := Vector([P]);
```

Check spelling to make sure input vector elements match an element of the name vector:

```
> Checkinputs(Namevec,Inputvec);
```
Translation function (execute only one from below)

Execute only the option you wish to use; leave the other option unexecuted:

    Translation function, Option 1: Expected value, Fig 3,2c (uniform); Results

```
> trans := proc(w,t)
local p, yprop;
 yprop :=
evalf(exp(3.45962*w+0.03417*w*t)/(1+exp(3.45962*w+0.03417*w*t)));
 p := evalf((4/3)*yprop-1/3);
p;
end:
NoFBtrans := trans(1.0, 0):
```

    Translation function, Option 2: 95% bound, Fig 2c (uniform); Appendix C

```
> trans := proc(w,t)
local p, yprop;
 yprop :=
evalf(exp(9.766*w+0.139*w*t)/(1253.992+exp(9.766*w+0.139*w*t)));
 if yprop < 0.5 then
  p := evalf(1/3);
 else
  p := evalf((4/3)*yprop-1/3);
 fi;
p;
end:
NoFBtrans := trans(1.0, 0):
> X := CPTconstruct(Namevec,Modelvec,Inputvec,trans,NoFBtrans,no);
```

APPENDIX F. EPIDEMICS IN HOSTS, IN HETEROGENEOUS POPULATIONS, AND IN ENDEMIC AREAS

F.1 Elevated prevalence in hosts

We determine the condition for an epidemic elevating the prevalence within hosts for the standard model. Similar calculations can be made for the vector bias and modified vector behavior models. Epidemics elevate prevalence in hosts when the angle θ (see Figure 4.1) between the eigenvectors at the DFE is obtuse. The matrix $\mathbf{J}_0$ has negative entries on the main diagonal and positive entries in the off-diagonal elements. The slope of the eigenvector associated with $s(\mathbf{J}_0)$ is always positive, and the slope of the eigenvector associated with $\rho(\mathbf{J}_0)$ is always negative. The vertical (opposite) angle of θ therefore always includes part of the positive quadrant.

Let the matrix $\mathbf{W}$ contain the right eigenvectors of the matrix $\mathbf{J}_0$. Let $\mathbf{w}^{(1)}$ denote the right eigenvector corresponding to the maximum eigenvalue, $\lambda_1(\mathbf{J}_0) = s(\mathbf{J}_0)$, and $\mathbf{w}^{(2)}$ denote the right eigenvector corresponding to the minimum eigenvalue, $\lambda_2(\mathbf{J}_0) = \rho(\mathbf{J}_0)$, of $\mathbf{J}_0$. The angle θ is determined by the Law of Cosines:

$$\theta = \arccos\left[\frac{\mathbf{w}^{(1)} \bullet \mathbf{w}^{(2)}}{\left\|\mathbf{w}^{(1)}\right\|\left\|\mathbf{w}^{(2)}\right\|}\right]. \tag{F.1}$$

The sign of the numerator in Eq. (F.1) determines whether the angle θ is obtuse:

$$\operatorname{sgn}\left(\mathbf{w}^{(1)} \bullet \mathbf{w}^{(2)}\right) < 0 \Leftrightarrow \theta \text{ is obtuse.}$$
$$\operatorname{sgn}\left(\mathbf{w}^{(1)} \bullet \mathbf{w}^{(2)}\right) > 0 \Leftrightarrow \theta \text{ is acute.} \tag{F.2}$$

For the standard model, Eq. (F.2) gives $\operatorname{sgn}\left(b_y e^{-\mu n} - b_x m\right)$. Epidemics will elevate prevalence in human hosts when $b_x m > b_y e^{-\mu n}$ and the angle θ is obtuse. Epidemics will elevate prevalence in vectors when $b_x m < b_y e^{-\mu n}$ and the angle θ is acute.

F.2 Heterogeneous susceptibility

F.2.1 Stability of equilibria

Hasibeder and Dye (1988) use the results of Lajmanovich and Yorke (1976) to show that their patchy host-vector model of infected individuals has the same properties as the standard model. In the model of gonorrhea transmission investigated by Lajmanovich and Yorke (1976), either the DFE is globally asymptotically stable, or there is a single globally asymptotically stable endemic equilibrium. The heterogeneous susceptibility model is equivalent to the model of Lajmanovich and Yorke (1976) following appropriate substitution, and so it also shares the same properties.

F.2.2 Threshold indices for endemicity and epidemicity

For the $N+1$ dimensional system, the matrix $\mathbf{F}_{\mathbf{J}_0}\mathbf{V}_{\mathbf{J}_0}^{-1}$ (see Appendix A) has nonnegative entries, and this matrix has rank 2. Only two of the $N+2$ coefficients in the characteristic polynomial of $\mathbf{F}_{\mathbf{J}_0}\mathbf{V}_{\mathbf{J}_0}^{-1}$ are nonzero, giving

$$\det\left(\mathbf{F}_{\mathbf{J}_0}\mathbf{V}_{\mathbf{J}_0}^{-1}-\lambda\right)=\lambda^{N+1}+c_2\lambda^{N-1}. \tag{F.3}$$

In Eq. (F.3), the terms within the coefficient $c_2<0$ are formed by the cycles of length 2 that define disease transmission between the vector and the host subpopulations. There are $N-1$ zero eigenvalues. The two nonzero eigenvalues are $\lambda=\pm\sqrt{-c_2}$. A similar result holds for $H(\mathbf{J}_0)$ since $H(\mathbf{V}_{\mathbf{J}_0})$ is diagonal. The cone of epidemicity includes a portion of the nonnegative orthant because the matrix $H(\mathbf{J}_0)$ is quasipositive.

F.3 Epidemicity at the endemic equilibrium

The endemic equilibrium for the standard model (provided that $\mathbf{R}_0 > 1$) is

$$x^* = \frac{a^2 b_x b_y m e^{-\mu n} - r\mu}{a b_y \left(a b_x m e^{-\mu n} + r\right)}, \quad y^* = \frac{a^2 b_x b_y m e^{-\mu n} - r\mu}{a b_x m \left(a b_y + \mu\right)}. \tag{F.4}$$

van den Driessche and Watmough (2002) show that if the matrix $\mathbf{F}$ is nonnegative and the matrix $\mathbf{V}$ is a non-singular M-matrix, then the spectral radius $\rho\left(\mathbf{FV}^{-1}\right) > 1$ if the spectral abscissa $s(\mathbf{F} - \mathbf{V}) > 0$, and $\rho\left(\mathbf{FV}^{-1}\right) < 1$ if $s(\mathbf{F} - \mathbf{V}) < 0$. The Hermitian part of the Jacobian matrix of Eq. evaluated at the endemic equilibrium, $H(\mathbf{J}^*)$, has negative entries on the main diagonal and positive entries in the off-diagonal elements. The matrix $H(\mathbf{J}^*)$ may be partitioned into nonnegative matrix $H(\mathbf{F}_{\mathbf{J}^*})$, containing the offdiagonal elements of $H(\mathbf{J}^*)$, and matrix $H(\mathbf{V}_{\mathbf{J}^*}) = H(\mathbf{F}_{\mathbf{J}^*}) - H(\mathbf{J}^*)$, where $H(\mathbf{V}_{\mathbf{J}^*})$ is a positive diagonal matrix. Thus, the methods described in Section 4.2 and Appendix F.1 may also be applied to the standard model at the endemic equilibrium. The threshold index for epidemicity at the endemic equilibrium is

$$\mathbf{E}^* = \rho\left(H(\mathbf{F}_{\mathbf{J}^*})H(\mathbf{F}_{\mathbf{J}^*})^{-1}\right) = \sqrt{\frac{\left[b_x^2 m^2 r\left(a b_y + \mu\right)^2 + b_y^2 \mu\left(a b_x m e^{-\mu n} + r\right)^2\right]^2}{4 a^2 b_x^3 b_y^3 m^3 e^{-\mu n}\left(a b_y + \mu\right)^2 \left(a b_x m e^{-\mu n} + r\right)^2}}. \tag{F.5}$$

An epidemic elevates prevalence within hosts if $b_x^2 m^2 r\left(a b_y + \mu\right)^2 > b_y^2 \mu\left(a b_x m e^{-\mu n} + r\right)^2$. The eigenvector associated with $s\left(H(\mathbf{J}^*)\right)$ lies in the quadrant of higher prevalence levels relative to the endemic equilibrium, and also continues into the quadrant of lower prevalence levels relative to the endemic equilibrium.